

INFORMATION TO USERS

This manuscript has been reproduced from the microfilm master. UMI films the text directly from the original or copy submitted. Thus, some thesis and dissertation copies are in typewriter face, while others may be from any type of computer printer.

The quality of this reproduction is dependent upon the quality of the copy submitted. Broken or indistinct print, colored or poor quality illustrations and photographs, print bleedthrough, substandard margins, and improper alignment can adversely affect reproduction.

In the unlikely event that the author did not send UMI a complete manuscript and there are missing pages, these will be noted. Also, if unauthorized copyright material had to be removed, a note will indicate the deletion.

Oversize materials (e.g., maps, drawings, charts) are reproduced by sectioning the original, beginning at the upper left-hand corner and continuing from left to right in equal sections with small overlaps.

Photographs included in the original manuscript have been reproduced xerographically in this copy. Higher quality 6" x 9" black and white photographic prints are available for any photographs or illustrations appearing in this copy for an additional charge. Contact UMI directly to order.

**Bell & Howell Information and Learning
300 North Zeeb Road, Ann Arbor, MI 48106-1346 USA
800-521-0600**

UMI[®]

**ASSESSMENT OF HYDROLOGIC PROCESSES ACROSS MULTIPLE SCALES
IN SOIL/PALEOSOL SEQUENCES USING ENVIRONMENTAL TRACERS**

A Dissertation

**Presented in Partial Fulfillment of the Requirements for the
Degree of Doctor of Philosophy**

with a

Major in Soil Science

in the

College of Graduate Studies

University of Idaho

by

Anthony Tobin O'Geen

May 2002

Major Professor: Paul A. McDaniel, Ph.D.

UMI Number: 3055391

UMI[®]

UMI Microform 3055391

Copyright 2002 by ProQuest Information and Learning Company.

**All rights reserved. This microform edition is protected against
unauthorized copying under Title 17, United States Code.**

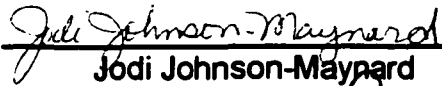
**ProQuest Information and Learning Company
300 North Zeeb Road
P.O. Box 1346
Ann Arbor, MI 48106-1346**

AUTHORIZATION TO SUBMIT DISSERTATION

This dissertation of Anthony Tobin O'Geen, submitted for the degree of Doctor of Philosophy with a major in Soil Science and titled "Assessment of hydrologic processes across multiple scales in soil/paleosol sequences using environmental tracers", has been reviewed in final form. Permission, as indicated by the signatures and dates given below, is now granted to submit final copies to the College of Graduate Studies for approval.

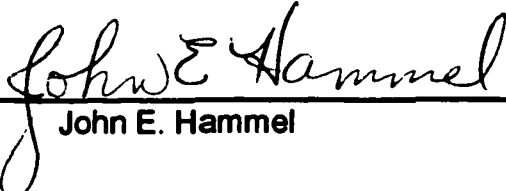
Major Professor  Date 14 May 2002
Paul A. McDaniel

Committee Members  Date 14 May 2002
C. Kent Keller


 Date May 14, 2002
Jodi Johnson-Maynard

 Date May 15, 2002
John D. Marshall

Department Administrator  Date May 14 2002
Mike J. Weiss

Discipline's College Dean  Date 14 May 2002
John E. Hammel

Final Approval and Acceptance by the College of Graduate Studies

 Date 15 May 2002
Charles R. Hatch

ABSTRACT

In the Palouse Basin of eastern Washington and northern Idaho, ground water is the principal municipal-water resource. Reliance on ground water continues to increase in the region, yet recharge mechanisms and rates are poorly understood in thick loess deposits that blanket the Basin. The main objective of this study was to assess the ability of soil/paleosol sequences in loessial hillslopes to accommodate deep percolation using environmental tracers. Patterns between vadose zone stratigraphy and Cl^- tracer profiles were established in heterogeneous regolith. Characterization of deep strata revealed sequences of extremely dense paleosol fragipans interstratified with less-dense eluvial horizons. Abrupt changes in $[\text{Cl}^-]$ reflect boundaries between stratigraphic units that display contrasting physical and morphological properties. Results illustrate that Cl^- depth profiles can be used as indicators of deep stratigraphy across various landscape positions. To assess regional recharge rates and mechanisms, environmental tracer distributions were measured in three catchments reflecting a regional climosequence. Tracer profiles and stratigraphy illustrate three major hydrostratigraphic units: 1) uplands with homogeneous regolith and short pore-water residence times; 2) uplands with heterogeneous regolith and long pore-water residence times; and 3) valleys with heterogeneous regolith that display dynamic hydraulic processes. Regional relationships between deep regolith and surface soils were established in order to use the Soil Survey Geographic database to estimate spatial extent of hydrostratigraphic

units. Results indicate that recharge is less than 3 mm yr⁻¹ in 33% of the loess-covered Basin where precipitation is greatest, and regolith is heterogeneous. Recharge is 10 mm yr⁻¹ in 37% of the Basin where loessial regolith is homogeneous. Hydraulically dynamic valley positions constitute 10% of the study area. Hydrometric measurements and natural tracers were used to assess hydrologic processes active in vadose zones, near-surface perched water tables, and streams of valley positions. Deep tensiometer readings and secondary Mn distributions indicate that ground-water recharge occurs as bypass flow. Indirect evidence from $\delta^{18}\text{O}$ signatures of water samples suggests that near-surface perched water tables are a major source of stream flow. Representative Cl^- profiles of valley soils reflect differences in pore-water residence time that are governed by regional patterns of soil development.

ACKNOWLEDGMENTS

I regretfully admit that this acknowledgement section was composed in haste, and I'm not sure that these words can express my gratitude for those who have helped me along the way. First, I would like to thank Mike Weiss, John Hammel, and all members of the Department of Plant, Soil, and Entomological Sciences for their support and encouragement. I am also grateful for the guidance and insight of my committee members Jodi Johnson-Maynard, Kent Keller, and John Marshall. Most importantly, I feel privileged to have worked with my advisor and mentor Paul McDaniel. Paul has donated countless hours of his time providing me with precious opportunities, training, and advice. In addition, I would like to acknowledge the financial support of the Stillinger Trust Fund, Idaho National Environmental Engineering Laboratory, and the Idaho Water Resource Research Institute. Finally, I would like to thank Henny and my family for their understanding and patience over the last four years. I made it guys!

TABLE OF CONTENTS

ABSTRACT	iii
ACKNOWLEDGMENTS.....	v
LIST OF FIGURES.....	viii
LIST OF TABLES.....	xii
CHAPTER 1: INTRODUCTION.....	1
Justification.....	1
Overview.....	1
Organization of the Dissertation.....	3
References.....	3
CHAPTER 2: CHLORIDE DISTRIBUTIONS AS INDICATORS OF VADOSE	
ZONE STRATIGRAPHY IN PALOUSE LOESS DEPOSITS.....	5
Abstract.....	5
Introduction.....	5
Materials and Methods.....	10
Environmental setting.....	10
Experimental methods.....	11
Results and Discussion.....	12
Morphology and physical properties of soils.....	12
Morphology and physical properties of deep loess.....	15
Chloride depth profiles and stratigraphic relationships.....	19
Mechanisms of recharge.....	21

Recharge estimates.....	23
Conclusions.....	25
References.....	26
CHAPTER 3: PALEOSOLS AS DEEP REGOLITH: IMPLICATIONS FOR	
GROUND-WATER RECHARGE ACROSS A LOESSIAL	
CLIMOSEQUENCE.....	31
Abstract.....	31
Introduction.....	32
Materials and Methods.....	36
Environmental setting.....	36
Core collection.....	37
Chloride.....	37
Stable isotopes.....	39
Stratigraphic analysis.....	40
Results and Discussion.....	40
Stratigraphy of the eastern catchment.....	40
Environmental tracers in the eastern catchment.....	41
Stratigraphy of the central catchment.....	45
Environmental tracers in the central catchment.....	47
Stratigraphy of the western catchment.....	49
Environmental tracers in the western catchment.....	49
Recharge estimates.....	52
Regional basin analysis.....	55

Conclusions.....	60
References.....	60
CHAPTER 4: HYDROLOGIC PROCESSES IN VALLEY SOILSCAPES	
OF THE EASTERN PALOUSE BASIN.....	65
Abstract.....	65
Introduction.....	66
Materials and Methods.....	68
Environmental setting.....	68
Field methods.....	70
Laboratory methods.....	70
Results and Discussion.....	72
Vadose zone stratigraphy.....	72
Near-surface perched water.....	74
Vadose zone hydrology.....	76
Secondary manganese.....	78
Oxygen isotopes.....	80
Regional trends of Cl ⁻ depth profiles	83
Conclusions.....	85
References.....	85
APPENDIX 1: Chloride distributions.....	90
APPENDIX 2: Stable isotope data.....	102
APPENDIX 3: Stratigraphic measurements.....	106
APPENDIX 4: Diffusion calculations.....	115

LIST OF FIGURES

- Figure 2.1. Location of the study site showing distribution of soils with hydraulically restrictive horizons in eastern Washington and northern Idaho. Topographic attributes are displayed using a 2-m grid elevation model and locations of core samples are indicated with X..... 7**
- Figure 2.2. Pedo-stratigraphic descriptions and depth profiles of chloride, θ_m , clay, and $Mn_d:Fe_d$ at the summit position. Shading represents zones of soil strength greater than 3.0 kg cm^{-2} 16**
- Figure 2.3. Pedo-stratigraphic descriptions and depth profiles of chloride, θ_m , clay, and $Mn_d:Fe_d$ at the side slope position. Shading represents zones of soil strength greater than 3.0 kg cm^{-2} 17**
- Figure 2.4. Pedo-stratigraphic descriptions and depth profiles of chloride, θ_m , clay, and $Mn_d:Fe_d$ at the valley position. Shading represents zones of soil strength greater than 3.0 kg cm^{-2} 18**
- Figure 2.5. Recharge rates calculated from water inventory vs. chloride inventory. Linear-line segments represent constant chloride accumulation 24**

Figure 3.1. Digital elevation model of the Palouse Basin and its location in the Pacific Northwest. Western, central and eastern Basin study sites are indicated using the letters W, C, and E respectively. Approximate physiographic boundary of the Basin is indicated by the white line.....	33
Figure 3.2. Morphologic and stratigraphic descriptions of the eastern catchment.....	42
Figure 3.3. Chloride and $\delta^{18}\text{O}$ depth profiles at summit, side slope, and valley positions in the eastern catchment.....	44
Figure 3.4. Morphologic and stratigraphic descriptions of the central catchment.....	46
Figure 3.5. Chloride and $\delta^{18}\text{O}$ depth profiles at summit, side slope, and valley positions in the central catchment.....	48
Figure 3.6. Morphologic and stratigraphic descriptions of the western catchment.....	50
Figure 3.7. Chloride and $\delta^{18}\text{O}$ depth profiles at summit, side slope, and valley positions in the western catchment.....	51
Figure 3.8. Cumulative water-cumulative chloride plots showing recharge estimates for valley and upland sites. Straight-line segments represent episodes of constant Cl^- accumulation.....	53

Figure 3.9. Conceptual representation of the degree of soil development in deep regolith across depositional and climatic gradients.....	57
Figure 3.10. Spatial representation of recharge rates of major hydrostratigraphic units identified from the SSURGO database. P and M represent locations of Pullman and Moscow; western, central, and eastern study sites are indicated by W, C, and E.....	59
Figure 4.1. Location of the Palouse Basin of northern Idaho and the Troy study catchment. Letters a, b, and c indicate sampling locations for Cl⁻ depth profiles. Shading indicates the approximate distribution of valley. Topographic attributes for the Troy study catchment are displayed using a 2-m grid elevation model and location of core samples are indicated with X.....	67
Figure 4.2. Schematic diagram of morphology and stratigraphy of soil/paleosol sequences in valley positions at the Troy catchment.....	73
Figure 4.3. Hydrographs for upper- and lower-slope well positions at the Troy catchment for 1998 through 1999. Genetic horizon and depths are indicated at the right of each hydrograph.....	75

Figure 4.4. Measurements of saturated thickness recorded by multilevel tensiometers for the lower-slope position at the Troy catchment. Data points represent the elevation head above the indicated depth of each tensiometer.....	77
Figure 4.5. Vertical distributions of dithionite-extractable manganese (Mn_d) for upper- and lower-slope positions of the Troy catchment.....	79
Figure 4.6. Chloride depth profiles at representative valley soils in the eastern Palouse Basin.	84

LIST OF TABLES

Table 2.1. Selected soil morphological and physical characteristics at summit, side slope, and valley sites.....	13
Table 2.2. Correlation of the vertical change in measured stratigraphic variables with pore-water Cl⁻ concentrations in a Palouse hillslope.....	21
Table 3.1. Spatial extent of the three major hydrostratigraphic units in the Palouse Basin.....	58
Table 4.1. The $\delta^{18}\text{O}$ signature of perched water tables, snowpack, and streams in 2000.....	82

CHAPTER 1

INTRODUCTION

Justification

Like many communities in the western U.S.A., the cities of Moscow, ID and Pullman, WA are struggling to maintain a sustainable water resource. Ground water is the sole municipal water supply for the region, and as a result, potentiometric surfaces of pumping wells have decreased approximately 0.45 m per year over the last century in response to increased demand by the growing communities (Barker, 1979). To date, mechanisms of ground water recharge remain unclear; however, many believe that infiltration of precipitation through thick loess deposits is the most likely avenue. Loess deposits of the region have traditionally been treated as a single homogeneous unit for purposes of modeling. Loess blankets over 75% of the Palouse Basin (Williams and Allman 1969), and therefore understanding the ability of the loessial regolith to accommodate deep percolation is an important component to the assessment of water resource sustainability for the region.

Overview

A major role of pedology in science today is working within multiple scales of investigation to extrapolate information from individual sampling points within a soil profile to regional scale. This involves the recognition of the soil continuum within a region into discrete bodies that coexist on a landscape. This project entails an added level of complexity that involves the linkage of hydraulic

characteristics of surface soils to that of deep regolith, which traditionally is ignored for purposes of soil inventory.

The goal of this dissertation was to obtain a basin-wide understanding of hydrologic processes operating in loessial hillslopes of the Palouse Basin. Several time-tested tools and techniques were implemented to analyze of near-surface and vadose zone hydrologic processes. These tools and techniques included environmental tracers, spatial databases, stratigraphic observations, and hydrometric measurements. The unique aspect of this study is the interpretation and scaling of recharge mechanisms based on a pedologic analysis of soil/paleosol stratigraphic relationships to obtain a regional understanding of deep regolith hydrology.

The conceptual framework of this project is organized around the hypothesis that the permeability of loessial regolith is controlled by the degree of pedogenic alteration, which is in turn, governed by a Basin-wide climatic gradient. More specifically, we hypothesize that regional patterns in the degree of anisotropy and heterogeneity of deep regolith result from differences in soil development. The Palouse Basin is a perfect natural laboratory to test this hypothesis because several of the soil-forming factors including time, topography, parent material, and organisms are similar across the Basin. Therefore, pedogenic differences among contemporary soils result primarily from the strong climatic gradient (Busacca, 1989).

A second major source of variation across the Basin is the rate of loess deposition, which is related to distance from the sediment source. The western

Basin is proximal to the loess source, and as a result, deposition rates are high (Busacca and McDonald, 1994). Rapid rates of landscape aggradation counteract the rate of pedogenesis. In contrast, the eastern Basin is more distal to the loess source, and therefore loess deposition rates are much lower, which allows for greater superposition and overprinting of soil forming intervals (Kemp et al., 1998). As a result, deep regolith can be conceptualized as a single soil profile extending several meters to bedrock and as a discrete body with a spatial extent defined by the climatic gradient and loess deposition rate.

The foundation of this research is based upon a fundamental understanding of the depositional and pedogenic environment inherent to eastern Palouse loess. The linkage of hydrologic processes to the morphologic character of regolith provides a means of scaling the results Basin-wide.

Organization of the Dissertation

This dissertation is organized in journal style format consisting of three chapters: 1) Chloride distributions as indicators of vadose zone stratigraphy in Palouse loess deposits; 2) Paleosols as deep regolith: implications for ground water recharge across a loessial climosequence; and 3) Hydrologic processes in valley soils of the eastern Palouse Basin.

References

- Barker, R.J., 1981. Soil Survey of Latah County area, Idaho. USDA-SCS. U.S. Gov. Print. Office, Washington, D.C.
- Busacca, A.J., 1989. Long Quaternary record in eastern Washington, USA, interpreted from multiple buried paleosols in loess. *Geoderma* 45:105-122.

- Busacca, A.J. and E.V. McDonald, 1994. Regional sedimentation of late Quaternary loess on the Columbia Plateau: sediment source areas and loess distribution patterns. P. 181-190 in R. Lasmanis and E.S. Cheney (eds.) Washington Div. Geol. Earth Res. Bull. 80.**
- Kemp, R.A., P.A. McDaniel and A.J. Busacca, 1998. Genesis and relationship of macromorphology and micromorphology to contemporary hydrological conditions of a welded Argixeroll from the Palouse in NW, USA. Geoderma 83:309-329.**
- Williams, R.E. and D.W. Allman, 1969. Factors affecting infiltration and recharge in a loess-covered basin. J. Hydrol. 8:265-281.**

CHAPTER 2

CHLORIDE DISTRIBUTIONS AS INDICATORS OF VADOSE ZONE STRATIGRAPHY IN PALOUSE LOESS DEPOSITS

Abstract

Chloride is often used as a conservative tracer to estimate groundwater recharge rates in arid and semiarid regions. Relationships between Cl^- depth profiles and vadose zone stratigraphy have revealed new information on the behavior of this dissolved constituent in pore waters of heterogeneous materials. We measured pore-water Cl^- in loess deposits of the eastern Palouse region in northern Idaho, where multiple sequences of buried soils extend to ~20 m depth. Three cores were collected to bedrock at summit, side slope, and valley positions. Pore-water Cl^- distribution, clay content, soil strength, and secondary $\text{Mn}_d:\text{Fe}_d$ ratios were measured to identify relationships between natural tracer migration and vadose zone stratigraphy. Characterization of deep strata revealed complex sequences of extremely dense paleosol fragipans interstratified with less dense leached horizons. Abrupt changes in $[\text{Cl}^-]$ reflect boundaries between these stratigraphic units that display contrasting physical and morphological properties. Results illustrate that loess stratigraphy influences vadose-zone water movement in the Palouse. In addition, Cl^- depth profiles can be used as indicators of deep stratigraphy across various landscape positions.

Introduction

Loess-derived soils in the eastern Palouse region of Washington and northern Idaho contain fragipans and horizons with fragic character that restrict vertical

percolation of water (Fig. 2.1) (McDaniel and Falen, 1994; McDaniel et al., 2001). Fragipans are brittle subsurface soil horizons that exhibit high bulk density to the extent that movement of water and roots is restricted (Soil Survey Staff, 1999). Soils that contain hydraulically restrictive horizons occupy areas of greatest mean annual precipitation in the Palouse Basin, which is a drainage basin that occupies approximately 60,000 ha of the eastern Palouse region (Fig. 2.1). Since water-restrictive horizons are believed to play a critical role in groundwater recharge, understanding the ability of soils to accommodate deep percolation is an important step towards characterizing the regional hydrology of the Palouse Basin.

Investigations of near-surface hydrological processes in soils with fragipans are common, yet no studies have directly measured deep percolation below a fragipan, particularly in xeric moisture regimes such as those found in the Pacific Northwest. Observations of perched water table dynamics at one site in the eastern Palouse region indicate that E horizons overlying restrictive horizons remain saturated for long periods and water moves laterally as throughflow in more permeable Ap and Bw horizons (Reuter et al., 1998; McDaniel et al., 2001). Measured saturated hydraulic conductivity values range from 0.06 to 0.9 cm d⁻¹ in restrictive horizons and 14 to 129 cm d⁻¹ in Ap and Bw horizons (McDaniel et al., 2001; Reuter et al., 1998). As a result, up to 90% of the perched water volume can be shed from uplands as lateral throughflow in Ap and Bw horizons (Brooks et al., 2000). Moreover, multilevel tensiometers indicate that saturation

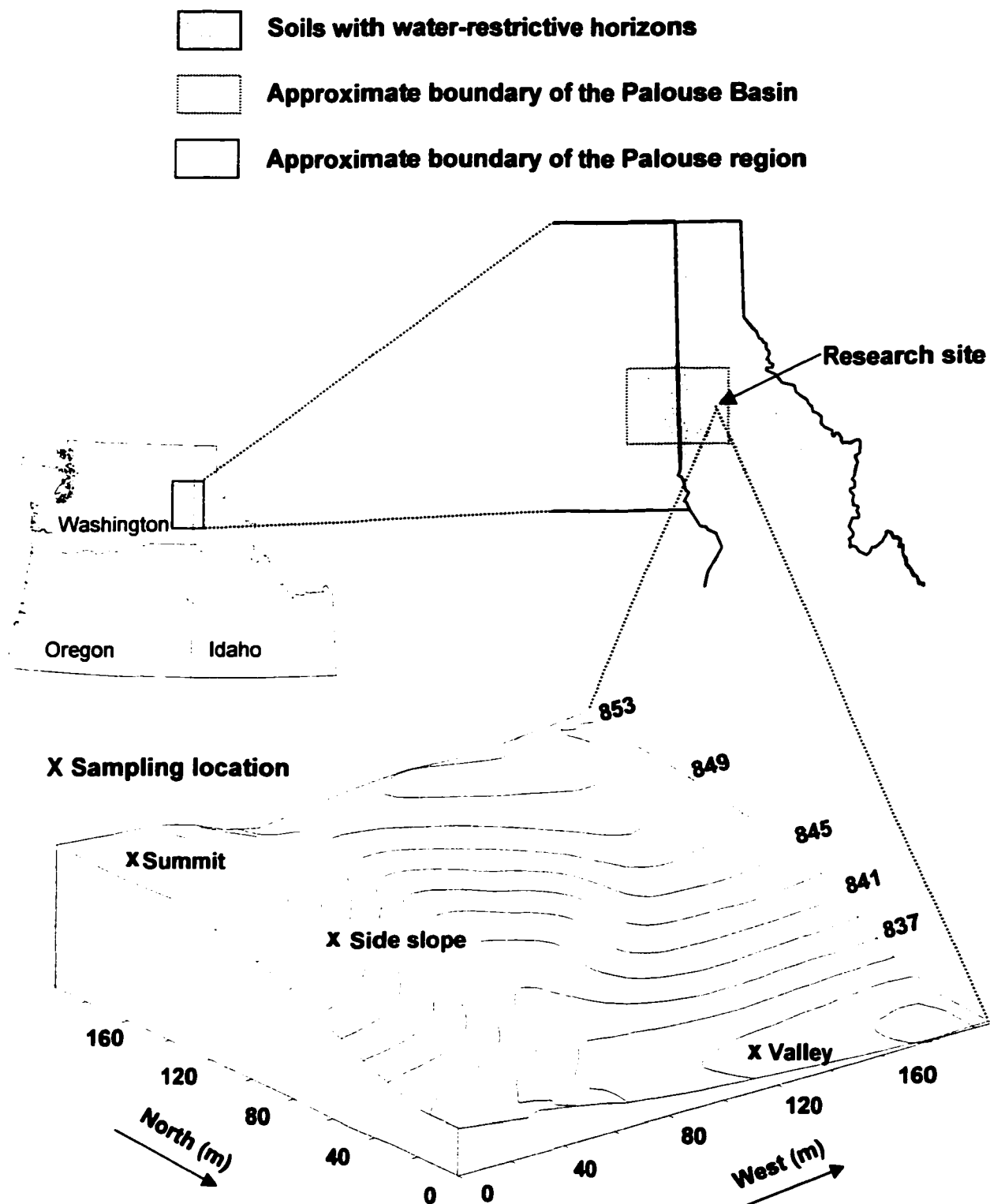


Figure 2.1. Location of the study site showing distribution of soils with hydraulically restrictive horizons in eastern Washington and northern Idaho. Topographic attributes are displayed using a 2-m grid elevation model and locations of core samples are indicated with X.

does not occur below the uppermost fragipan in uplands of the eastern Palouse region (O'Geen et al., 2001).

Water mass balance techniques are commonly used to assess water movement in soils with fragipans under udic soil moisture regimes. In New York, Parlange et al. (1989) discovered that a majority of irrigation water moved laterally through a network of cracks present within a fragipan. A similar study using *in situ* soil block experiments identified 23% of water flow as vertical percolation below the upper boundary of a fragipan (Day et al., 1998). A unifying concept among all studies is that permeability of fragipans is governed by frequency and distribution of cracks, which, in turn, is influenced by the degree of soil development (Van Vliet and Langohr, 1981; Parlange et al., 1989; Ciolkosz et al., 1995; Day et al., 1998).

Pore-water Cl^- is commonly used as a conservative natural tracer to assess deep percolation in vadose zones (Scanlon, 1992; Cook et al., 1992; Allison et al., 1994; Phillips, 1994; Murphy et al., 1996). In most cases, Cl^- is introduced into soils through atmospheric deposition and enriched in soil solution through evapotranspiration because plants do not assimilate significant amounts of Cl^- . Using Cl^- depth profiles, a mass balance approach can be applied to calculate water flux under steady-state conditions (Cook et al., 1992; Allison et al., 1994; Tyler and Walker, 1994; O'Brien et al., 1996; Murphy et al., 1996). If sources and sinks of Cl^- are defined and the deposition rate has remained constant through time, the flux of Cl^- below the root zone can be estimated by:

$$R = C_p P / C_s \text{ (eq. 1)}$$

Where: R - recharge

P - mean annual precipitation

C_s - average Cl⁻ concentration

C_p - Cl⁻ concentration in precipitation

Although several studies have documented sedimentologic and stratigraphic characteristics to accompany natural tracer studies, few have directly quantified the influences of stratigraphy on Cl⁻ depth profiles. Eriksson and Khunakasem (1969) discovered that spatial variability of recharge rates calculated from Cl⁻ mass balance in ground water was related to general trends in distribution of soils. Complex hydrological processes such as fluctuating water tables and bypass flow have been suggested as factors influencing the Cl⁻ profiles (Allison et al., 1994; Phillips 1994). In Australia, steep concentration gradients of Cl⁻ depth profiles reportedly reflecting boundaries between different stratigraphic units were recognized, but not directly quantified (Johnston, 1987). In addition, Hendry et al. (2000) identified distinct Cl⁻ signatures in different geologic units within a saturated aquitard. No studies have focused on relating the form of Cl⁻ depth profiles to stratigraphic sequences in unsaturated material.

Regional concerns regarding sustainability of ground water in the Palouse Basin have fueled a need to identify hydrologic processes in soils and deep vadose zones. The overall objective of this study was to use Cl⁻ depth profiles to interpret relationships between soil stratigraphic conditions and hillslope hydrologic processes in a Fragixeralf landscape of northern Idaho. Specifically,

we wanted to compare more traditional techniques for characterization of deep sediment stratigraphy such as morphology, physical properties, and mineralogy, with Cl^- depth profiles.

Materials and Methods

Environmental setting

The Palouse region is located on the eastern part of the Columbia Plateau and is characterized as a thick sequence of loess deposits that occupy 20,000 km^2 in northwestern USA (Fig. 2.1) (Busacca, 1989; Baker et al., 1991). The study area consists of a 1.7-ha catchment located near the eastern boundary of the Palouse region in northern Idaho (Fig. 2.1). The landscape of rolling loessial hills represents eolian deposition throughout the Quaternary Period (Busacca, 1989). Loess thickness ranges from ~ 20 m in uplands to less than 5 m in valleys. Soils are classified as Fragixeralfs (Soil Survey Staff, 1999).

In the western Palouse region, multiple episodes of soil development are interrupted by periods of rapid loess deposition resulting in a vertical sequence of buried ancient soils (paleosols) interstratified with relatively unaltered loess (Baker et al., 1991). Because the eastern Palouse receives greater mean annual precipitation and is more distal to the loess source, superposition of paleosols is common, and overprinting of soil-forming intervals results in a continuous sequence of hydraulically restrictive paleo-fragipans and highly leached (E) horizons (Busacca, 1989; King, 2000).

Mean annual precipitation is ~800 mm at the research site and falls predominantly during winter months. As a result, perched water tables form in

November or December and persist for periods up to seven months, disappearing in May or June in response to increased evapotranspiration (McDaniel et al., 2001). Observations of perched water table dynamics indicate that the uppermost fragipan extends across the catchment (McDaniel et al., 2001).

Experimental methods

Three hillslope positions were sampled within the study area using a truck-mounted hollow-stem auger. Seven, 4-cm diameter cores extending 6 m were saved for tracer and detailed stratigraphic analysis. These three sampling sites include summit, side slope, and valley positions. Cores ranged from 6 to 13 m in length and were sectioned into 20-cm sampling increments, sealed in plastic bags, and frozen until analyzed.

In the laboratory, cores were split longitudinally, providing samples for both stratigraphic description and for extraction of pore-water Cl^- . Gravimetric water content was determined for all samples prior to Cl^- extraction. After samples were oven dried, 20 g of sediment were mixed with 20 mL of triple-distilled water and shaken over night. Samples were centrifuged at 2500 RPM for 30 minutes, and supernatant solution was filtered through a 0.22- μm Millipore filter. Chloride concentration was measured in triplicate using a Dionex ion chromatograph, and pore-water Cl^- concentration was calculated using gravimetric water content (Murphy et al., 1996). Recharge rates were estimated from three representative cores.

Since the degree of soil development appears to control vadose zone hydrology in the eastern Palouse, we attempted to identify pedo-stratigraphic units across the catchment with measurements of clay, secondary Mn and Fe oxides, and soil strength. These measurements were used with morphologic descriptions of strata to further differentiate paleosol boundaries. Clay content was determined using the pipette method (Gee and Bauder, 1986). The distribution of secondary Mn and Fe oxides reflects changes between reducing and oxidizing environments, and $Mn_d:Fe_d$ ratios therefore are a good indicator of E-Btxb horizon boundaries in the Palouse region (McDaniel et al., 1992; McDaniel et al., 2001). $Mn_d:Fe_d$ ratios were measured using a citrate-bicarbonate-dithionite extracting solution (CBD) (Soil Conservation Service, 1972). Soil strength was used as a proxy for brittleness, a characteristic of fragipans, and assessed on peds using a pocket penetrometer, where deformation of the piston spring was recorded and expressed as unconfined compressive strength in $kg\ cm^{-2}$.

Results and Discussion

Morphology and physical properties of soils

Detailed soil descriptions were made for each sampling location according to techniques described by the Soil Survey Staff (1993). Each profile is dominated by silt loam or silty clay loam textures and contain E horizons that overlie an extremely dense paleosol fragipan (Btxb) (Table 2.1). The lower boundary of the uppermost fragipan at the summit position contains filaments of calcium carbonate that coat relict Mn concentrations. The dendritic Mn concentrations

Table 2.1. Selected soil morphological and physical characteristics at summit, side slope, and valley sites.

Soil Horizon	Depth (cm)	Munsell Color (dry)	Pedogenic Structure*	Dry Consistence	Matrix Features	Clay (%)
Summit						
Ap	0-20	10YR 6/3	1 f g	Soft	none	22
Bw	20-44	10YR 6/4	2 m sbk	Soft	none	19
EB	44-65	10YR 8/2	1 m sbk	Very hard	1 f Fe/Mn conc.	26
Btxb1	65-85	10YR 6/4	3 vc pr	Extremely hard	2 f Fe/Mn conc. & depl.	35
Btxb2	85-134	10YR 7/3	3 vc pr	Extremely hard	1 f Fe/Mn conc.	29
Btxb3	134-174	10YR 5/4	3 vc pr / 3 f abk	Extremely hard	2 f Fe/Mn conc.	35
Btkxb	174-200	10YR 6/5	ma	Extremely hard	2 f CaCO ₃ filaments	34
Side Slope						
Ap	0-22	10YR 6/2	2 f g	Soft	none	19
Bw	22-40	10YR 6/3	2 f sbk	Soft	none	16
E	40-60	10YR 7/2	1 m sbk	Very hard	none	22
EB	60-90	10YR 7/3	1 m sbk	Very hard	1 f Fe/Mn conc. & depl.	26
Btxb1	90-145	10YR 6/4	3 vc pr	Extremely hard	2 f Fe/Mn conc. & depl.	35
Btxb2	145-170	10YR 6/4	3 v t pl	Extremely hard	2 f Fe/Mn conc.	33
BE	170-200	10YR 7/4	3 v t pl	Very hard	1 f Fe/Mn conc.	27
Valley						
Ap	0-30	10YR 6/3	2 f g	Soft	1 f Fe/Mn conc.	18
E	30-50	10YR 8/1	1 m sbk	Slightly hard	1 f Fe/Mn conc. & depl.	19
Btg	50-80	2.5Y 6/3	3 m abk	Very hard	2 f Fe/Mn conc. & depl.	43
EBb	80-100	2.5 Y 7/3	2 m sbk	Hard	1 f Fe/Mn conc. & depl.	37
Btxgb	100-160	2.5Y 6/3	3 c pr	Very hard	3 f Fe/Mn conc. & depl.	33

*1 = weak; 2 = moderate; 3 = strong; f = fine; m = medium; c = coarse; t = thick; v = very; g = granular; sbk = subangular blocky; abk = angular blocky; pr = prismatic ma = massive/structureless

suggest changes in redox status associated with seasonally saturated conditions, probably when the zone was nearer to land surface. The calcium carbonate coatings illustrate how superposition of paleosols in an aggrading landscape changes the hydrology of a horizon by effectively decreasing percolation (Table 2.1).

Side slopes, which receive more effective precipitation from redistribution of snow, display evidence of greater leaching with a thicker E horizon and a lack of calcium carbonate. Since valley soils receive the greatest amount of effective precipitation profiles display clay-rich horizons overlying the fragipan. Depth to redoximorphic features is less than 30 cm. Moreover, horizons display reduced matrices, indicating prolonged saturation.

Buried fragipans are dense, brittle, and continuous across the hillslope. In uplands, fragipans have extremely hard dry consistence with very coarse prismatic structure that changes to very thick platy or a massive condition with depth (Table 2.1). Redox concentrations and Mn coatings are common in ped interiors. Redox depletions are present along large cracks separating structural units and in overlying E horizons (Table 2.1). In valley positions, buried fragipans grade into slightly less dense, brittle horizons with very hard dry consistence and medium to coarse prismatic or thick platy structure. Redox concentrations and Mn coatings are common in ped interiors and redox depletions occupy over 50% of the horizon matrix (Table 2.1).

Morphology and physical properties of deep loess

We recognized several major zones of paleosol fragipan development (Bt_xb horizons) in the upper 6 m of loess (Figs 2.2-2.4). Each zone of fragipan development represents multiple episodes of soil formation spanning thousands of years in which profiles are superimposed into single units (Busacca, 1989). In many cases fragipan horizons are interstratified with subtle leached horizons (Eb horizons) that reflect periods of saturation when the horizon was near the land surface. Because superimposed profiles are sometimes difficult to recognize in core samples, we compared morphologic observations with measurements of soil strength, clay content, and secondary Mn and Fe oxides to distinguish between buried Eb horizons and fragipans (Figs. 2.2-2.4).

Physical and chemical properties differ sharply between Eb and paleo-fragipan horizons. In each profile, Eb horizons have lower clay content, lower Mn_d:Fe_d ratios, and decreased soil strength. For example, all fragipans have 6-10% more clay (absolute) than Eb horizons and have silty clay loam textures (Table 2.1; Fig 2.2-2.4). Striking differences in soil strength exist where average strength increases from 1.1 kg/cm² in Eb horizons to 3.1 kg/cm² in fragipans (Figs. 2.2-2.4). Horizon boundaries were identified by CBD-extractable Fe and Mn oxides, where Mn_d:Fe_d ratios at boundaries of overprinted fragipans display a two-fold change (Figs. 2.2-2.4). Superposition and overprinting of paleosols complicates interpretation of clay and Mn_d:Fe_d depth profiles and although peaks in clay and Mn_d:Fe_d ratios occur at slightly different depths, they occur within the same horizon (Fig. 2.2-2.4). These data illustrate that physical and chemical

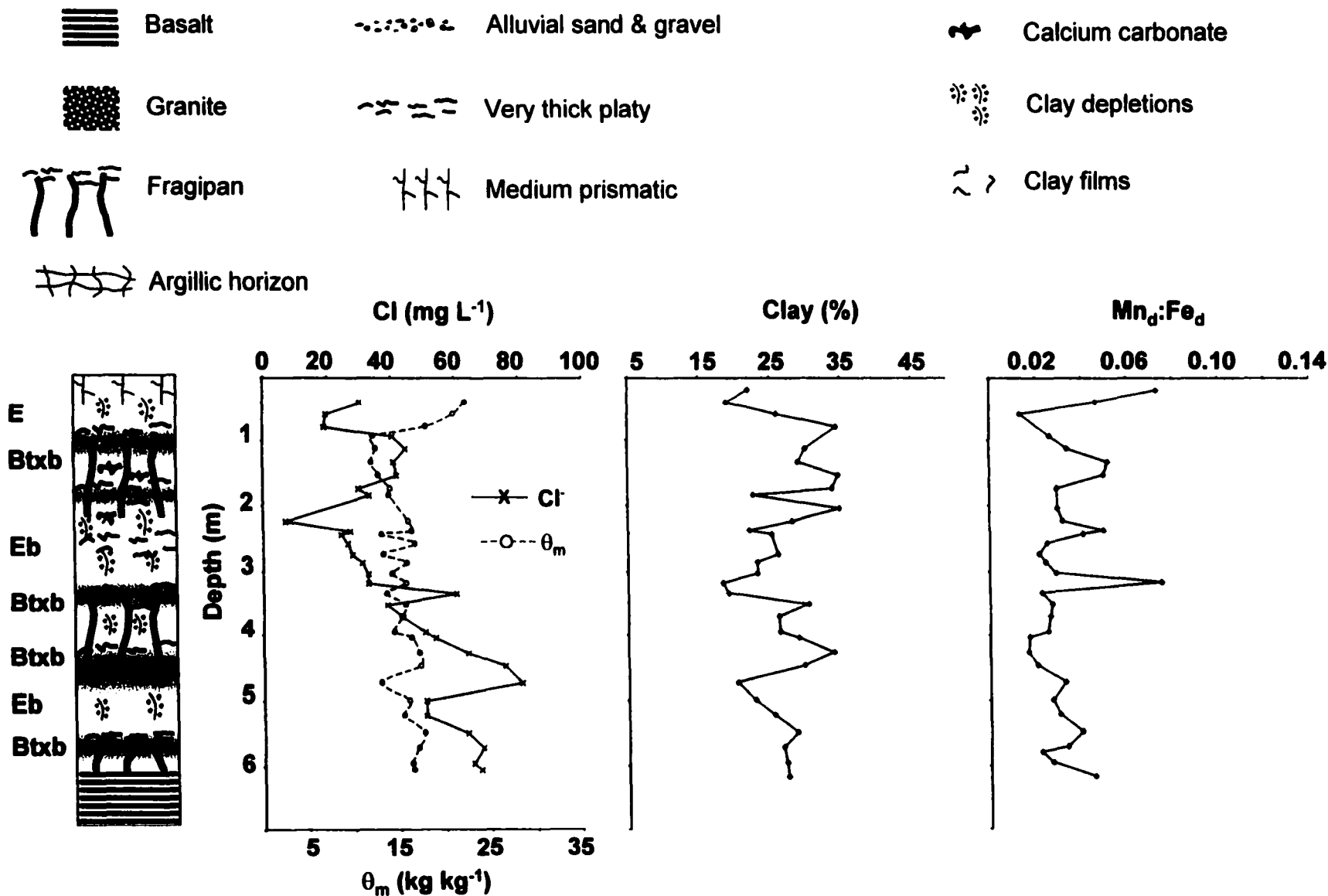


Figure 2.2. Pedo-stratigraphic descriptions and depth profiles of chloride, θ_m , clay, $Mn_d:Fe_d$ at the summit position. Shading represents zones of soil strength greater than 3.0 kg cm^{-2} .

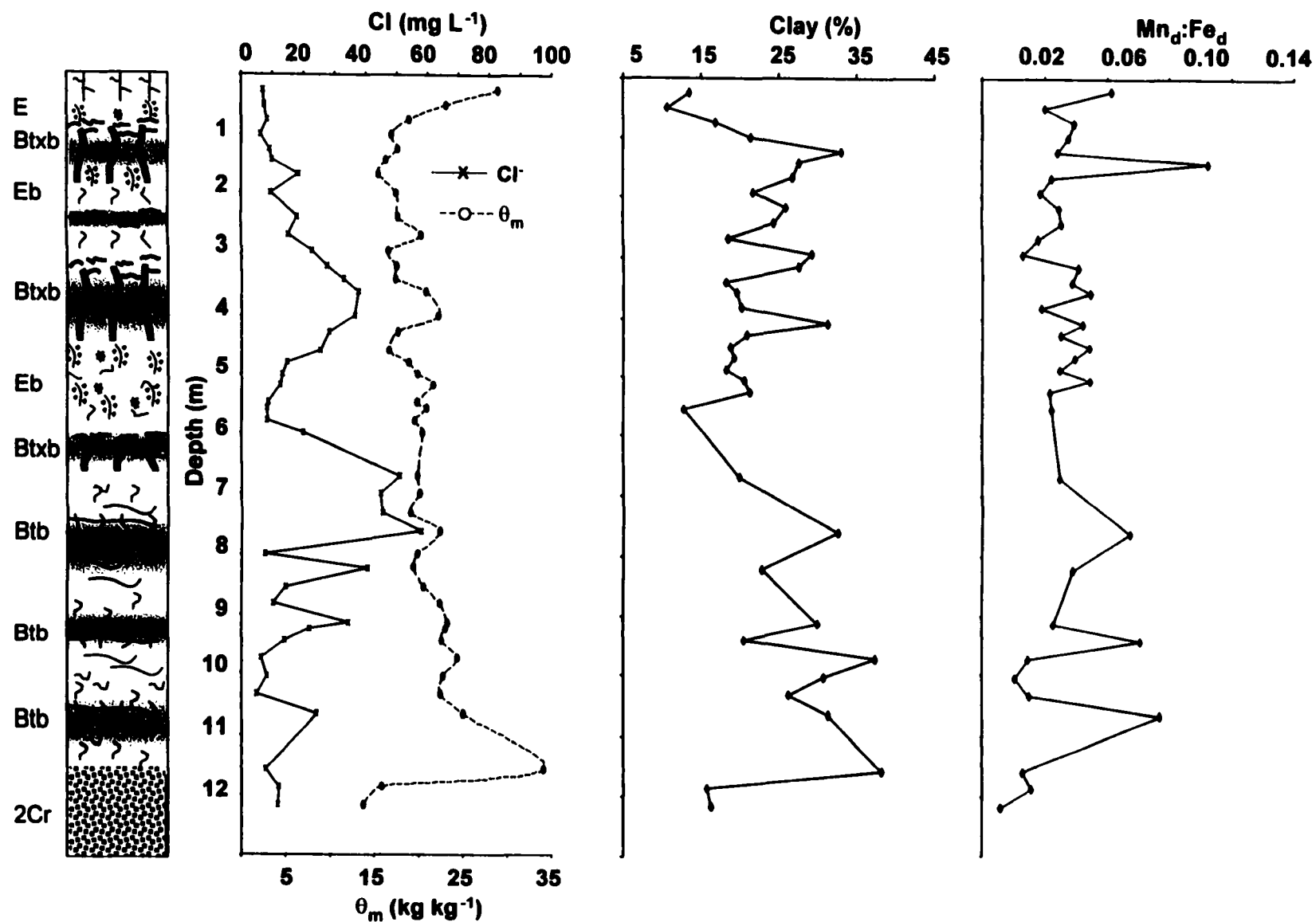


Figure 2.3. Pedo-stratigraphic descriptions and depth profiles of chloride, θ_m , clay, $\text{Mn}_d:\text{Fe}_d$ at the side slope position. Shading represents zones of soil strength greater than 3.0 kg cm^{-2} .

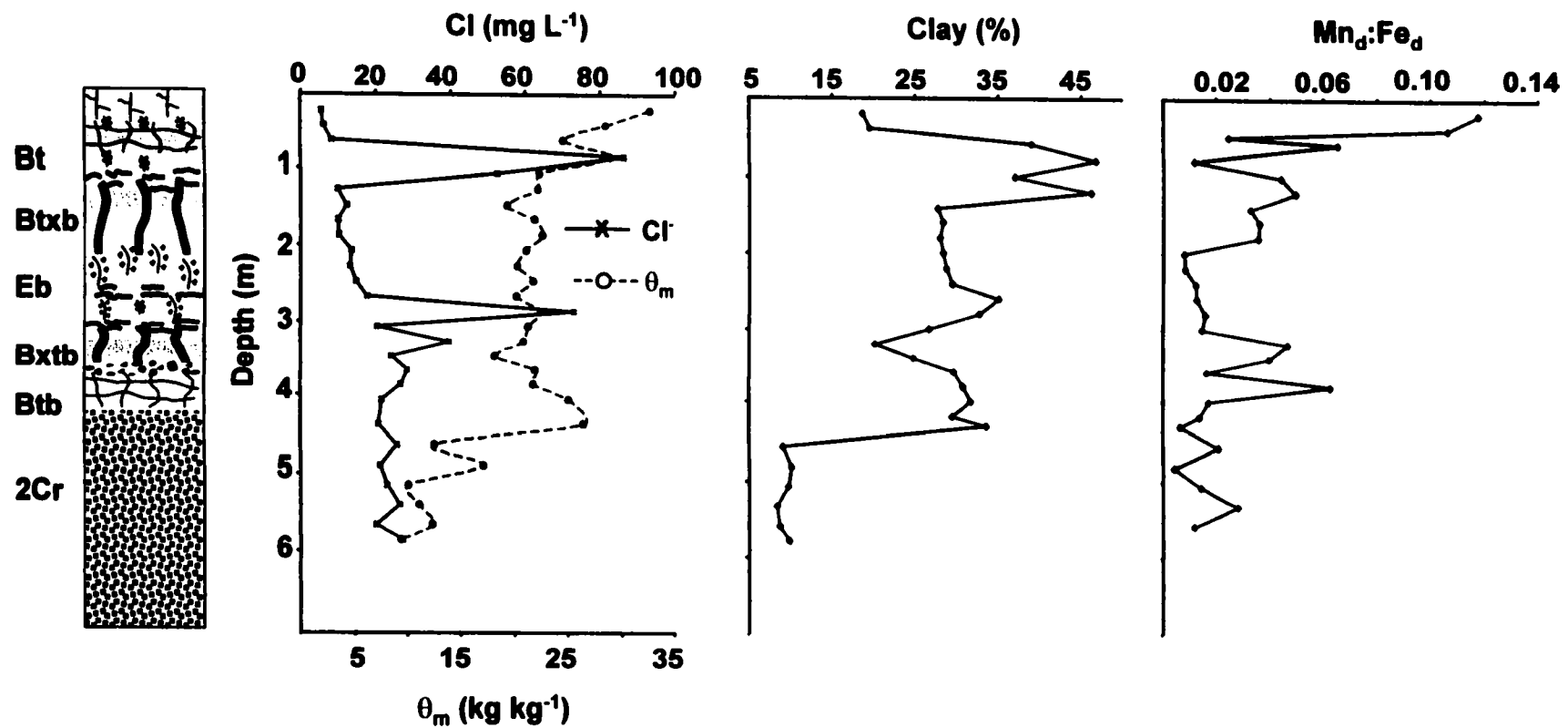


Figure 2.4. Pedo-stratigraphic descriptions and depth profiles of chloride, θ_m , clay, $\text{Mn}_d:\text{Fe}_d$ at the valley position. Shading represents zones of soil strength greater than 3.0 kg cm^{-2} .

properties can be used to distinguish pedo-stratigraphic units in loess sequences. Moreover, properties of paleosol fragipans and Eb horizons appear to contrast to the extent that hydrologic barriers are identifiable.

Chloride depth profiles and stratigraphic relationships

The Cl^- depth profile at the summit position is influenced by soil stratigraphy, where boundaries between Eb and paleo-fragipan horizons (Btxb) are associated with relatively large changes in $[\text{Cl}^-]$. Peaks in $[\text{Cl}^-]$ correspond with three buried fragipans that display changes in strength and clay content. Furthermore, their boundaries are identified by increases in $\text{Mn}_d:\text{Fe}_d$. Upper boundaries of each fragipan located at 1.00, 3.00, and 5.75 m reflect increases in $[\text{Cl}^-]$ of at least 20 mg L^{-1} compared to interstratified Eb horizons (Fig. 2.2).

The side slope position illustrates similar trends, where peaks in $[\text{Cl}^-]$ reflect boundaries between Eb horizons and four buried fragipans located at 1.00, 2.00, 3.00, and 6.50 m (Fig. 2.3). In the upper two fragipans, $[\text{Cl}^-]$ is 5 to 10 mg L^{-1} greater than in the interstratified Eb horizons, while the upper boundary of the third and fourth fragipans display greater than a 20 mg L^{-1} increase. Maximum $[\text{Cl}^-]$ is associated with the buried fragipans, and the Cl^- depth profile illustrates gradual changes in $[\text{Cl}^-]$. A greater degree of profile overprinting is observed at this landscape position. Hence, boundaries between Eb and fragipan horizons are more diffuse, resulting in depth profiles with smoother lines compared to the summit (Fig. 2.2 and 2.3).

In the valley, morphology of the Cl^- depth profile reflects changes in strata, but is also influenced by multiple perched water tables. An abrupt increase in $[\text{Cl}^-]$

from 5 to 90 mg L⁻¹ is associated with the restrictive layer 1.00 m below the soil surface (Fig. 2.4). A similar [Cl⁻] peak reflects a stratigraphic boundary at around 3.00 m. In addition to the near-surface perched water table at 0.50 m, as many as three zones of perched water are present in lowland positions located at 1.25, 2.50, and 8.00 m (Boll et al., 2001).

Chloride depth profiles can be used to identify hydro-stratigraphic units within the hillslope. At each sampling location, E horizons that overlie the uppermost fragipan display low [Cl⁻]s because this is where water contents are highest (Figs. 2.2-2.4). Water contents decrease below the uppermost fragipan in the upland positions, and high [Cl⁻]s are found in multiple paleosols (Figs. 2.2 & 2.3). [Cl⁻]s appear to be diluted or leached by perched water in the valley (Fig 2.4).

Additionally, a thick Eb horizon characterized by low [Cl⁻], is present between 2 and 3 m at the summit and valley, and 5 to 6 m at the side slope position (Figs. 2.2-2.4).

To assess relationships between individual stratigraphic measurements and Cl⁻ depth profiles, we correlated the vertical change in [Cl⁻] with the vertical change in clay, strength, and Mn_d:Fe_d (Table 2.2). In the upland positions, correlations of change in [Cl⁻] vs. change in clay and strength with depth are significant at the 0.01 and 0.05 levels. Change in [Cl⁻] was not significantly correlated with changes in Mn_d:Fe_d ratios (Table 2.2) probably because these ratios tend to change across horizon boundaries and do not necessarily remain constant within a horizon. The vertical distribution of secondary CBD-extractable

Mn and Fe has been affected by saturated flow that may have only occurred when the unit was near the land surface (O'Geen et al., 2001).

Changes in $[Cl^-]$ were not significantly related to stratigraphic measurements the valley position (Table 2.2). This lack of correlation is due to the dynamic hydrology of this position where ground water mounds extend into the lowermost fragipan and multiple perched water tables occur (O'Geen et al., 2001). In fact, peaks in $[Cl^-]$ within the valley core may reflect the transport of near-surface perched water from surrounding uplands, which perhaps explains why $[Cl^-]$ is significantly correlated to water content in the upper 4 m of the valley position (Table 2.2).

Table 2.2. Correlation of the vertical change in measured stratigraphic variables with pore-water Cl^- concentrations in a Palouse hillslope.

Variable	Summit	Side slope	Valley
	<i>r</i>		
Clay	0.914***	0.333**	0.098
Strength	0.391**	0.334**	0.046
Mn _d :Fe _d	0.159	0.055	-0.337
Water content	-0.452**	0.030	0.304*

***, **, * indicate significance at the 0.01, 0.05, and 0.10 levels, respectively. Data for the upper 4 m of loess were used at the valley position.

Mechanisms of recharge

Multiple buried soils with contrasting hydraulic properties within deep strata control the path of percolating water and therefore influence morphology of Cl^- depth profiles (Figs. 2.2-2.4). In the eastern Palouse region, rooting depth is limited to horizons that overlie the fragipan. Cracks in the fragipan extend only into the upper portions of the pan. Based on our understanding of the pedologic and depositional environment, we interpret zones of Cl^- -rich pore water that are

below the active rooting depth to represent "old" water that resides in deep sediment. Evidence from field observations and deep-well monitoring indicates that perched water tables do not exist below the uppermost fragipan in uplands (Boll et al., 2001). Moreover, secondary calcium carbonate coatings present below the uppermost fragipan indicate that little vertical flushing of water through the soil matrix has occurred at the summit position. Since a majority of saturated flow is redistributed downslope (Brooks et al., 2000), vertical movement of Cl^- -rich water must occur slowly as unsaturated flow and this water may reside in buried paleosol fragipans for extended periods of time.

Several studies have associated large increases in $[\text{Cl}^-]$ with long pore-water residence times at the lower boundary of the root zone (Stone, 1992; Allison et al., 1994; Tyler and Walker, 1994). In our case, we postulate that peaks in $[\text{Cl}^-]$ are relicts from times when these units were near the land surface. Cl^- deposition has remained constant over the last 15,000 years in the Palouse region and weathering of primary minerals in Palouse loess does not release significant Cl^- (Murphy et al., 1996). Therefore, duration of landscape stability and degree of evapotranspiration govern the extent of Cl^- accumulation within a horizon when the unit represented the land surface. In fact, buried paleosols in the Palouse are believed to have formed under conditions drier than present during periods of extended landscape stability (Kemp et al., 1998).

Similar processes likely influence Cl^- accumulation in valley positions, but multiple perched water tables complicate interpretation of Cl^- depth profiles. Monitoring of deep wells indicates that the ground water table extends to the

basal fragipan around 4-m below the soil surface. Piezometers installed below the uppermost fragipan indicate confined perched water tables around 1.5 and 2.5-m below the surface. Abrupt decreases in $[Cl^-]$ at 1.2 and 3.0 m may reflect boundaries of the ground water table and confined perched water tables (Fig. 2.4). There is insufficient evidence, however, to explain the complex hydraulic processes responsible for these observations.

Recharge estimates

If old water resides in buried paleosols, changes in recharge rates associated with climatic swings of the Holocene or late Pleistocene may be preserved. In order to estimate recharge rates through time we plotted cumulative water as a function of Cl^- inventory (Fig. 2.5). Slopes of straight-line segments represent reciprocals of $[Cl^-]$ for a particular depth interval (Selker et al., 1999). Straight-line segments reflect episodes of relatively constant precipitation and Cl^- deposition, thus recharge rates can be calculated for these particular depth intervals (Murphy et al., 1996; Selker et al., 1999).

Plots of cumulative Cl^- vs. cumulative water at the summit and side slope positions illustrate a characteristic stair-step appearance that corresponds to stratigraphic changes (Fig. 2.5). Recharge estimates are highest (3 mm y^{-1} and 6 mm y^{-1}) in a well-developed buried E horizon located 2 m below the surface at the summit and 4.75 m at the side slope. In addition, the lowest recharge rates (1 mm y^{-1}) are preserved in buried fragipans (Fig 2.5).

Estimates of recharge in uplands probably reflect maximum rates because we can not assess the dilution effects associated with the formation and lateral

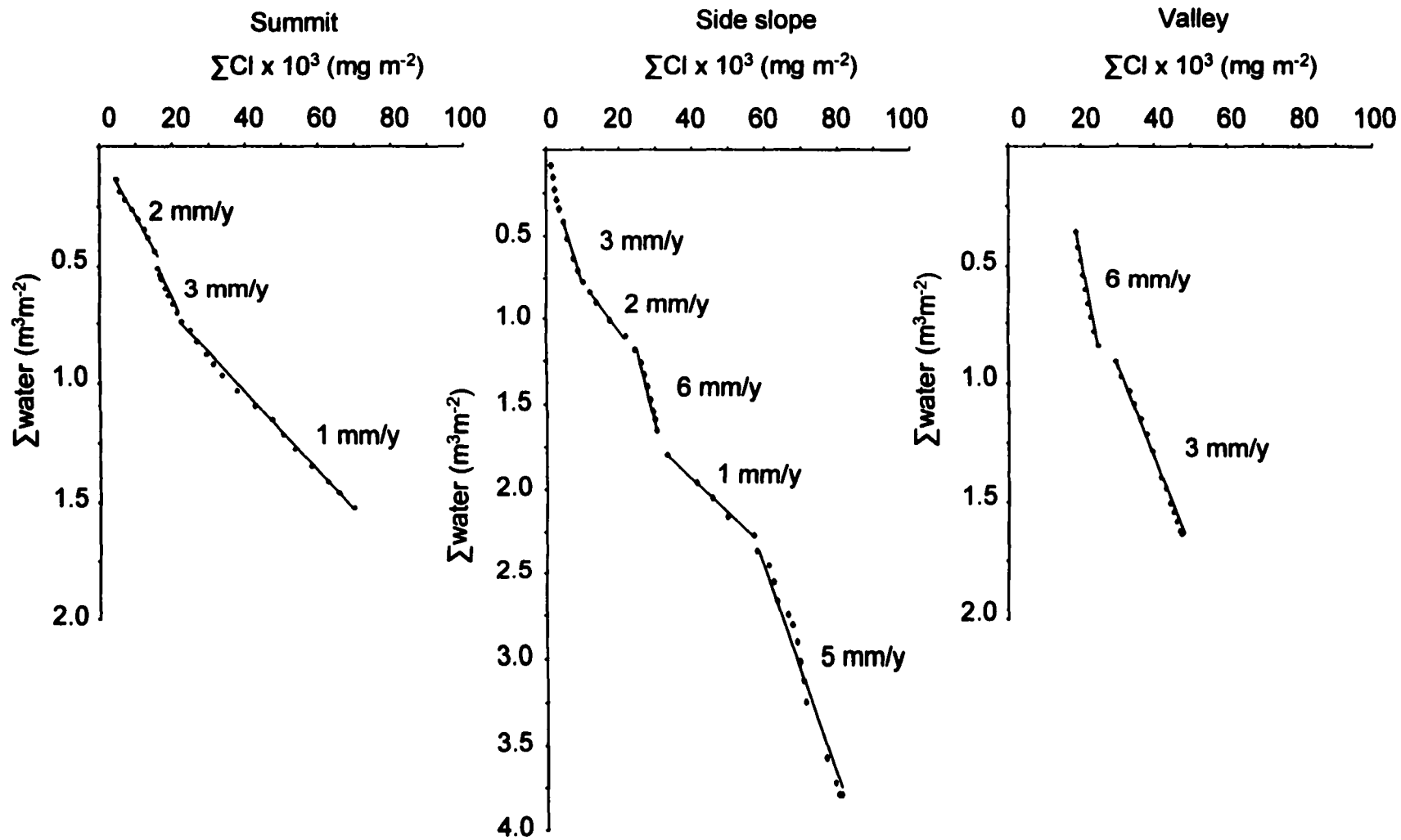


Figure 2.5. Recharge rates calculated from water inventory vs. chloride inventory. Linear-line segments represent constant chloride accumulation.

redistribution of perched water. In upland positions, Cl^- is concentrated in the root zone during the growing season, but is likely redistributed as lateral flow in perched water tables to valley positions in the winter months. Furthermore, the presence of pedogenic CaCO_3 in the summit position located at 2 m having a radiocarbon age of 9,220 years BP suggests even longer pore-water residence times. Discrepancies in pore-water residence time and pedogenic carbonate dates further indicate that Cl^- -bearing strata represent Cl^- accumulation at discrete intervals through time and the profile as whole does not reflect a continuous chronological sequence of Cl^- accumulation.

Conclusions

Results of this study illustrate how Cl^- concentration varies with depth and pedo-stratigraphic boundaries in the vadose zone. Abrupt changes in $[\text{Cl}^-]$ occur across boundaries between buried Eb and paleo-fragipan horizons because these boundaries impose hydro-stratigraphic barriers that restrict vertical flow. Moreover, the abrupt changes in $[\text{Cl}^-]$ at upland sites may indicate that water is “trapped” in buried, hydraulically restrictive horizons. Calculations of diffusion rates using Fick’s law, however, suggest that abrupt concentration boundaries can only persist for decades rather than hundreds of years (Appendix 4). The partially diluted signature of the valley site illustrates hydraulically active conditions. Understanding variability of regolith is important to assess hydrologic processes in the vadose zone. Cl^- depth profiles can be used as a relatively simple technique to characterize hydro-stratigraphic units in deep regolith. We

know of no other single technique that can be so easily used to characterize hydro-stratigraphy within the vadose zone.

References

- Allison, G.B., G.W. Gee and S.W. Tyler, 1994. Vadose-zone techniques for estimating groundwater recharge in arid and semiarid regions. *Soil Sci. Soc. Am. J.* 58:6-14.
- Baker, V.R., B.N. Bjornstad, A.J. Busacca, K.R. Fecht, E.P. Kiver, U.L. Moody, J.G. Rigby, D.F. Stradling and A.M. Tallman, 1991. Quaternary geology of the Columbia Plateau. P. 215-250. *In* R.B. Morrison (ed.) Quaternary nonglacial geology: Conterminous U.S. The geology of North America, Vol. K-2 Geol. Soc. Am., Boulder, CO.
- Boll, J., P. McDaniel, E. Brooks, J. Linard and S. Barndt, 2001. Hydrologic characterization of perched water systems: from hillslope to watershed scale. *In* Annual Abstracts. Soil Science Soc. Am. Charlotte, NC.
- Brooks, E.S., P.A. McDaniel and J. Boll, 2000. Hydrologic modeling in watersheds of the eastern Palouse: Estimation of subsurface flow conditions. Presented at the 2000 Pacific Northwest Region Meeting, Paper no. PNW2000-10. ASAE, St. Joseph, MI.
- Busacca, A.J., 1989. Long Quaternary record in eastern Washington, USA, interpreted from multiple buried paleosols in loess. *Geoderma* 45:105-122.
- Ciolkosz E.J., W.J. Waltman and N.C. Thurman, 1995. Fragipans in Pennsylvania soils. *Soil Surv. Horiz.* 36:5-20.

- Cook, P.G., W.M. Edmunds and C.B. Gaye, 1992. Estimating paleorecharge and paleoclimate from unsaturated zone profiles. *Water Resour. Res.* 28:2721-2732.
- Day, R.L., M.A. Calmon, J.M. Stiteler, J.D. Jabro and R.L. Cunningham, 1998. Water balance and flow patterns in a fragipan using in situ soil block. *Soil Sci.* 163:517-528.
- Ericksson, E. and V. Khunakasem, 1969. Chloride concentration in groundwater, recharge rate and rate of deposition of chloride in the Israel Coastal Plain. *J. Hydrol.* 7:178-197.
- Gee, G.W. and J.W. Bauder, 1986. Particle-size analysis. P383-411. In A. Klute (ed.) *Methods of soil analysis. Part 1.* 2nd ed. Agron. Monogr. 9. ASA and SSSA, Madison, WI.
- Hendry, M.J., L.I. Wassenaar and T. Kotzer, 2000. Chloride and chlorine isotopes (^{36}Cl and $\delta^{37}\text{Cl}$) as tracers of solute migration in a thick, clay-rich aquitard system. *Water Resour. Res.* 36:285-296.
- Johnston, C.D., 1987. Preferred water flow and localized recharge in a variable regolith. *J. Hydrol.* 94:129-142.
- Kemp, R.A., P.A. McDaniel and A.J. Busacca, 1998. Genesis and relationship of macromorphology and micromorphology to contemporary hydrological conditions of a welded Argixeroll from the Palouse in NW, USA. *Geoderma* 83: 309-329.

- King, M., 2000. Late Quaternary loess-paleosol sequences in the Palouse, Northwest USA: pedosedimentary and paleoclimatic significance. Ph.D. thesis. Univ. of London Royal Holloway.
- McDaniel, P.A., G.R. Bathke, S.W. Buol, D.K. Cassel and A.L. Falen, 1992. Secondary manganese/iron ratios as pedochemical indicators of field-scale throughflow water movement. *Soil Sci. Soc. Am. J.* 56:1211-1217.
- McDaniel, P.A. and A.L. Falen, 1994. Temporal and spatial patterns of episaturation in a Fragixeralf landscape. *Soil Sci. Soc. Am. J.* 58:1451-1457.
- McDaniel, P.A., R.W. Gabehart, A.L. Falen, J.E. Hammel and R.J. Reuter, 2001. Perched water tables on Argixeroll and Fragixeralf hillslopes. *Soil Sci. Soc. Am. J.* 65:805-810.
- Murphy, E.M., T.R. Ginn and J.L. Phillips, 1996. Geochemical estimates of paleorecharge in the Pasco Basin: Evaluation of the chloride mass balance technique. *Water Resour. Res.* 32:2853-2868.
- O'Brien, R., C.K. Keller and J.L. Smith, 1996. Multiple tracers of shallow ground-water flow and recharge in hilly loess. *Ground Water* 34:675-682.
- O'Geen, A.T., J. Boll, E.S. Brooks, J.I. Linard, P.A. McDaniel, J.B. Sisson and A. Wylie, 2001. Detection of multiple perched water tables using natural tracers and multilevel tensiometers in deep loess. *EOS Trans. AGU* 82 p.47 Fall Meet. Suppl. Abstract H52A-0383, San Francisco, CA.
- Parlange, M.B., T.S. Steenhuis, D.J. Timlin, F. Stagnitti and R.B. Bryant, 1989. Subsurface flow above a fragipan horizon. *Soil Sci.* 148:77-86.

- Phillips, F.M., 1994. Environmental tracers for water movement in desert soils of the American Southwest. *Soil Sci. Soc. Am. J.* 58:15-24.
- Reuter, R.J., P.A. McDaniel, J.E. Hammel and A.L. Falen, 1998. Solute transport in seasonal perched water tables in loess-derived soils. *Soil Sci. Soc. Am. J.* 62:977-983.
- Scanlon, B.R., 1992. Moisture and solute flux along preferred pathways characterized by fissured sediments in desert soils. *J. Contam. Hydrol.* 10:19-46.
- Selker, J.S., C.K. Keller and J.T. McCord, 1999. *Vadose zone processes*. CRC Press. Boca Raton, FL.
- Soil Conservation Service, 1972. *Soil survey laboratory methods and procedures for collecting soil samples*. Soil Surv. Invest. Rep. 1. U.S. Gov. Print. Office, Washington, DC.
- Soil Survey Staff, 1993. *Soil Survey Manual*. USDA-SCS Agric. Handb. 18. U.S. Gov. Print. Office, Washington, D.C.
- Soil Survey Staff, 1999. *Keys to soil taxonomy*, 8th Ed. USDA-NRCS. Washington, D.C.
- Stone, W.J., 1992. Paleohydrologic implications of some deep soil water chloride profiles, Murray Basin, South Australia. *J. Hydrol.* 132:201-223.
- Tyler, S.W. and G.R. Walker, 1994. Root zone effects on tracer migration in arid zones. *Soil Sci. Soc. Am. J.* 58:25-31.

Van Vliet, B. and R. Langohr, 1981. Correlation between fragipans and permafrost with special reference to silty Weishselian deposits in Belgium and northern France. Catena 8:137-154.

CHAPTER 3

PALEOSOLS AS DEEP REGOLITH: IMPLICATIONS FOR GROUND-WATER RECHARGE ACROSS A LOESSIAL CLIMOSEQUENCE

Abstract

Thick loess deposits consisting of paleosol sequences comprise the deep regolith of the Palouse region in eastern Washington and northern Idaho. Ground water is the principal water supply for the Palouse Basin, yet recharge mechanisms and rates through this regolith are poorly understood. Forecasting the sustainability of the water supply has been hampered because models that predict ground-water recharge are complicated by deep regolith that has complex stratigraphy and, in some instances, multiple buried hydraulically restrictive horizons. To assess water movement, pore-water Cl^- and $\delta^{18}\text{O}$ distributions were measured to 6-m depths in three catchments representing a climosequence across the Basin, and interpreted using catchment and basin-wide stratigraphic relationships. Vertical facies between dense and soft horizons coincide with variations in $[\text{Cl}^-]$. In the eastern Basin, pore-water $[\text{Cl}^-]$ ranged from 15 to 150 mg/L and increased with depth. In addition, shifts in isotopic signature of oxygen in pore water coincide with Cl^- -rich horizons, and suggest long pore-water residence times. In contrast, $[\text{Cl}^-]$ in the central and western Basin ranges from 1 to 15 mg/L and changes little with depth. Tracer profiles illustrate three major hydrostratigraphic units in the Basin: 1) uplands with relatively homogeneous regolith that has short pore-water residence times; 2) uplands with

heterogeneous regolith that has long pore-water residence times; and 3) valleys with heterogeneous regolith that display dynamic hydraulic processes. Regional relationships between deep regolith and surface soils were established in order to use the SSURGO database to estimate the spatial extent of each hydrostratigraphic unit. The degree of paleosol development mimics that of contemporary soils across the climosequence. Results indicate that recharge may be less than 1 mm yr⁻¹ in 33% of the study area where precipitation is greatest and regolith is heterogeneous. Recharge increases to 1 mm yr⁻¹ in 37% of the study area where regolith is homogeneous. Valley positions having active hydraulic regimes constitute 10% of the Basin.

Introduction

A thick mantle of loess blankets over 75 percent of the Palouse Basin in eastern Washington and northern Idaho (Williams and Allman, 1969) (Fig. 3.1). As is the case with most wind-transported parent materials, loess deposits are well sorted, resulting in a relatively uniform porous medium. The rate of soil development, however, strongly influences regolith heterogeneity; hence, hydraulic properties of loessial hillslopes can vary across spatial and temporal scales. As a result, deep regolith of the Palouse Basin consists of a complex vertical sequence of superimposed and over-printed paleosols that in some cases extend to a depth of 75 m (Busacca, 1989; McDonald and Busacca, 1992; Kemp et al., 1998).

Communities in the Palouse Basin rely on ground water as the principal water supply. Municipal water use has resulted in a continual decline in the regional

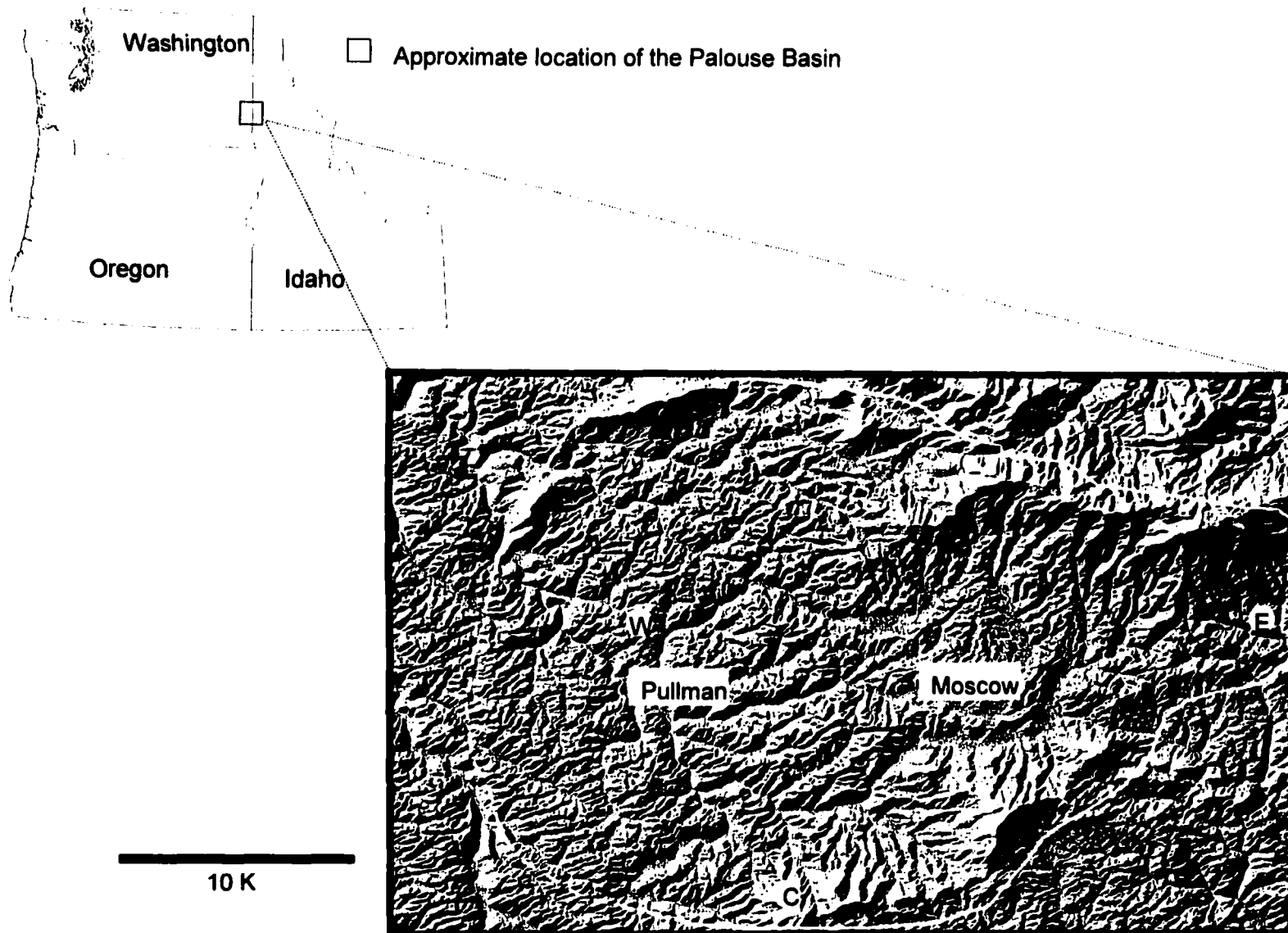


Figure 3.1. Digital elevation model of the Palouse Basin and its location in the Pacific Northwest. Western, central, and eastern Basin study sites are indicated using the letters W, C, and E respectively. Approximate physiographic boundary of the Basin is indicated by the white line.

basalt aquifer system since 1890, and a steady decrease of 0.45 ft per year in response to pumping from 1976 to 1985 (Barker, 1979). Existing ground-water recharge models for the Palouse Basin predict an unsustainable ground-water resource. Moreover, these models assume that the loessial regolith is a single homogenous and isotropic unit. To better evaluate the sustainability of this resource, an understanding of relationships between hydrological processes and deep-regolith stratigraphy is necessary.

The Palouse region extends across a broad climatic gradient and therefore hydraulic properties of deep regolith vary significantly. For example, in arid regions of central Washington environmental tracers were used to identify long pore-water residence times that ranged from 13,000 to 28,000 years (Murphy et al., 1996). In semiarid regions of the western Palouse Basin, Cl^- mass balance techniques revealed recharge rates that range from 0.3 cm y^{-1} at the summit to $2\text{--}3 \text{ cm y}^{-1}$ at mid- and toe-slope positions (O'Brien et al., 1996). Long-term hydrographs of deep monitoring wells in the western Palouse Basin indicate that ground-water recharge occurs during the winter months, and likely through hydraulically continuous worm-like channels extending vertically over 15 m (Williams and Allman, 1969). Current recharge models suggest that deep percolation is greatest in the east where mean annual precipitation is greatest (Lum et al., 1990).

Soil stratigraphic relationships dramatically affect near-surface hydrological processes and the resulting redistribution of precipitation in the eastern Palouse Basin (McDaniel and Falen, 1994; Reuter et al., 1998; McDaniel et al., 2001).

Observations of perched water table dynamics indicate that water moves laterally as throughflow in more permeable Ap and Bw horizons (Reuter et al., 1998; McDaniel et al., 2001). Measured saturated hydraulic conductivity values range from 0.06 to 0.9 cm d⁻¹ in restrictive horizons and 14 to 129 cm d⁻¹ in Ap and Bw horizons (McDaniel et al., 2001; Reuter et al., 1998). As a result, up to 90% of incident precipitation is redistributed as lateral throughflow (Brooks et al., 2000).

Regional trends in hydraulic characteristics of deep regolith appear to be driven by the pedogenic character of soils and buried paleosols. Studies have documented relationships between stratigraphic characteristics and natural tracers used to estimate water flux. For example, in Australia, steep concentration gradients of Cl⁻ depth profiles were recognized as reflecting boundaries between different stratigraphic units (Johnston, 1987). In addition, Hendry et al. (2000) identified distinct Cl⁻ signatures in different geologic units within a saturated aquitard. Stable isotopes and Cl⁻ depth profiles were used to identify spatially uniform water fluxes in areas with homogeneous soils and to identify changes in water flux that coincided with changes in soil stratigraphy (Newman et al., 1997). Eriksson and Khunakasem (1969) discovered that spatial variability of recharge rates calculated from Cl⁻ mass balance in ground water was related to general trends in the distribution of soils. Based on these observations, it is possible that stratigraphic relationships can be used as a scaling mechanism to extrapolate from profile- to basin-wide scales.

Regional concerns regarding sustainability of ground water in the Palouse Basin have fueled a need to identify Basin-wide hydrologic processes in soils and

deep vadose zones. Soil survey databases are an excellent source of geographic data in this region, but are not designed to provide spatial information regarding processes in deep regolith. However, if relationships between deep regolith and surface soils are established, then soil survey databases can be used as a powerful spatial scaling mechanism. Our approach was to link the following research objectives in order to evaluate regional hydrologic relationships of deep regolith: 1) assess the ability of soil/paleosol sequences to accommodate deep percolation across the Basin using environmental tracers such as Cl^- and $\delta^{18}\text{O}$; 2) identify the spatial distribution of hydraulically significant, pedo-stratigraphic relationships between contemporary sola and deep regolith that are controlled by the existing climosequence; and 3) extract and retrieve these hydraulically significant relationships between deep regolith and contemporary sola from the USDA-NRCS Soil Survey Geographic (SSURGO) spatial database to scale recharge estimates Basin wide.

Materials and Methods

Environmental setting

The Palouse Basin is a 60,000 ha area situated in northern Idaho and eastern Washington (Fig. 3.1). The Basin consists of a landscape of rolling hillslopes that formed as a result of loess accumulation over the last two million years (Busacca, 1989; Baker et al., 1991). Loess thickness varies from up to 75 m in the west to less than 10 m in the eastern portion of the Basin.

A strong climatic gradient exists across the Basin, and controls the degree of soil development. Isohyets of precipitation are parallel to each other, and mean

annual precipitation (MAP) increases from ~450 mm in the west to over 750 mm in the east. Precipitation falls predominantly during the winter months. Soils with weak calcic, cambic, argillic, and albic horizons dominate the western and central portions of the Basin where MAP ranges from 450 mm to 650 mm. Soils with strong albic, argillic, and fragipan horizons dominate the eastern portion of the Basin where MAP exceeds 650 mm (Busacca, 1989).

Core collection

We selected three 2-5 ha catchments in the western, central, and eastern Basin that reflect regional differences in soils, loess thickness, and mean annual precipitation (MAP) (Fig. 3.1). Three hillslope positions were sampled at each catchment using a tractor-mounted hollow-stem auger and a 6-m extension hand auger. All cores were sampled during the summer months (May-September) at summit, side slope, and valley positions. Two cores were collected at each slope position. For stable-isotope analysis, hand-auger samples were collected in 25- to 50-cm increments, sealed in Nalgene[®] containers, and frozen immediately until analyzed for pore-water $\delta^{18}\text{O}$. For Cl^- and stratigraphic analysis, cores were collected using a tractor mounted hollow-stem auger and were sectioned in to 20-cm increments, sealed in zip-lock bags, and frozen until analyzed.

Chloride

In the laboratory, cores were split longitudinally providing samples for stratigraphic description and for extraction of pore-water Cl^- . Gravimetric water content was determined for all samples prior to Cl^- extraction. After samples were oven dry, 20 g of sediment were mixed with 20 mL of triple distilled water and

shaken overnight. Samples were centrifuged at 2500 RPM for 30 minutes, and supernatant solution was filtered through a 0.22- μm Millipore® filter. Chloride concentration was measured in triplicate using a Dionex ion chromatograph, and pore-water $[\text{Cl}^-]$ was calculated using gravimetric water content (Murphy et al., 1996).

The chloride mass balance method (CMB) was used to calculate recharge rates from plots of cumulative water vs. cumulative Cl^- (Selker et al., 1999). Several assumptions are necessary to apply this technique: 1) water movement occurs as piston flow; 2) atmospheric Cl^- deposition has remained constant through time and is the sole source of Cl^- ; 3) Cl^- is an inert tracer, and 4) plant uptake is minimal (Allison et al., 1994). Recharge can then be estimated using the following equation:

$$R = (C_p \times P)/C_r$$

Where: R = recharge

C_p = average $[\text{Cl}^-]$ in precipitation

P = mean annual precipitation

C_r = average $[\text{Cl}^-]$ in pore water

Mean pore-water residence time (MRT) at a given depth can be estimated by:

$$\text{MRT} = C_{ri}/q_{ac}$$

where MRT is in years, C_{ri} is the cumulative Cl pool from ground surface to a given depth in mg m^{-2} , and q_{ac} is the accumulation flux in $\text{mg m}^{-2} \text{ yr}^{-1}$ (Selker et al. 1999). For all sites a C_p value of 0.09 mg L^{-1} was used to calculate q_{ac} and

determined for the region by the National Atmospheric Deposition Program [1985-1991].

Stable isotopes

Stable-isotope analyses were performed at the University of Idaho Stable Isotope Laboratory. A direct-CO₂ equilibration technique was used to measure the oxygen isotope signature ($\delta^{18}\text{O}$) of pore water (Scrimgeour, 1995; Hsieh et al., 1998). The method involves the equilibration of a soil sample with a known pressure and isotopic signature of CO₂ for several days at 25° C. After equilibration, an aliquot of the gas was injected into a Finnigan-Mat Delta-Plus stable-isotope-ratio mass spectrometer. The original $\delta^{18}\text{O}$ signature of pore water was determined using a mass balance calculation (Hsieh et al., 1998). Values of ^{18}O analysis were reported in delta (δ) notation as per mil (‰) deviations relative to the Vienna-Standard Mean Ocean Water (VSMOW) international standard. The analytical precision for the direct-CO₂ $\delta^{18}\text{O}$ analysis was $\pm 0.5\text{‰}$. Samples of A horizons display much poorer precision due to microbial decomposition of organic matter, which produces CO₂, and therefore we did not include these data.

In many instances the source of percolating water (glacial precipitation, snow melt, monsoon rains, or evaporated water) can be identified through its isotopic signature (Newman et al., 1997). Isotopes of oxygen such as ^{18}O and ^{16}O display different chemical and physical behavior based on slight differences in mass. In the case of water, physical processes that facilitate change in phase result in fractionation of the relative proportions of ^{18}O and ^{16}O in a water molecule. Thus

the $\delta^{18}\text{O}$ signature of precipitation is influenced by phase changes of water through processes such as evaporation, condensation, and freezing.

Generally speaking the isotopic signature of precipitation displays a global pattern. Precipitation in polar regions is depleted with respect to the heavy isotope (^{18}O) and therefore displays δ -values that are more negative compared to VSMOW (Kendall and Caldwell, 1998). Precipitation of equatorial regions is enriched with respect to ^{18}O and therefore displays δ values near zero. Thus the signature of precipitation is controlled by global weather patterns, temperature, and timing and magnitude of the rain event (Kendall and Caldwell, 1998).

Stratigraphic analysis

Since the degree of soil development appears to control vadose zone hydrology in the Palouse Basin, we attempted to identify pedo-stratigraphic units across each catchment. Strata were differentiated based upon soil horizon and paleosol boundaries using soil morphological field criteria. Soil strength was used as a proxy for brittleness and bulk density, and assessed on peds using a pocket penetrometer, where deformation of the piston spring was recorded and expressed as unconfined compressive strength in kg cm^{-2} .

Results and Discussion

Stratigraphy of the eastern catchment

In the eastern Basin, the upper 6 m of deep regolith consists of a welded sequence of hydraulically restrictive paleosols. We recognized multiple zones of buried paleosol fragipan development through measurements of soil strength and morphological observations. Each zone of fragipan development represents

multiple episodes of soil formation spanning thousands of years in which profiles have superimposed and overprinted into single units (Busacca, 1989). In many cases, buried fragipan horizons are interstratified with subtly expressed eluviated horizons (EBb horizons) that reflect periods of saturation when the horizon was near the land surface (Fig. 3.2).

Trends in hillslope stratigraphy are controlled by topography. A perched water table extends across the catchment above the uppermost fragipan. The most stable landscape position is the summit and therefore buried paleo-fragipans are interstratified with less-dense EBb horizons (Fig. 3.2). Effective precipitation is lowest at the summit due to redistribution of the snowpack by wind. As a result, coatings of CaCO_3 are encountered 2.0 m below the soil surface, representing decalcification of early Holocene loess. A greater degree of profile overprinting is present at the side slope position where erosion rates are high. As a result a thick, welded sequence of paleo-fragipans extends from 1.0 to 5.5 m. A highly eluviated E horizon is present below this unit (Fig. 3.2).

Effective precipitation is greatest at the valley position and as a result dense paleosols have reduced matrix (Fig. 3.2). Zones of saturation are present due to a seasonally high ground-water table and complex stratigraphic relationships with upland strata that may redirect near-surface perched water.

Environmental tracers in the eastern catchment

Stratigraphic relationships among upland positions in the eastern catchment influence the vertical distribution of Cl^- . Both profiles illustrate increases in $[\text{Cl}^-]$ from less than 10 mgL^{-1} near the soil surface to over 100 mgL^{-1} in deep regolith

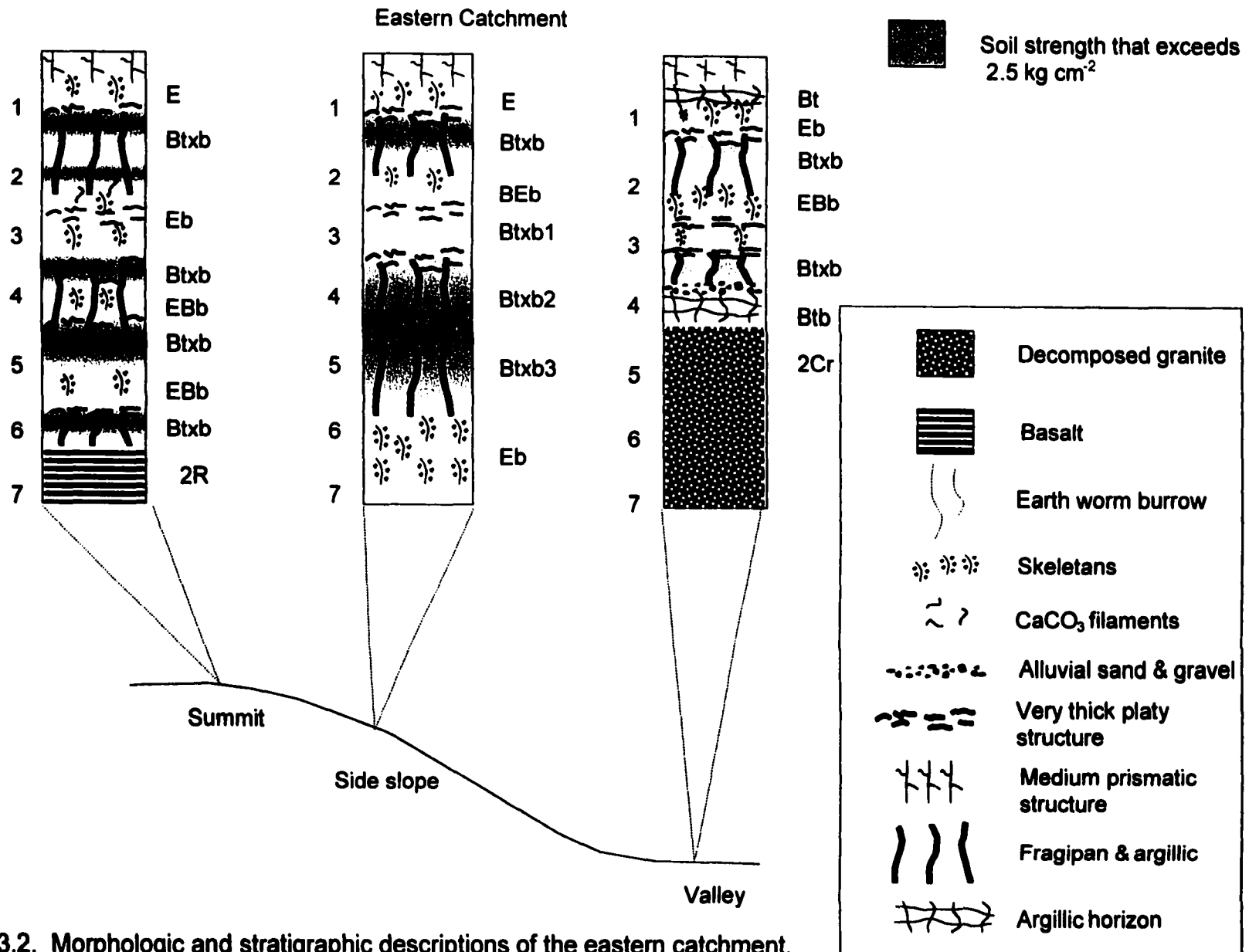


Figure 3.2. Morphologic and stratigraphic descriptions of the eastern catchment.

(Fig. 3.3). Maximum $[Cl^-]$ at summit and side slope positions is associated with a pedo-stratigraphic unit consisting of a sequence of extremely dense paleosol fragipans welded together between 3 and 5 m below the surface (Figs. 3.2 & 3.3). Decreases in $[Cl^-]$ are associated with buried E and EB horizons located at depths of 2.25 and 5.25 m at the summit position and 1.75 and 5.50 m at the side slope position (Figs. 3.2 & 3.3).

The $\delta^{18}O$ depth profiles are similar in upland positions of the eastern Basin catchment. Each profile illustrates a maximum $\delta^{18}O$ -value 1 m below the surface, which is just below the upper boundary of the fragipan. The $\delta^{18}O$ signature of pore water decreases from a maximum value of -10‰ to -11‰ in the uppermost fragipan to a minimum value of -14.5‰ to -15‰ at the base of the core (Fig. 3.3). The most negative values are associated with Cl^- -rich zones of superimposed and overprinted paleosol fragipans located 3-5 m below the surface. Profiles display a 4-5‰ negative shift in $\delta^{18}O$ with increasing depth below the uppermost fragipan (Figs. 3.2 & 3.3). A shift in $\delta^{18}O$ of similar magnitude and direction is observed when comparing shallow aquifers recharged by current precipitation to deep ground water having a ^{14}C age date of 8,000 to 18,000 yr. B.P. (Crosby & Chatters, 1963; Larson et al., 1999). High $[Cl^-]$ and the negative shift in $\delta^{18}O$ signature indicate long pore-water residence times where buried paleosol fragipans contain “old water” precipitated during different climatic regimes.

In the valley, morphology of the Cl^- depth profile is influenced by multiple perched water tables. In addition to the near-surface perched water table at 0.5 m, as many as three zones of perched water are present in lowland positions

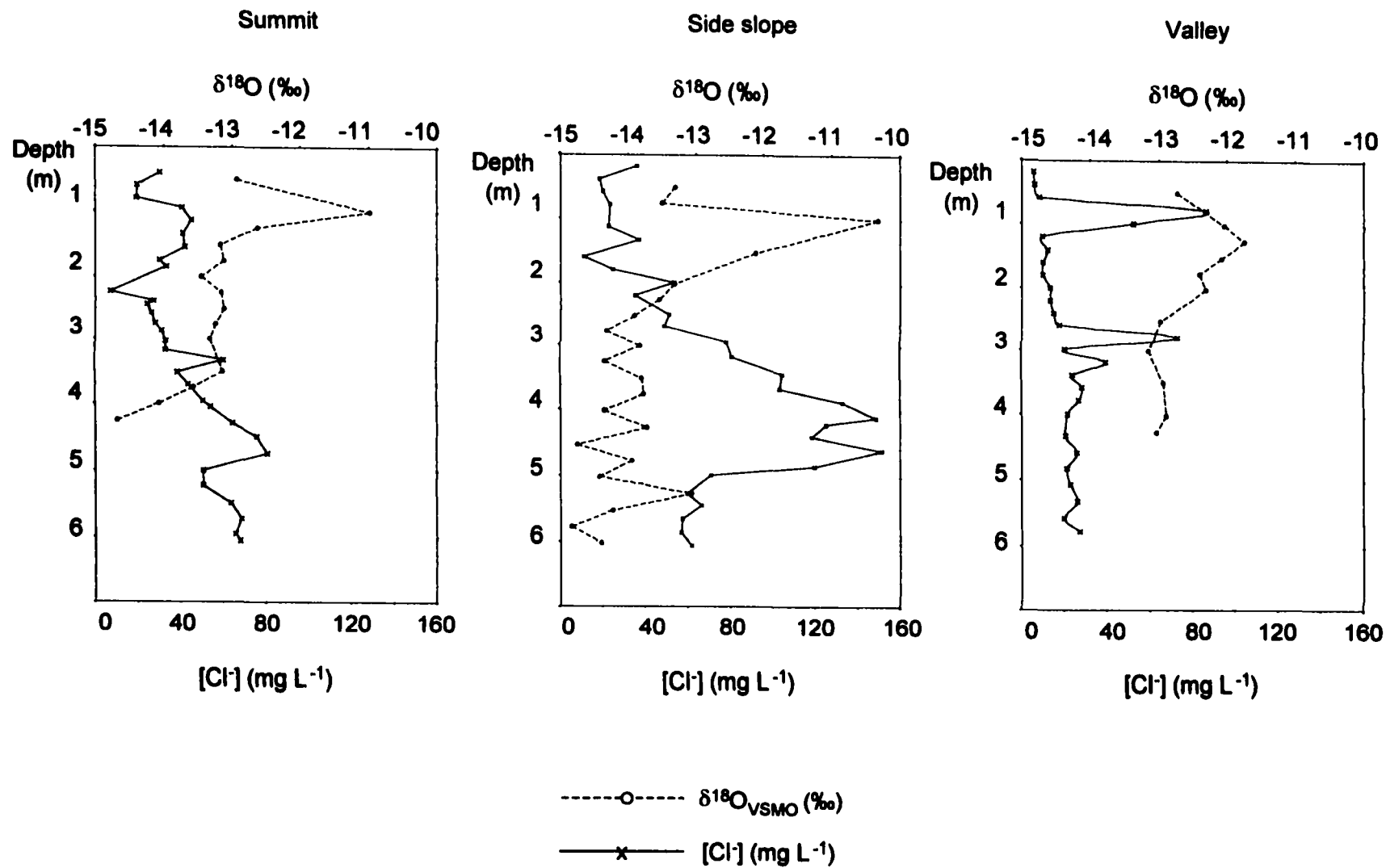


Figure 3.3. Chloride and $\delta^{18}O$ depth profiles at summit, side slope, and valley positions in the eastern catchment.

located at 1.25, 3.0, and 8.00 m (O'Geen et al., 2001). An abrupt increase in $[Cl^-]$ from 5 to 90 mg L⁻¹ is associated with a restrictive layer 1.25 m below the soil surface (Fig. 3.3). A similar $[Cl^-]$ peak reflects a stratigraphic boundary at 3 m.

The $\delta^{18}O$ signature of pore water is different than that of uplands. Although the maximum $\delta^{18}O$ value occurs just below 1 m as is the case in the uplands, the profile displays 1‰ to 1.5‰ negative shift in $\delta^{18}O$, which reflects the isotopic variability of hydrostratigraphic units recharged by contemporary precipitation (Fig. 3.3) (Larson, 1999). These measurements along with observations of multiple perched water tables and reduced horizon matrices indicate a dynamic hydraulic environment.

Stratigraphy of the central catchment

Upland positions of the central Basin display relatively homogeneous regolith in the upper 6 m of loess. Summit positions have well-developed overprinted argillic horizons that extend from 0.5 to 6 m with diffuse horizon boundaries. Side slopes display slightly more heterogeneity. In the solum, a weak albic horizon overlies an argillic horizon having slightly higher soil strength, and extending to 6 m as a continuous welded horizon (Fig. 3.4).

Valleys receive the greatest amount of effective precipitation; therefore, rates of pedogenesis exceed loess deposition rates, which results in heterogeneous deep regolith having abrupt horizon boundaries. A sequence of well-developed argillic and albic horizons occur with depth. Multiple perched water tables were associated with these well-developed horizons (Fig. 3.4).

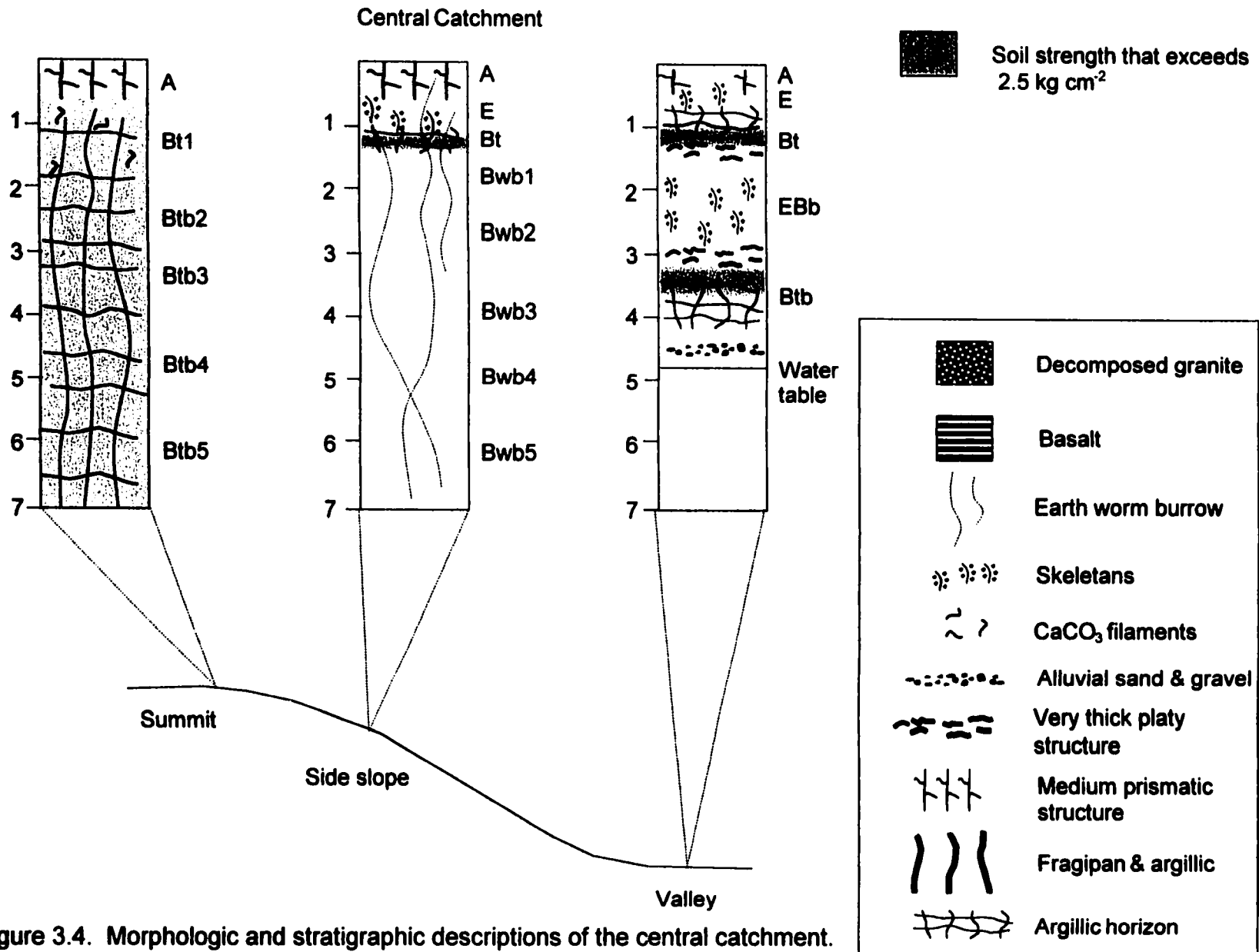


Figure 3.4. Morphologic and stratigraphic descriptions of the central catchment.

Environmental tracers in the central catchment

Tracer profiles in upland positions of the central Basin differ from those of the eastern Basin because deep regolith consists of homogeneous strata with diffuse horizon boundaries. At summit and side slope positions, $[Cl^-]$ is less than 5-10 mg L^{-1} and relatively uniform with depth (Fig. 3.5). The maximum $\delta^{18}O$ values are located 2-3 m below the soil surface, which is 1 m deeper than soils of the eastern Basin. The $\delta^{18}O$ signature of pore water displays a 1‰ to 2‰ negative shift with depth and reflects the isotopic variability of hydraulically active sites such as the valleys of the eastern Basin (Fig. 3.5).

In the valley, the morphology of Cl^- depth profiles resembles valley positions of the eastern Basin. Multiple perched water tables and a high ground-water table correspond to small but abrupt changes in $[Cl^-]$ at depths of 2.25 and 3.25 m (Fig. 3.5). The $\delta^{18}O$ signature of pore water above the water table varies 1‰ to 2‰ and reflects the isotopic variability displayed in hydraulically active sites (Fig. 3.5).

Tracer profiles illustrate evidence for deep percolation in the central Basin. Across the catchment, cumulative $[Cl^-]$ is low, which is indicative of short pore-water residence times. In uplands, the depth to the maximum $\delta^{18}O$ value is 1 m deeper compared to the eastern Basin. This $\delta^{18}O$ maximum could represent a high-intensity rain event or the maximum depth of the evaporative front. The greater depth of this maximum suggests greater permeability in the central Basin. In addition, the low degree of variability in $\delta^{18}O$ reflects contemporary recharge processes.

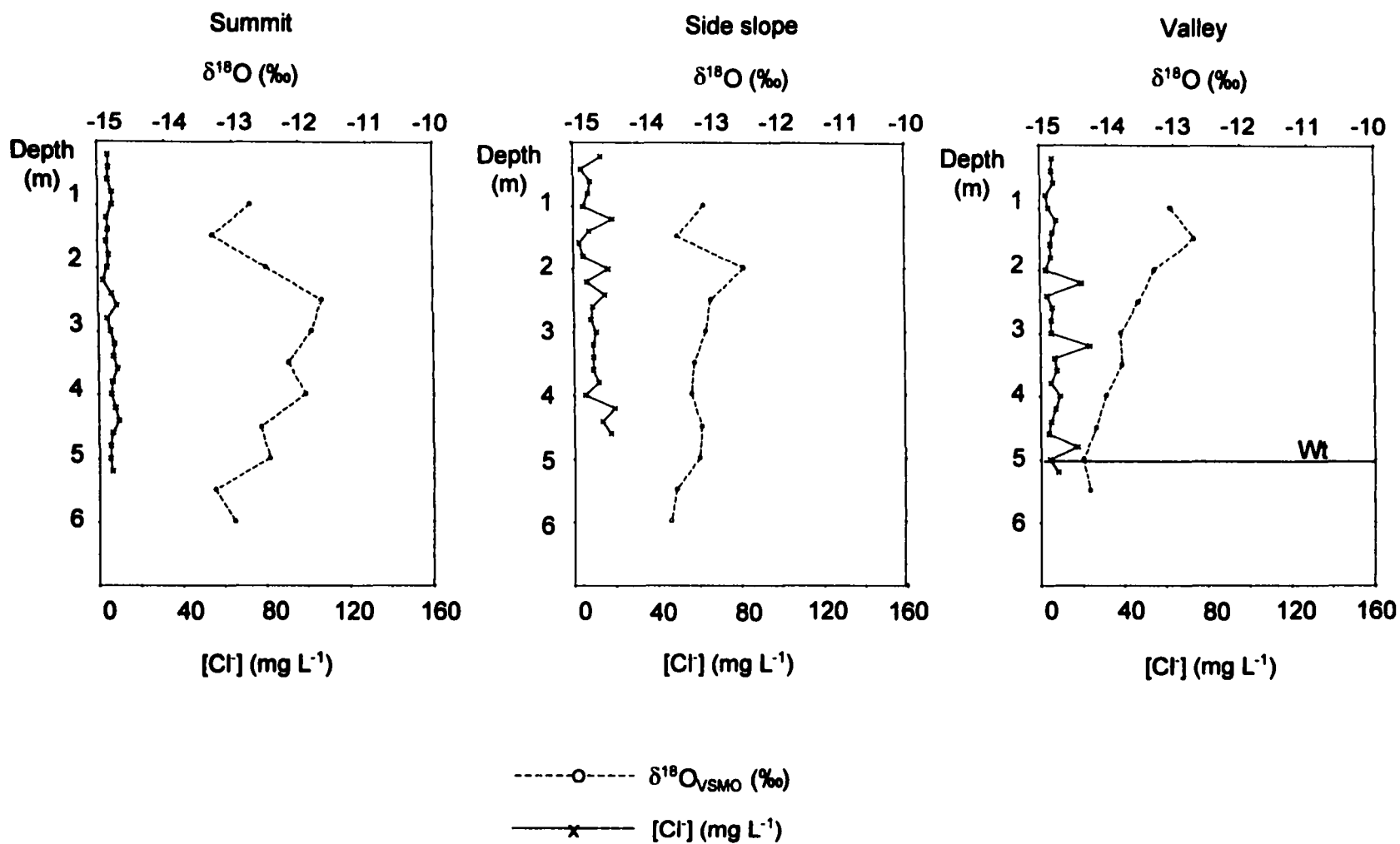


Figure 3.5. Chloride and $\delta^{18}O$ depth profiles at summit, side slope, and valley positions in the central catchment.

Stratigraphy of the western catchment

Stratigraphic relationships with regolith of the western and central Basin are similar. Upland positions display homogeneous deep regolith and valley soils have a sequence of hydraulically restrictive horizons. The summit position supports deep regolith consisting of a continuous overprinted cambic horizon that extends from 0.5 to 6 m with diffuse horizon boundaries. Soft masses of pedogenic carbonate are present in the upper 2 m of regolith (Fig. 3.6). Side slopes display slightly more heterogeneity. In the solum, an albic horizon overlies a weak argillic horizon having slightly higher soil strength, yet deep regolith displays pedogenic character similar to a continuous welded cambic horizon (Fig. 3.6). In addition, both landscape positions contain extensive open channels less than 1 cm in diameter that extend beyond the depths of investigation possibly formed by earthworms or plant roots (Williams and Allman, 1969). Pedo-stratigraphic relationships of valley positions in the western Basin are identical to that of the central Basin, displaying multiple perched water tables with depth (Fig. 3.6).

Environmental tracers in the western catchment

Stratigraphic relationships are similar in regolith of the western and central Basin, and, as a result, environmental tracer depth profiles were also similar. In upland positions, $[Cl^-]$ is low and uniform with depth. The depth to the maximum $\delta^{18}O$ value coincides with that found in the central Basin. Pore water $\delta^{18}O$ depth profiles fluctuated more with depth compared the eastern and central catchments, and displayed 1‰ to 2.5‰ shifts (Fig. 3.7). These vertical

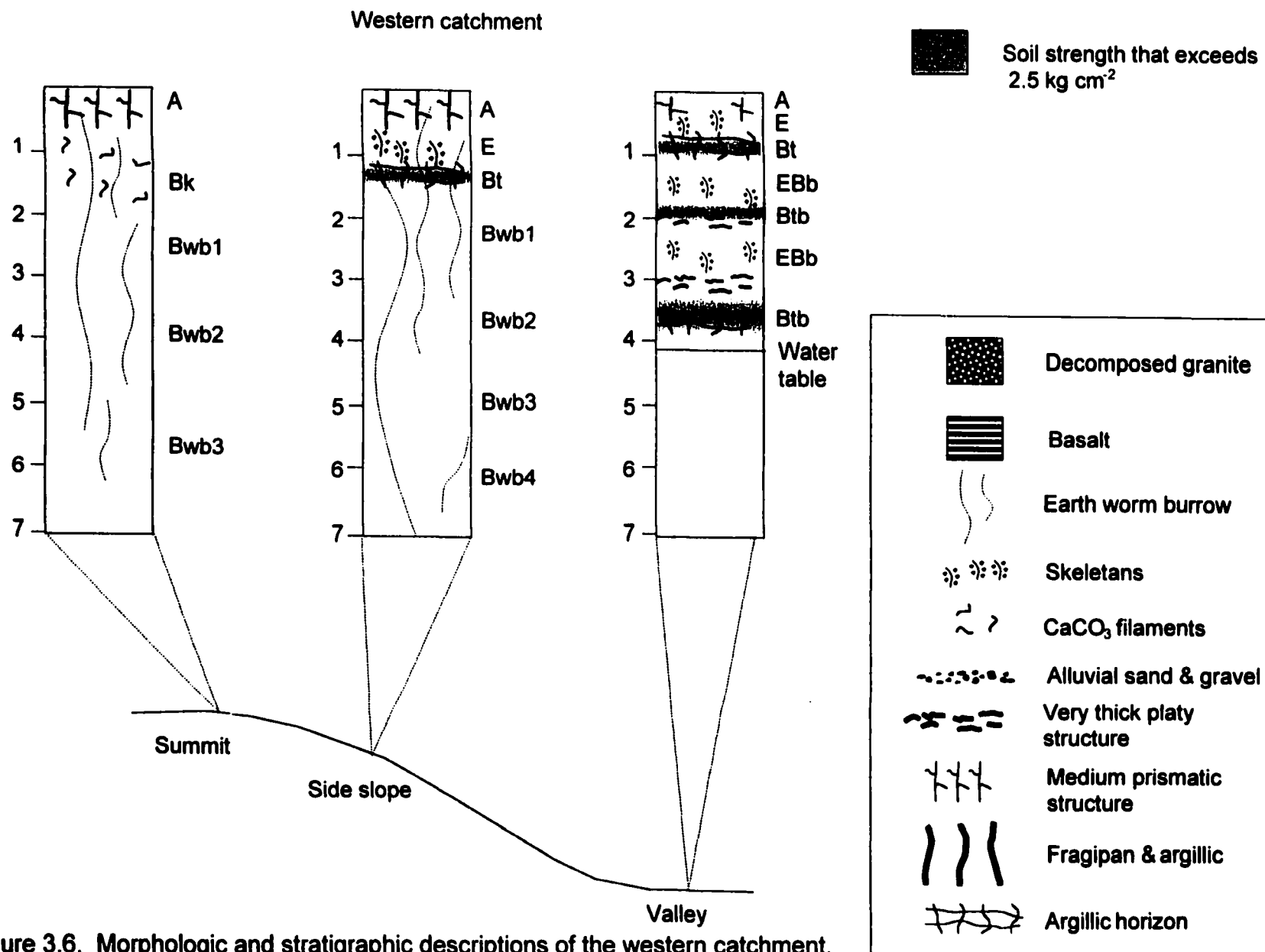


Figure 3.6. Morphologic and stratigraphic descriptions of the western catchment.

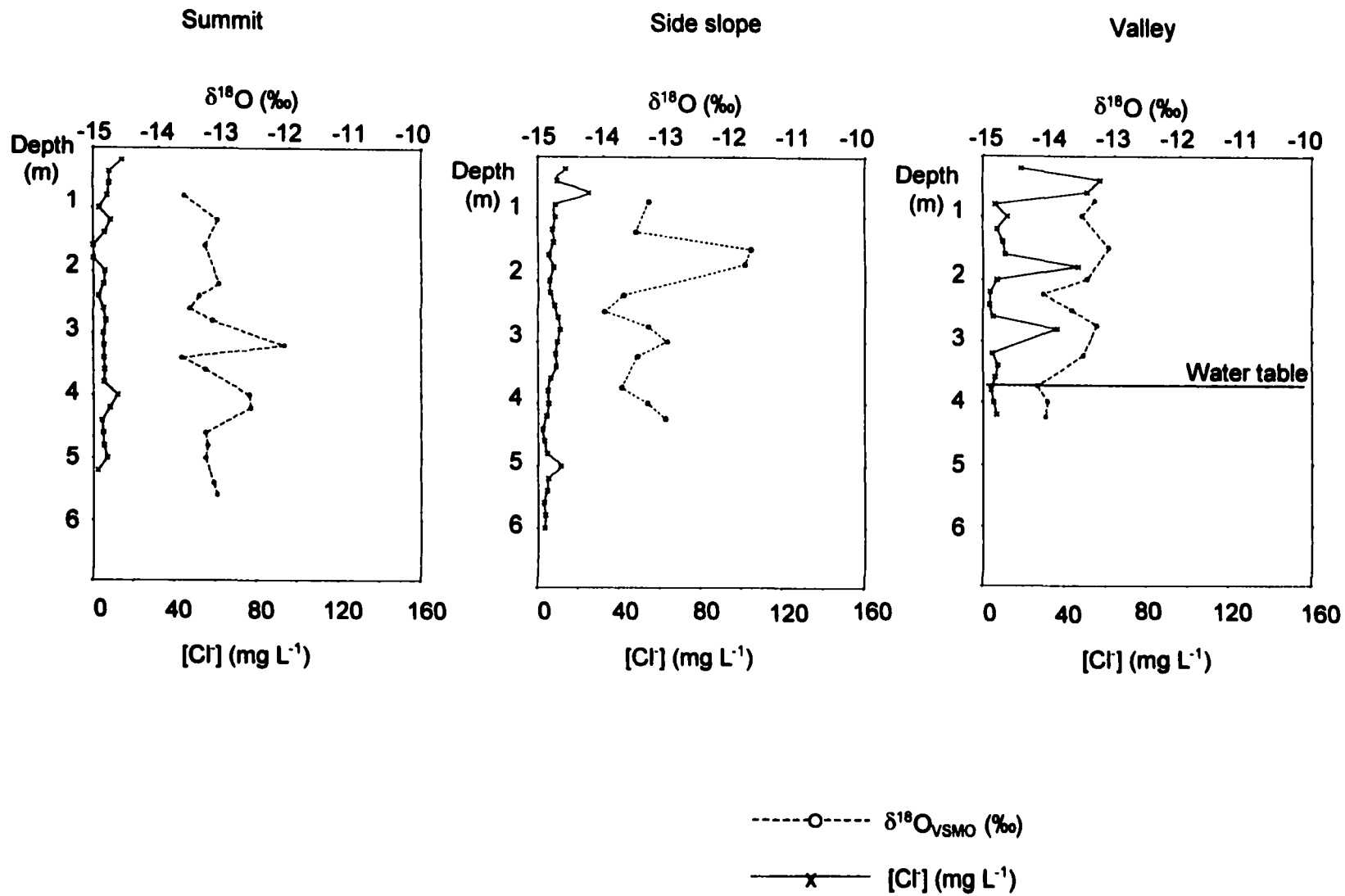


Figure 3.7. Chloride and $\delta^{18}\text{O}$ depth profiles at summit, side slope, and valley positions in the western catchment.

fluctuations in $\delta^{18}\text{O}$ are probably due to the presence of CaCO_3 at the summit or high organic matter content associated with earthworm activity, which can affect the measured value during equilibration (Hsieh et al., 1998).

Recharge estimates

Based on the natural tracer profiles, we identified three major hydrostratigraphic units in the Palouse Basin: 1) uplands of the eastern Basin with heterogeneous regolith that display evidence of long pore-water residence times; 2) uplands of the western and central Basin with homogeneous regolith that display evidence of short pore-water residence times; and 3) valley positions with heterogeneous regolith that display dynamic hydraulic processes.

Plots of cumulative water as a function of Cl^- inventory were developed from representative cores of each hydrostratigraphic unit to estimate recharge rates (Fig. 3.8). Estimated recharge rates represent mean values from duplicate core samples that were collected (Fig. 3.8). Straight-line segments reflect episodes of relatively constant Cl^- accumulation (Murphy et al., 1996; Selker et al., 1999). The slopes of these straight-line segments represent the reciprocal of the cumulative $[\text{Cl}^-]$ for a particular depth interval, thus recharge rates can be calculated by dividing the Cl^- accumulation flux by the cumulative $[\text{Cl}^-]$ (Selker et al., 1999).

Recharge rates in uplands of the eastern Basin are low ranging from 3 to 0.6 mm yr^{-1} because sequences of paleosol fragipans restrict vertical percolation (Fig. 3.8). Plots of cumulative water versus cumulative Cl^- display a characteristic

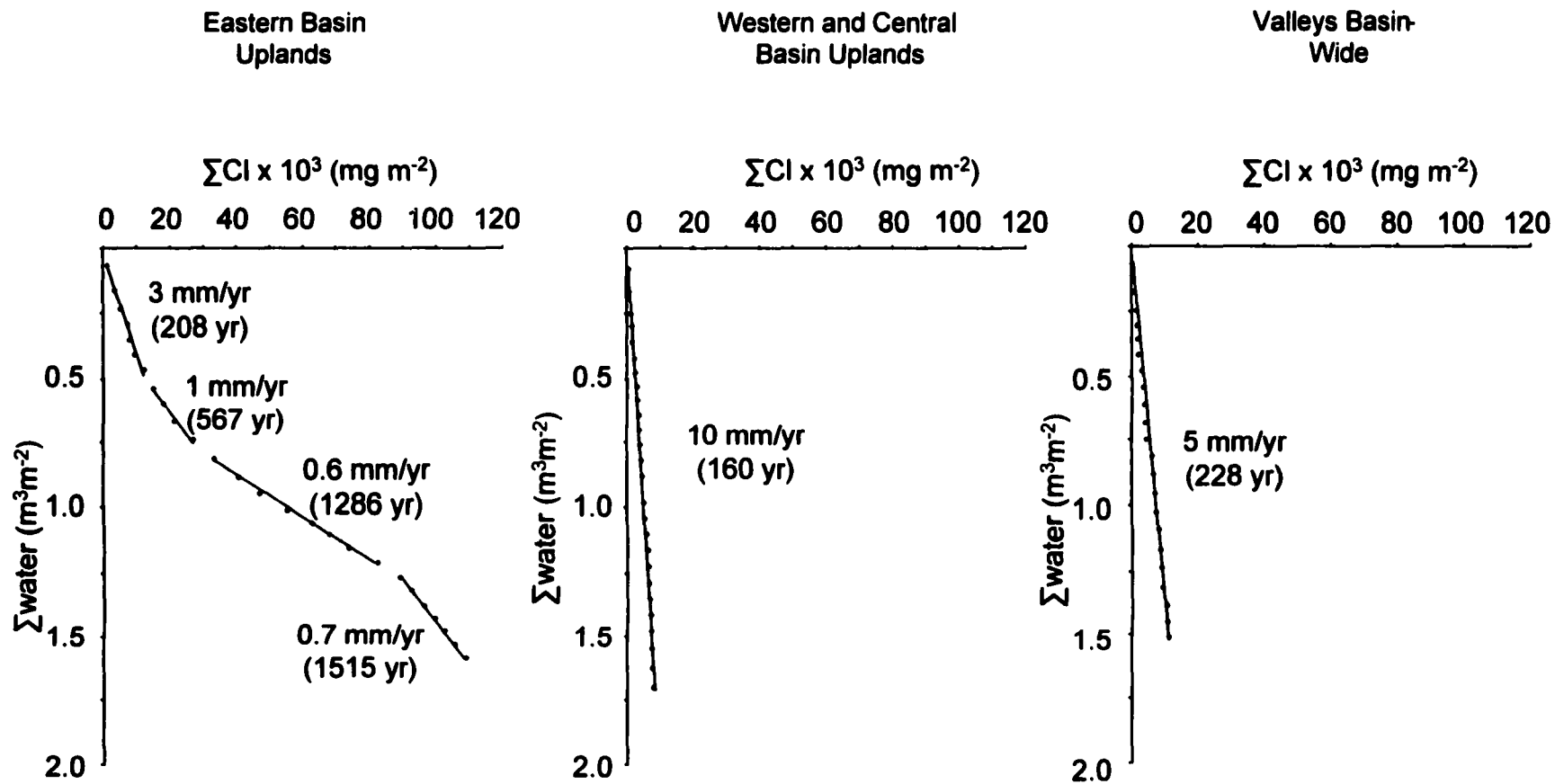


Figure 3.8. Cumulative water-cumulative chloride plots showing recharge estimates for valley and upland sites. Straight-line segments represent episodes of constant Cl^- accumulation.

“stair-step” pattern, which is indicative of long pore-water residence times where episodes of Cl^- accumulation associated with changes in climate have been preserved (Murphy et al., 1996). In fact, the mean pore-water residence time (MRT) at 6 m was 1,515 yr (Fig. 3.8).

Estimates of recharge in uplands of the eastern Basin may reflect maximum rates because we can not assess the impact associated with the formation and lateral redistribution of perched water on Cl^- accumulation. This hypothesis is supported by presence of pedogenic CaCO_3 located at a 2-m depth having a radiocarbon age of 9,220 yr BP. Although the radiocarbon date does not represent the age of pore water at that depth, it does suggest that deep percolation has not been significant over the last 10,000 yr. The presence of pedogenic carbonates that formed from decalcification of Holocene loess is commonly observed in contemporary soils in the western Palouse region in areas that receive less than 400 mm of MAP (Busacca, 1989).

The recharge rate is as high as 10 mm yr^{-1} for uplands of the western and central Basin because deep regolith does not contain water-restrictive horizons and is homogeneous throughout (Fig. 3.8). Plots illustrate continuous straight-line segments, which reflect short pore-water residence times. The MRT at a depth of 6 m is less than 200 years (Fig. 3.8).

Estimated recharge rates of the dynamic valleys are not reliable due to seasonally high water tables and multiple perched water tables. Valley positions that display relatively uniform Cl^- depth profiles illustrate short pore-water residence times up to 228 years (Fig. 3.8).

It is difficult to interpret recharge rates in the valleys because of complex hydrology. We cannot accurately assess lateral contributions of Cl^- from surrounding uplands, hence the actual Cl^- deposition rate at these sites is unknown. Near-surface perched water tables may deliver water that is relatively rich in Cl^- compared to rain water. In contrast, high water tables may have a dilution effect on the signature in deep sediment that is shut off from the Cl^- -concentrating effects of the root zone (Allison et al., 1994).

Regional basin analysis

We used the SSURGO database to scale our results from catchment level to a regional basin analysis. Because the Basin boundaries are not clearly defined we used a slightly larger land area to perform the basin analysis, which is referred to as the "study area". Spatial data that characterizes the vadose zone does not exist in the Palouse Basin, nor in many other locations. Therefore we attempted to link attributes of surface soils in the SSURGO database with those of deep regolith.

Broad-scale spatial variability of soils is controlled by regional patterns in climate and the rate of loess deposition across the Palouse Basin (Busacca, 1989). Loess thickness decreases with increasing distance from the Columbia Basin, which is the loess source (Busacca and McDonald, 1994). Therefore, loess deposition rates decrease along the west-to-east gradient where the eastern portion of the Basin is distal to the loess source. In addition, MAP increases to the east as a result of the orographic effect imposed by the Clearwater Mountains. As a result, soils display a greater degree of soil

development in the eastern portion of the Basin (Busacca, 1989). Magnitudes of loess deposition rates and MAP have changed through time, although the gradients have remained in place (Busacca, 1989).

Gradients of MAP and loess deposition appear to have existed throughout the Quaternary Period (Busacca, 1989). Therefore, we can link the degree of pedogenesis in the solum with that of deep regolith. For example, regolith heterogeneity is most pronounced in the eastern portion of the Palouse Basin where loess deposition rate is low and MAP is high. Therefore, rates of pedogenesis greatly exceed that of loess accumulation. As a result, a continuous sequence of buried E and Btxb horizons occur throughout the deep regolith (Fig. 3.9) (Busacca, 1989; King, 2000). In areas of the western and central Palouse Basin the rate of pedogenesis and loess deposition are "in phase" because MAP is low and loess deposition rate is high compared to the eastern Basin. Therefore, rates of pedogenesis and loess deposition are roughly equivalent. As a result, a relatively homogeneous deep regolith that is similar to the contemporary sola has formed through time (Fig. 3.9). The relationships between regional distribution of soils and the degree of pedogenesis in deep regolith form the foundation of our attempt to "scale-up" the results from catchment- to basin-wide using the SSURGO database.

To identify the spatial distribution of the three major hydrostratigraphic units that were illustrated by natural tracers, we selected soil permeability attributes from the SSURGO database that illustrate the regional patterns observed between sola and deep regolith. Permeability data from the SSURGO database

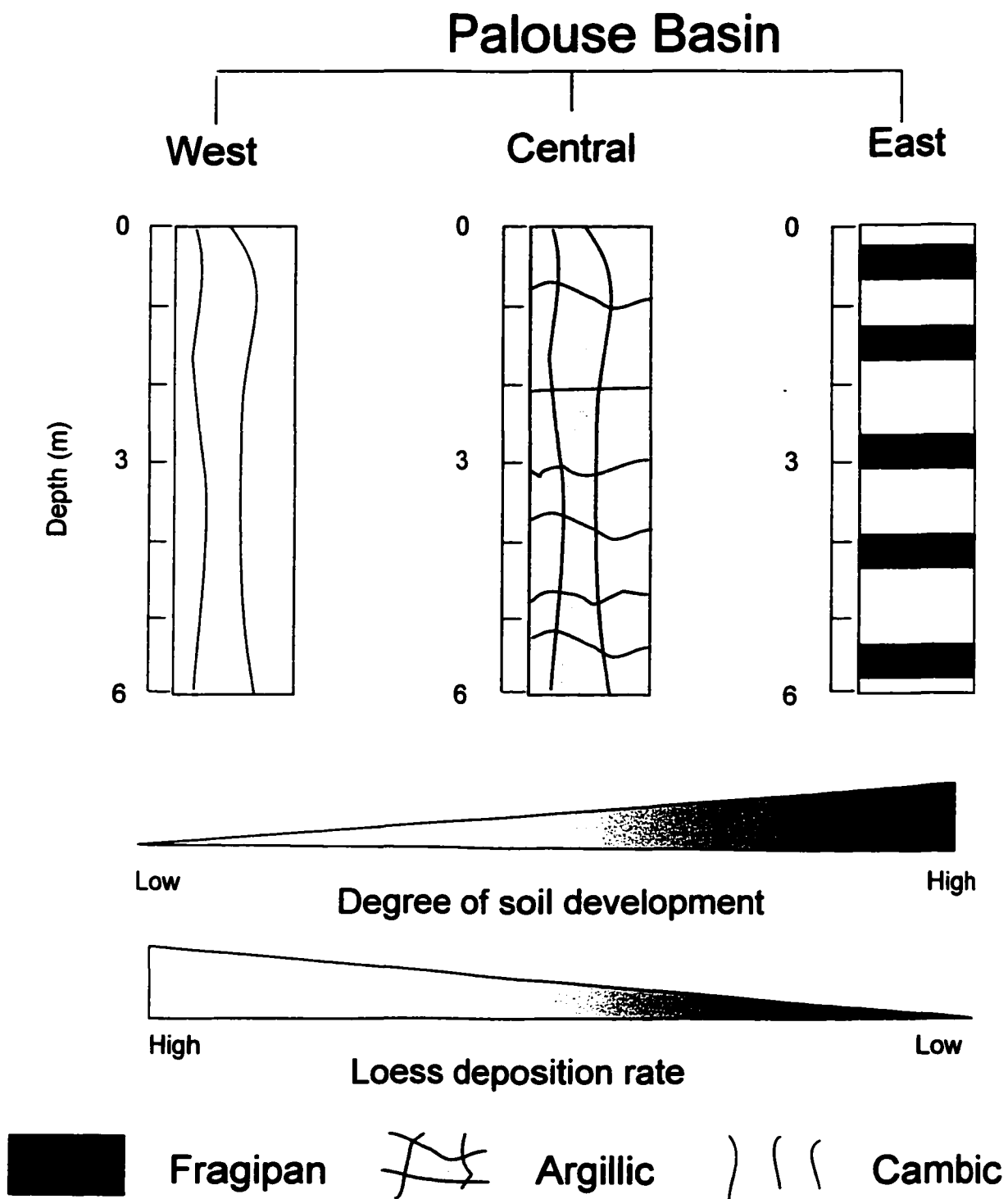


Figure 3.9. Conceptual representation of the degree of soil development in deep regolith across depositional and climatic gradients.

were correlated with recharge rates of deep regolith using the Spearman's Coefficient of Rank, and were significant at the 0.05 level. Regions of heterogeneous deep regolith such as valleys and uplands of the eastern study area were identified through top- and subsoil permeability values that differed by greater than one order of magnitude. These two hydrostratigraphic units were then separated based on slope. Uplands with homogeneous deep regolith in the western and central study area were identified based on soils with uniform permeability values in the topsoil and subsoil (Fig. 3.10).

The three major hydrostratigraphic units combined represent 80% of the study area. The remaining 20% consist of shallow soils and profiles formed from residuum. Hydraulically active valley positions occupy 15,424 ha, constituting 10% of the study area (Table 3.1). Homogeneous deep regolith having a recharge rate $\sim 10 \text{ mm yr}^{-1}$ occupies 56,467 ha and is the most spatially extensive hydrostratigraphic unit, constituting 37% of the study area. Recharge through heterogeneous deep regolith where estimated recharge rates range from 3 to 0.6 mm yr^{-1} constitutes 1,569 ha, which corresponds to 33% of the study area (Fig. 3.10; Table 3.1).

Table 3.1. Spatial extent of the three major hydrostratigraphic units in the Palouse Basin.

Hydrostratigraphic Unit	Total area	Component of study area
	ha	%
Homogeneous uplands	56,467	37
Heterogeneous uplands	50,278	33
Heterogeneous valleys	15,424	10

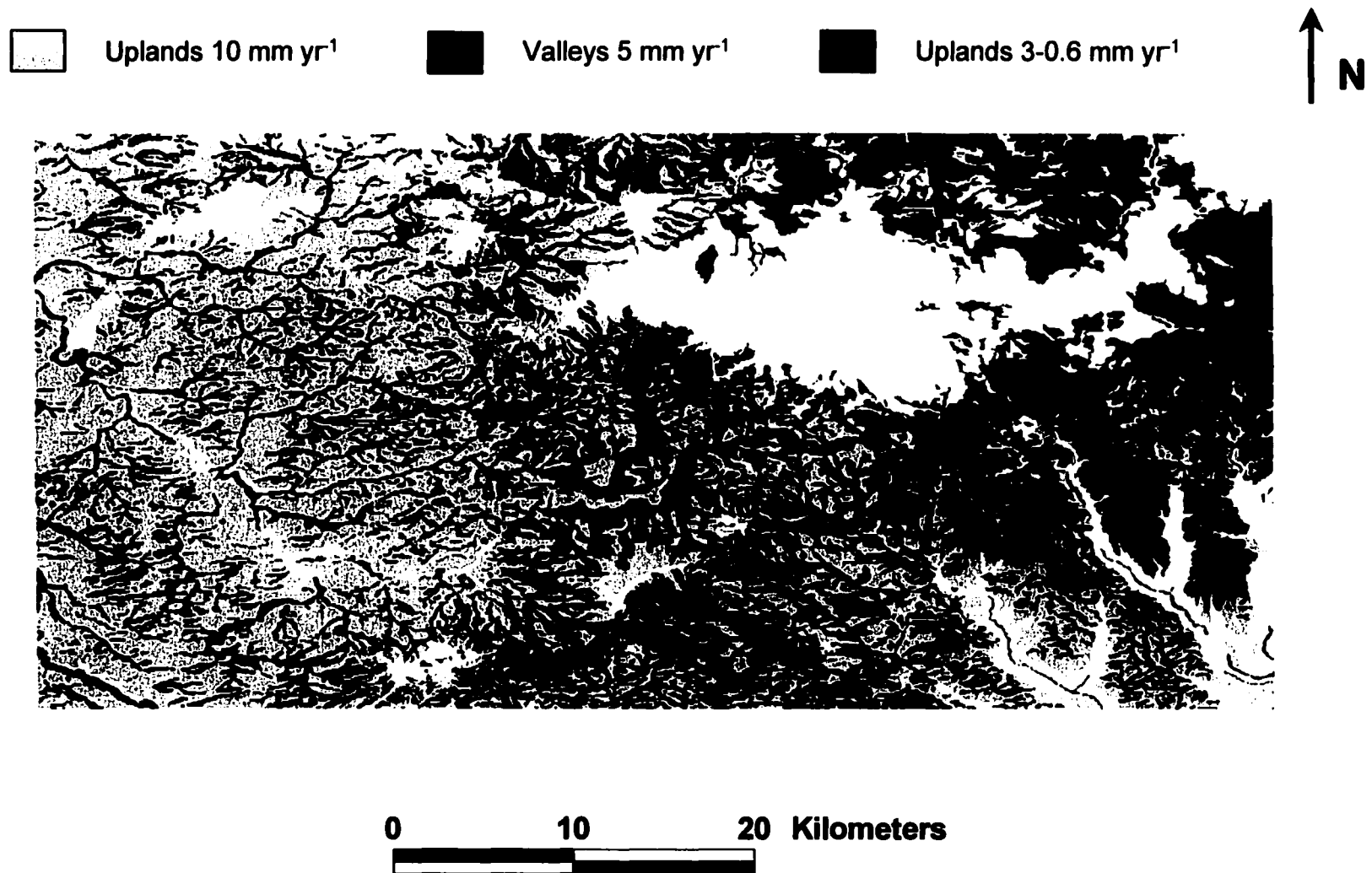


Figure 3.10. Spatial representation of recharge rates of major hydrostratigraphic units identified from the SSURGO database. P and M represent locations of Pullman and Moscow; western, central, and eastern study sites are indicated by W, C, and E.

Conclusions

Existing hydrologic models that assume homogeneous and isotropic deep regolith predict that ground-water recharge is greatest in the eastern Basin where MAP is highest. We found that recharge is lower in the eastern Basin because soils and deep regolith display greater degree of soil development, which restricts the vertical percolation of water. In contrast ground-water recharge is higher in the western and central Basin where soils and regolith are less developed and deep regolith is more homogeneous. Although hydraulically active valley positions are the least spatially extensive, these areas may represent the most significant locations for recharge and further information is needed to better characterize hydraulic processes within this hydrostratigraphic unit.

References

- Allison, G.B., G.W. Gee and S.W. Tyler, 1994. Vadose-zone techniques for estimating ground-water recharge in arid and semiarid regions. *Soil Sci. Soc. Am. J.* 58:6-14.
- Baker, V.R., B.N. Bjornstad, A.J. Busacca, K.R. Fecht, E.P. Kiver, U.L. Moody, J.G. Rigby, D.F. Stradling and A.M. Tallman, 1991. Quaternary geology of the Columbia Plateau. P. 215-250. *In* R.B. Morrison (ed.) Quaternary nonglacial geology: Conterminous U.S. The geology of North America, Vol. K-2 Geol. Soc. Am., Boulder, CO.
- Barker, R.A., 1979. Computer simulation and geohydrology of a basalt aquifer system in the Pullman-Moscow Basin, Washington and Idaho: Washington Department of Ecology Water-Supply Bulletin 48.

- Boll, J., P. McDaniel, E. Brooks, J. Linard and S. Barndt, 2001. Hydrologic characterization of perched water systems: from hillslope to watershed scale. *In Annual Abstracts. Soil Science Soc. Am. Charlotte, NC.*
- Brooks, E.S., P.A. McDaniel and J. Boll, 2000. Hydrologic modeling in watersheds of the eastern Palouse: Estimation of subsurface flow conditions. Presented at the 2000 Pacific Northwest Region Meeting, Paper no. PNW2000-10. ASAE, St. Joseph, MI.
- Busacca, A.J., 1989. Long Quaternary record in eastern Washington, USA, interpreted from multiple buried paleosols in loess. *Geoderma* 45:105-122.
- Busacca, A.J. and E.V. McDonald, 1994. Regional sedimentation of late Quaternary loess on the Columbia Plateau: sediment source areas and loess distribution patterns. P. 181-190 in R. Lasmanis and E.S. Cheney (eds.) *Washington Div. Geol. Earth Res. Bull.* 80.
- Cook, P.G., W.M. Edmunds, and C.B. Gaye, 1992. Estimating paleorecharge and paleoclimate from unsaturated zone profiles. *Water Resour. Res.* 28:2721-2732.
- Crosby, J.W. III. and R.M. Chatters, 1965. Water dating techniques as applied to the Pullman-Moscow ground-water basin. *Bulletin 296, Washington State University College of Engineering Research Division, Pullman, WA.*
- Ericksson, E. and V. Khunakasem, 1969. Chloride concentration in groundwater, recharge rate and rate of deposition of chloride in the Israel Coastal Plain. *J. Hydrol.* 7:178-197.

- Hendry, M.J., L.I. Wassenaar and T. Kotzer, 2000. Chloride and chlorine isotopes (^{36}Cl and $\delta^{37}\text{Cl}$) as tracers of solute migration in a thick, clay-rich aquitard system. *Water Resour. Res.* 36:285-296.
- Hsieh, J.C.C., S.M. Savin, E.F. Kelly, and O.A. Chadwick, 1998. Measurement of soil-water $\delta^{18}\text{O}$ values by direct equilibration with CO_2 . *Geoderma* 82:255-268.
- Johnston, C.D., 1987. Preferred water flow and localized recharge in a variable regolith. *J. Hydrol.* 94:129-142.
- Kendall, C. and E.A. Caldwell, 1998. Fundamentals of Isotope Geochemistry. *In*. Kendall and McDonnell (eds.) *Isotope tracers in catchment hydrology*. Elsevier Science. Amsterdam.
- Kemp, R.A., P.A. McDaniel and A.J. Busacca, 1998. Genesis and relationship of macromorphology and micromorphology to contemporary hydrological conditions of a welded Argixeroll from the Palouse in NW, USA. *Geoderma* 83:309-329.
- King, M., 2000. Late Quaternary loess-paleosol sequences in the Palouse, Northwest USA: pedosedimentary and paleoclimatic significance. Ph.D. thesis. Royal Holloway, Univ. of London.
- Larson, K.R., C.K. Keller, P.B. Larson and R.M. Allen-King, 2000. Water resource implications of ^{18}O and ^2H distributions in a basalt aquifer system. *Ground Water* 38:947-953.

- Lum, W.E., J.L. Smoot and D.R. Ralston, 1990. Geohydrology and numerical model analysis of ground-water flow in the Pullman-Moscow area, Washington and Idaho. U.S. Geol. Surv. Water-Res. Invest. Rep. 89-4103.
- McDaniel, P.A. and A.L. Falen, 1994. Temporal and spatial patterns of episaturation in a Fragixeralf landscape. Soil Sci. Soc. Am. J. 58:1451-1457.
- McDaniel, P.A., R.W. Gabehart, A.L. Falen, J.E. Hammel and R.J. Reuter, 2001. Perched water tables on Argixeroll and Fragixeralf hillslopes. Soil Sci. Soc. Am. J. 65:805-810.
- McDonald, E.V. and A.J. Busacca, 1992. Late Quaternary stratigraphy of loess in the Channeled Scabland and Palouse regions of Washington state. Quaternary Res. 38:141-156.
- Murphy, E.M., T.R. Ginn and J.L. Phillips, 1996. Geochemical estimates of paleorecharge in the Pasco Basin: Evaluation of the chloride mass balance technique. Water Resour. Res. 32:2853-2868.
- Newman, B.D., A.R. Campbell and B.P. Wilcox, 1997. Tracer-based studies of soil water movement in semi-arid forests of New Mexico. J. Hydrol. 196:251-270.
- O'Brien, R., C.K. Keller and J.L. Smith, 1996. Multiple tracers of shallow ground-water flow and recharge in hilly loess. Ground Water 34:675-682.
- O'Geen, T., J. Boll, E.S. Brooks, J.I. Linard, P.A. McDaniel, J.B. Sisson and A. Wylie, 2001. Detection of multiple perched water tables using natural tracers and multilevel tensiometers in deep loess. EOS Trans. AGU. 82 p.47 Fall Meet. Suppl. Abstract H52A-0383 San Francisco, CA.

- Reuter, R.J., P.A. McDaniel, J.E. Hammel and A.L. Falen, 1998. Solute transport in seasonal perched water tables in loess-derived soils. *Soil Sci. Soc. Am. J.* 62:977-983.
- Scrimgeour, C.M., 1995. Measurement of plant and soil water isotope composition by direct equilibration methods. *J. Hydrol.* 172:261-274.
- Selker, J.S., C.K. Keller and J.T. McCord, 1999. *Vadose zone processes*. CRC Press. Boca Raton, FL.
- Williams, R.E. and D.W. Allman, 1969. Factors affecting infiltration and recharge in a loess-covered basin. *J. Hydrol.* 8:265-281.

CHAPTER 4

HYDROLOGIC PROCESSES IN VALLEY SOILSCAPES OF THE EASTERN PALOUSE BASIN

Abstract

Vadose zone hydrology is poorly understood in the eastern Palouse Basin of northern Idaho because loess deposits often contain multiple, hydraulically restrictive horizons that impede water flow. Valley soilsclapes are of particular interest from a hydrologic perspective, because a majority of precipitation is redistributed as runoff and throughflow into these landscape positions. We implemented a combined approach to assess hydrologic processes in valley positions using hydrometric measurements, natural tracers, and stratigraphic observations. Hydrographs of near-surface monitoring wells indicate that valley positions maintain a thicker zone of saturation for longer duration compared to upland positions. Deep tensiometers illustrate that valley positions develop multiple zones of seasonal saturation within the vadose zone in response to sediments with contrasting physical nature, while saturation only occurs above the uppermost fragipan in uplands. Together with deep tensiometer readings, secondary Mn distributions suggest that ground-water recharge occurs as bypass flow. Indirect evidence from the $\delta^{18}\text{O}$ signature of water samples suggests that near-surface perched water tables are a major source of stream flow. In addition, representative chloride profiles of valley soilsclapes reflect differences in the rate of deep percolation that is governed by regional patterns of

soil development. Results suggest that valley soils play an important role in surficial and deep regolith hydrological processes in the Palouse Basin.

Introduction

Undulating topography of the Palouse Basin in northern Idaho redistributes a majority of precipitation as surface runoff and throughflow. As recipients of redistributed precipitation, valley soils play an important role in the regulation of stream flow and ground-water recharge, while only occupying approximately 17,000 ha in the Palouse Basin (Fig. 4.1) (Murray, 2002). Recent studies in the region have shown that lower slope positions are dynamic hydrostratigraphic units (O'Brien et al., 1996), while uplands have deep vadose zones with long pore-water residence times (O'Geen et al., in press). In addition to topographic patterns, the redistribution of soil water across a landscape is also influenced by the variability of soil features such as vertical and horizontal saturated hydraulic conductivity (Bathke and Cassel, 1991; McDaniel and Falen, 1994; Reuter et al., 1998; McDaniel et al., 2001).

Loess-derived soils in the Palouse region of northern Idaho contain hydraulically restrictive horizons that retard vertical percolation of water (McDaniel and Falen, 1994; McDaniel et al., 2001). Measured saturated hydraulic conductivity values range from 0.06 to 0.9 cm d⁻¹ in restrictive horizons and 14 to 129 cm d⁻¹ in Ap and Bw horizons (McDaniel et al., 2001; Reuter et al., 1998). Observations of perched water table dynamics in the eastern Palouse region indicate that water moves laterally as throughflow in more permeable Ap and Bw horizons (Reuter et al., 1998; McDaniel et al., 2001). As a result, up to

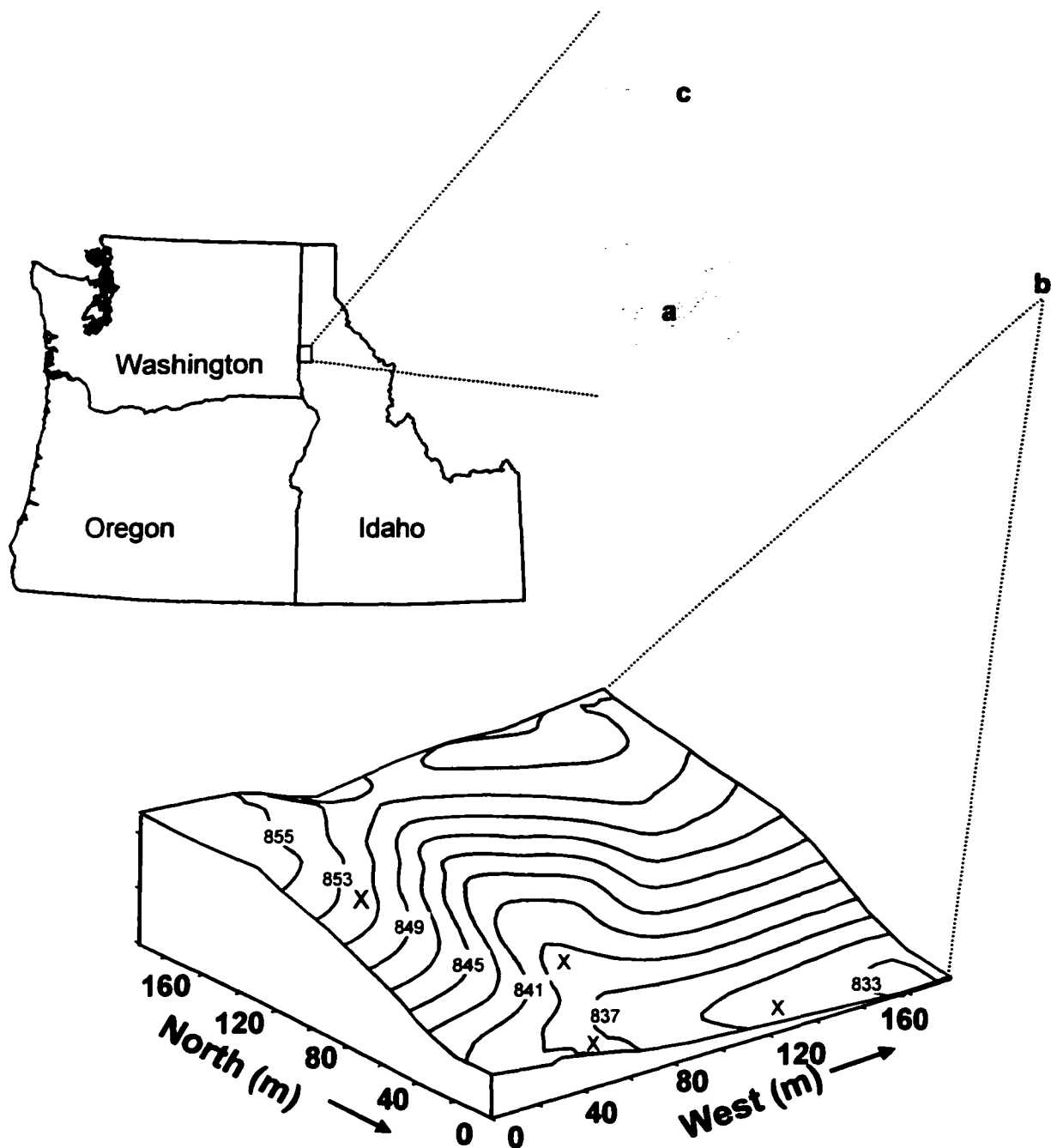


Figure 4.1. Location of the Palouse Basin of northern Idaho and the Troy study catchment. Letters a, b, and c indicate sampling locations for Cl⁻ depth profiles. Shading indicates the approximate distribution of valley soils. Topographic attributes for the Troy study catchment are displayed using a 2-m grid elevation model and location of core samples are indicated with X.

90% of incident precipitation may be redistributed as lateral throughflow (Brooks et al., 2000).

Regional concerns regarding the sustainability of ground water in the Palouse Basin have fueled a need to identify hydrologic processes in valley soils. Studies that integrate hydrometric measurements with environmental and geochemical tracers have clarified relationships between hillslope hydrology, stream flow, and ground-water recharge (McDaniel et al., 1992; McDonnell, 1990; Bazemore et al., 1994; Harris et al., 1995; Rodhe et al., 1996; Park and Burt, 1999; Marc et al., 2001). The approach of this investigation was to use natural tracers, hydrometric measurements, and stratigraphic observations to interpret dynamic flow regimes in valley soils of the eastern Palouse Basin. The specific objectives of this study were to: 1) monitor perched water table dynamics in near-surface perched water tables and within the vadose zone of valley and upland positions; 2) utilize secondary Mn profiles to help interpret flow mechanisms in the vadose zone; 3) evaluate the contributions of snowmelt and perched water to streams using oxygen isotopes; and 4) use representative chloride depth profiles to obtain a regional understanding deep percolation within valley soils.

Materials and Methods

Environmental setting

Soils of the Palouse region have formed from thick loess deposits that blanket a majority of eastern Washington and northern Idaho. Soils that have formed in loess are dominated by silt loam and silty clay loam textures, due to the nature of the transport process. The degree of soil development is controlled by a strong

climatic gradient where mean annual precipitation (MAP) ranges from ~ 550 mm in the vicinity of Moscow, ID to >800 mm at the eastern margin of the Palouse. In response to this gradient, Argixerolls with dense argillic horizons and Fragixeralfs with very dense brittle fragipans occupy much of the eastern Palouse region (Barker, 1981). Surface soils consist of friable A and Bw horizons formed in Holocene loess that overly dense brittle E, Btb, or Btxb horizons that have formed from late Pleistocene loess (Kemp et al., 1998).

The presence of dense argillic and fragipan horizons plays an important role in the near-surface hydrology of the eastern Palouse because most of the annual precipitation falls during the winter months when evapotranspiration is low. As a result, percolating precipitation is impeded by these horizons that are slowly permeable to water, and therefore, seasonal perched water tables develop and persist from late November through May (Barker, 1981; McDaniel and Falen, 1994; Reuter et al., 1998).

The study site is a small catchment located 3 km north of Troy, ID at the eastern boundary of the Palouse region (Fig. 4.1). It consists of a well-defined sub-watershed that drains toward the north into a larger drainage system that contains an ephemeral stream running east to west. The study site has been in the Conservation Reserve Program for the last 10 years.

Loess thickness ranges from less than 4 m in the valley to over 12 m in the upland positions. The dominant soil mapped in the region is a Fragixeralf (Barker, 1981), however, field investigations suggest that Fragiaqualfs are present in lowlands.

Field methods

The study site is part of an ongoing project designed to monitor temporal and spatial changes in near-surface perched water tables (PWTs). The catchment is instrumented with 120 monitoring wells installed on a 15-m by 10-m grid format to monitor perched water table dynamics. Each well is designed to measure the perched water table thickness above the fragipan using electronic pressure transducers.

To monitor water potential in the vadose zone, multilevel tensiometers were placed at major stratigraphic boundaries below the uppermost fragipan in upper- and lower-slope positions. In the lower-slope position, tensiometers were placed at 0.6, 4.2, and 5.5 m and sealed above and below with bentonite. At the upper slope position, tensiometers were installed at 1.2, 5.2, and 7.0 m.

To construct subsurface stratigraphy of the valley, seven cores were collected. Three were collected using a tractor mounted hollow-stem auger, and four were sampled using an extension hand auger. Morphologic field descriptions were performed on each core.

Laboratory methods

The distribution of secondary Mn oxides reflects changes between reducing and oxidizing environments, and Mn_d therefore is a good indicator of saturated conditions in the Palouse region (McDaniel et al., 1992; McDaniel et al., 2001). The Mn_d distribution in the vadose zone of upper- and lower-slope positions was measured using a citrate-bicarbonate-dithionite extracting solution (CBD) (Soil Conservation Service, 1972).

To assess the contributions of PWTs to ground water and streams, subplots consisting of nine monitoring wells were established near the research site in pasture and forest. PWT samples were collected monthly during the course of the 1999 water year for oxygen isotope ($\delta^{18}\text{O}$) analysis. The signatures of PWTs were compared to those of streams, snowpack, and ground water.

Stable-isotope analyses were performed at the University of Idaho Stable Isotope Laboratory. A direct- CO_2 equilibration technique was used to measure $\delta^{18}\text{O}$ of water (Epstein and Mayeda, 1953). After equilibration, an aliquot of the gas was injected into a Finnigan Mat Delta-Plus stable-isotope-ratio mass spectrometer. Values of ^{18}O analysis were reported in delta (δ) notation as per mil (‰) deviations relative to the Vienna-Standard Mean Ocean Water (VSMOW) international standard. The analytical precision for the direct- CO_2 $\delta^{18}\text{O}$ analysis was $\pm 0.3\text{‰}$.

Distributions of $[\text{Cl}^-]$ were measured for three representative cores that were collected across the eastern Palouse in order to assess hydrologic differences influenced by soil variability of valley soils. A single core was sampled from the Troy site. Two additional cores were collected at locations in the eastern Palouse that reflect differences in the degree of soil development (Fig. 4.1). All cores were sampled during the summer months (May-September). Samples were sectioned in to 20-cm increments, sealed in plastic bags, and frozen until analyzed.

In the laboratory, cores were split longitudinally providing samples for stratigraphic description and half for extraction of pore-water Cl^- . Gravimetric

water content was determined for all samples prior to Cl^- extraction. After soil samples were oven dry, 20 g of sediment were mixed with 20 mL of triple-distilled water and shaken overnight. Samples were centrifuged at 2500 RPM for 30 minutes, and supernatant solution was filtered through a 0.22- μm filter. Chloride concentration was measured in triplicate using a Dionex ion chromatograph, and pore-water $[\text{Cl}^-]$ was calculated using gravimetric water content (Murphy et al., 1996).

Results and Discussion

Vadose zone stratigraphy

The recognition of dynamic flow regimes within lower slope positions of the Palouse Basin (O'Brien et al., 1996; O'Geen et al., in press) warrants a better understanding of the vadose zone stratigraphy in these soils. Loess thickness at the site ranges from 5.5 to 4.5 m and thins toward the north. Interestingly, the granite bedrock slopes to the south, which is the opposite direction that the catchment drains towards (Fig. 4.2). The vadose zone consists of a complex sequence of buried paleosol fragipans, clay-enriched horizons, and eluvial layers (Fig. 4.2).

The pedogenic character of buried fragipans changes across the landscape. The northern portion of the valley, which is proximal to the east-west running ephemeral stream, has very dense B-horizons with reduced matrix. The southern portion of the landscape consists of moderately dense B-horizons with fragic character (Fig. 4.2). In addition, a thick eluvial horizon is present in the center of the valley at a 4-m depth. It appears as if the spatial variability of pedogenic

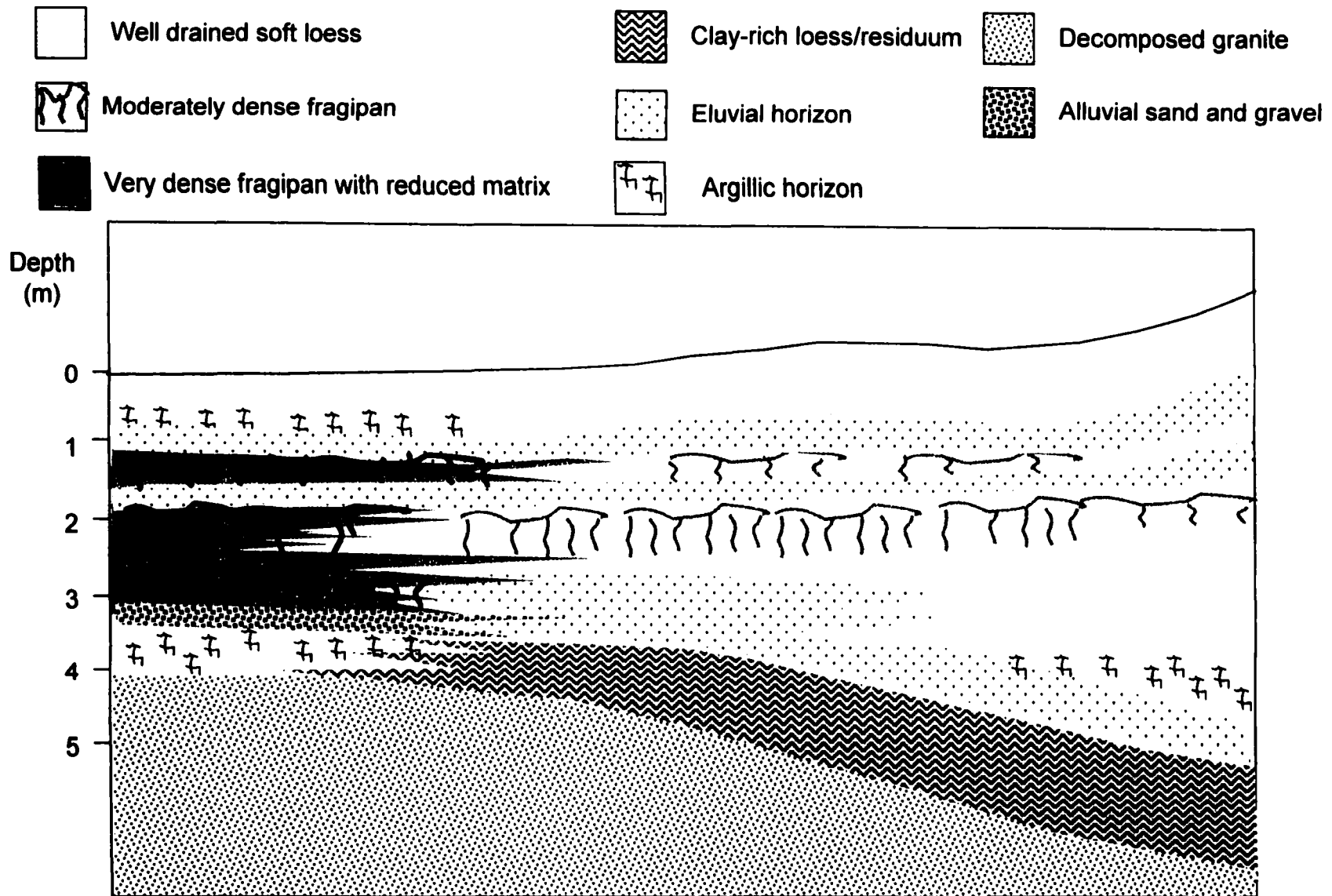


Figure 4.2. Schematic diagram of morphology and stratigraphy of soil/paleosol sequences in valley positions at the Troy study catchment.

character in paleosols may allow for the development of localized conduits through which preferential recharge can occur within the vadose zone.

Near surface perched water

Hydrographs of near-surface perched water tables for upper- and lower-slope positions display several similarities. Episodes of saturation above the fragipan developed abruptly over the wet season in 1998 and 1999 (Fig. 4.3). Although the formation of PWTs varies from year to year, they form simultaneously at each slope position. Sharp fluctuations in PWT height are associated with rain and snow-melt events, and in some instances, PWT levels rise over 40 cm within a period of less than 24 hours (Fig. 4.3) (McDaniel et al., 2001). Interestingly, the rise and fall of PWTs is only associated with a 4 to 5% change in volumetric water content, and therefore, relatively small inputs result in large and rapid increases in PWT levels (Regan, 2000; McDaniel et al., 2001).

Patterns of saturated conditions within the solum differ between upper- and lower-slope positions. The hydrograph of the upland position illustrates several short-duration events of saturation within Ap, Bw, and BE horizons. In contrast, the Ap horizon remains saturated for several days at the lower-slope position. As a result, the PWT is approximately twice as thick as in the upland position (Fig. 4.3). Rapid decreases in perched water thickness associated with upland positions are a result of water that drains laterally in permeable A and Bw horizons (Reuter et al., 1998; McDaniel et al., 2001).

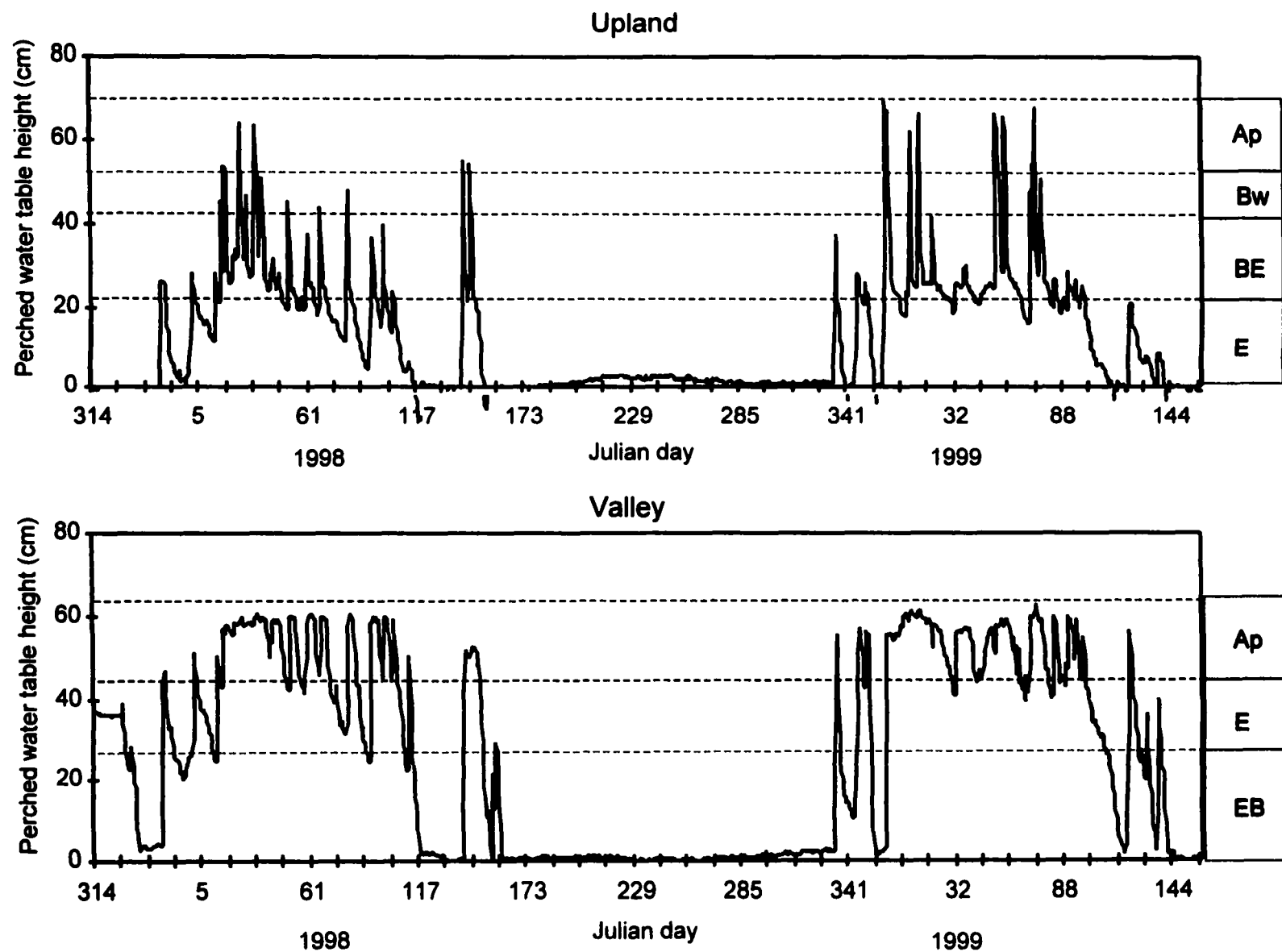


Figure 4.3. Hydrographs for upper- and lower-slope well positions at the Troy catchment for 1998 through 1999. Genetic horizons are indicated at the right of each hydrograph.

Vadose zone hydrology

In 2001, multilevel tensiometers were installed to monitor water potential in the vadose zone. At the lower-slope position, three saturated layers were identified below the uppermost fragipan and will be referred to as vadose zone water tables (VZWTs). Conditions were exceptionally dry in 2001, and as a result, sustained episodes of near-surface perched water were only present in March (Fig. 4.4). The duration of saturation of VZWTs, however, lasted 1 to 2 months longer than the PWT disappearing in late May and June (Fig. 4.4). The VZWTs developed sequentially, starting at the deepest depth, which we interpret to be the ground-water table at 5.5 m. The VZWTs diminished in reverse order beginning with the near surface PWT at 0.6 m (Fig. 4.4). VZWTs were not present below the contemporary fragipan in upper-slope positions (O'Geen et al., 2001).

Patterns in wetting and drying of the VZWTs help clarify flow pathways in the vadose zone of valley soils. Multilevel tensiometers illustrate a vertical hydraulic connection between the near-surface PWT and the ground-water table. The PWT and ground-water table develop simultaneously, while the 4.2 and 1.5 m VZWTs lag slightly behind (Fig. 4.4). The sequential development of VZWTs indicates that water percolates through deep strata as preferential flow, initially bypassing a majority of the vadose zone soil matrix. Zones of saturation disappear in reverse order beginning with the PWT, indicating that VZWTs slowly drain into the ground water (Fig. 4.4). An alternative explanation is that VZWTs move laterally towards the south following the slope of the bedrock, and

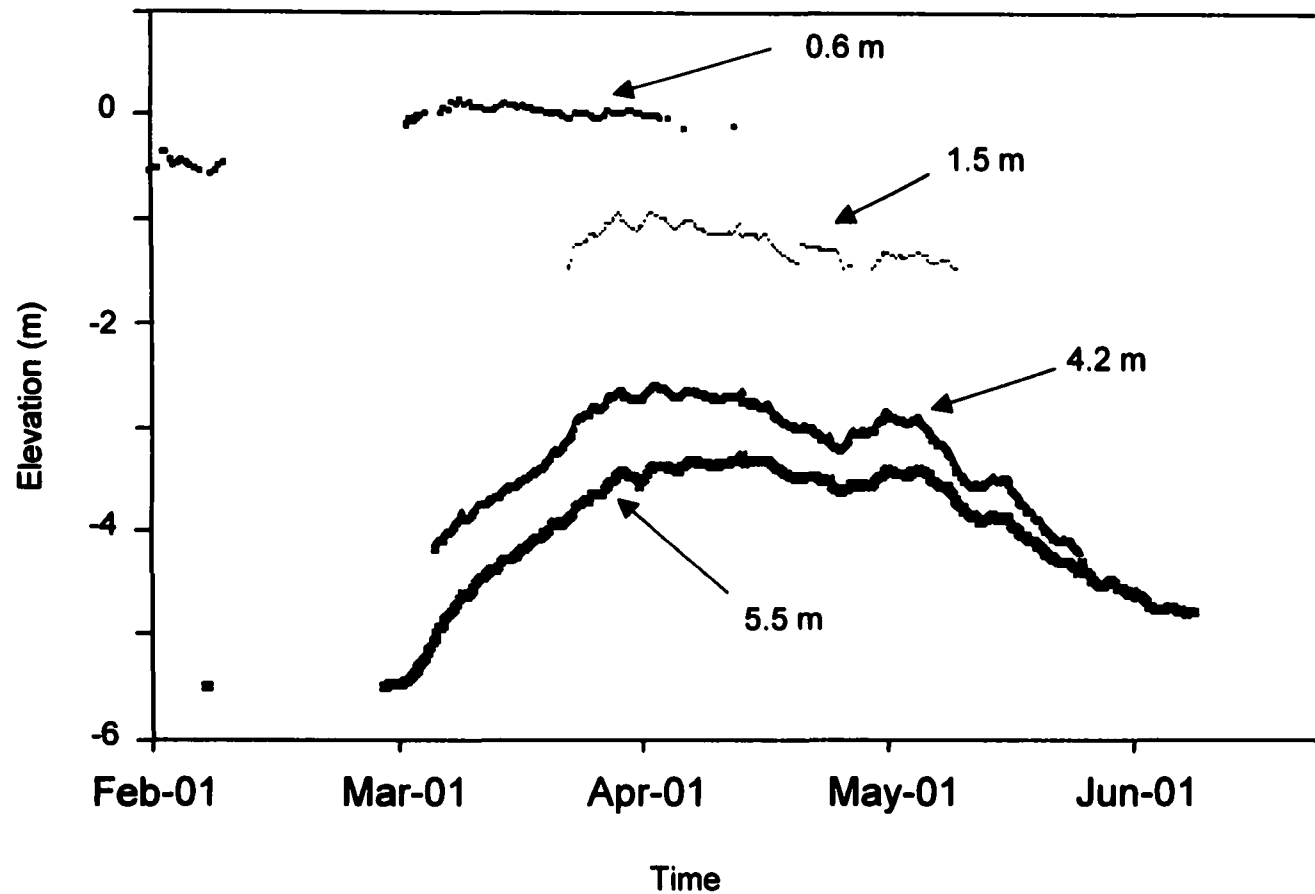


Figure 4.4. Measurements of saturated thickness recorded by multilevel tensiometers for the lower-slope position at the Troy catchment. Data points represent the elevation-head above the indicated depth of each tensiometer.

eventually percolate through less-dense strata in the center of the catchment (Fig. 4.2).

Secondary manganese

Secondary manganese (Mn_d) depth profiles can be used as geochemical indicators of hillslope hydrological processes (McDaniel et al., 1992; Park and Burt, 1999). Once released from primary minerals, Mn_d becomes soluble and subsequently redistributed across soilscares during periods of low redox potential.

Relationships between Mn_d profiles and landscape position illustrate contrasting hydrologic conditions within the vadose zone. The average Mn_d content in the upland position is 0.06%, which is twice as high as in the valley (Fig. 4.5). In the lower-slope position, the duration and degree of saturated thickness is greater throughout the vadose zone. As a result, redox potentials remain low enough to reduce and mobilize secondary Mn to the extent that it is eventually lost from the system. These patterns support evidence from multilevel tensiometers that illustrate the absence of VZWTs in upper-slope positions and the development of multiple VZWTs in lower-slope positions. (Fig. 4.4 & 4.5) (O'Geen et al., 2001).

Vertical changes in Mn_d in the lower-slope position reflect patterns of saturated conditions in the vadose zone. Fluctuations in Mn_d with depth correspond with zones of paleosol development (O'Geen et al., in press). Horizons of low Mn_d represent layers of prolonged saturation and redistribution of Mn_d located at depth intervals of 0.5 to 1.0 m, 2.0 to 3.0 m, and 4.0 to 6.0 m

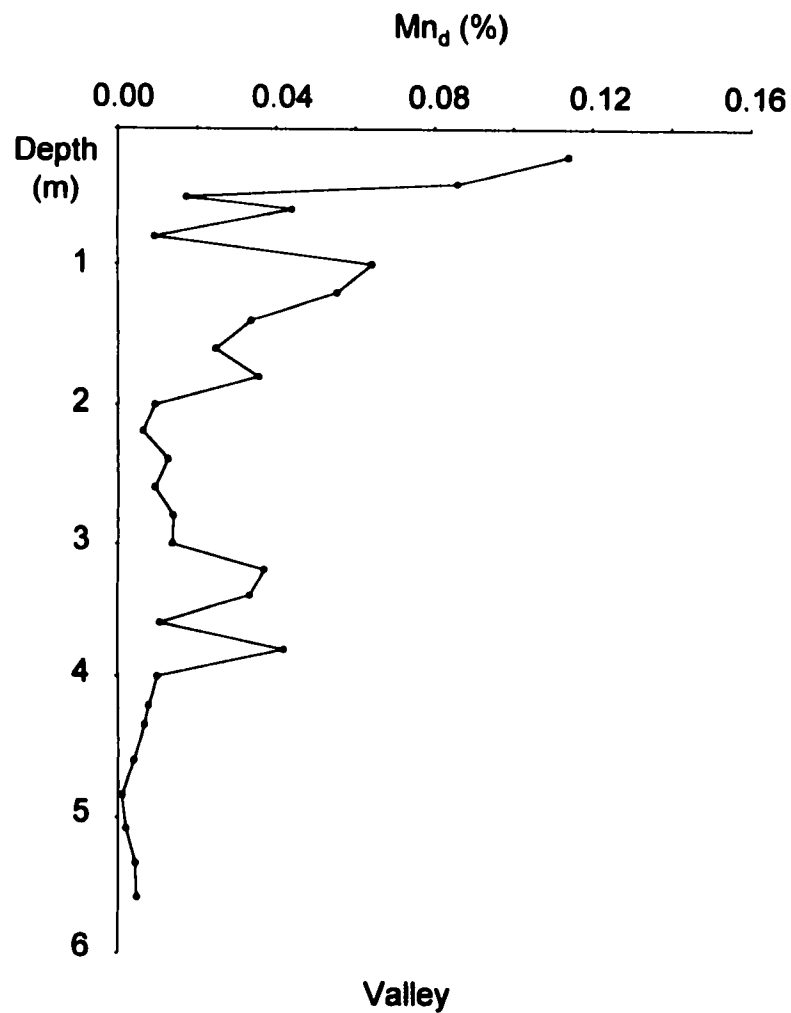
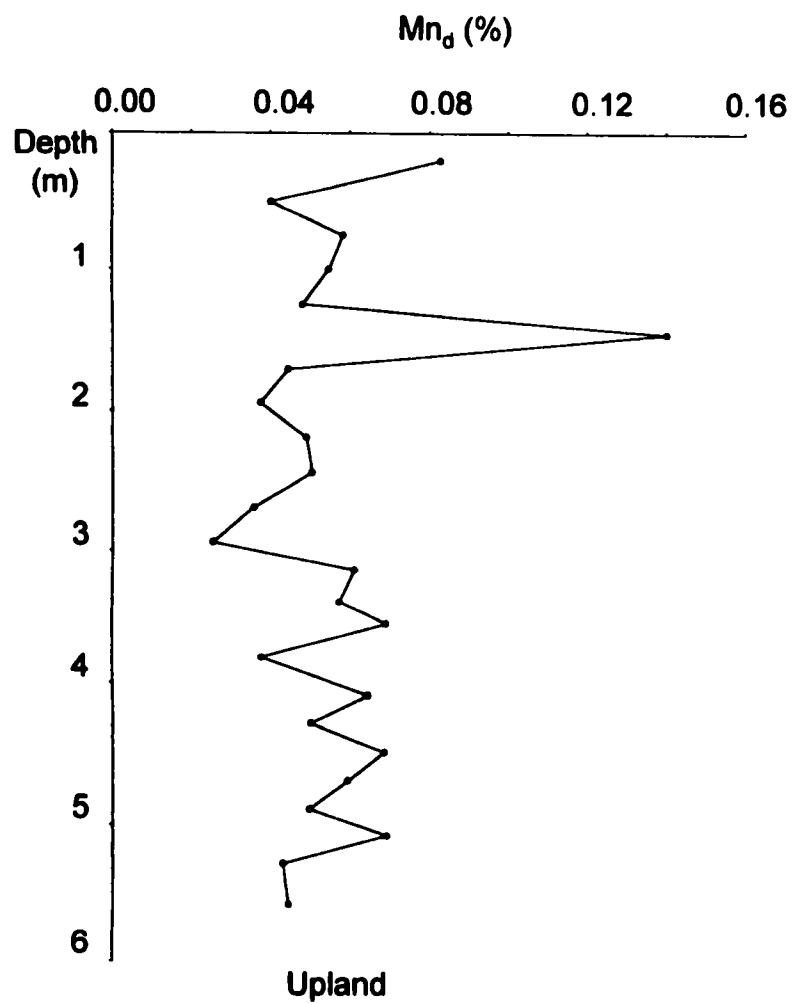


Figure 4.5. Vertical distributions of dithionite-extractable manganese (Mn_d) for upper- and lower-slope positions of the Troy catchment.

(Fig. 4.5). These layers coincide with zones of saturation identified by hydrometric measurements (Figs. 4.4 & 4.5). Furthermore, strata associated with the ground-water table display lowest Mn_d , which is to be expected due to prolonged saturation. In contrast, maximum Mn_d is located between 1 to 2 m and 3 to 4 m depths represent zones of fragipan development. A large increase in Mn_d is observed between 1 and 2 m below the surface, which underlies the near-surface PWT. An additional peak represents a buried fragipan that appears to confine the ground-water table identified by tensiometers at 4.2 and 5.5 m depths. Low Mn_d content in the valley position indicates that these soils remain saturated for long periods of time. Vertical fluctuations in Mn_d indicate that hydraulically restrictive horizons may confine VZWTs and redistribute water laterally or vertically via preferential pathways.

Oxygen isotopes

Many studies have been able to assess the compartmentalization of water in catchments using stable isotopes (Allison and Hughes, 1983; Harris et al., 1995; Rodhe and Nyberg, 1996; Neal et al., 1997; Tang and Feng, 2001). Stable isotopes of oxygen work best as natural tracers in catchment hydrology when the $\delta^{18}O$ signature of source- and sink-water contrast (Gonfiantini et al., 1998). The $\delta^{18}O$ signature of soil water is often different from that of precipitation due to mixing of event and pre-event water (Jordan, 1994; Marc et al., 2001). Moreover, snowmelt is often depleted with respect to ^{18}O compared to precipitation, therefore, the isotopic signature of runoff and infiltrating snowmelt may differ from that of the entire snowpack (Cooper, 1998; Rodhe, 1999; Unnikrishna et al.,

2002). Isotopic fractionation with respect to $\delta^{18}\text{O}$ can also occur when precipitation is intercepted and evaporated by forest canopies resulting in enrichment of canopy drip (Kelliher et al., 1993; Dawson and Ehleringer, 1998).

We measured the $\delta^{18}\text{O}$ signature of perched water, stream water, and snowpack in an attempt to clarify contributions of lateral throughflow to streams. We also compared the $\delta^{18}\text{O}$ signature of perched water under intact and cleared forest to assess the impacts of forest canopy on the perched water signature. It should be noted that the effective distribution of precipitation differed between the intact and cleared forest. The cleared forest consistently maintained greater snow pack and thicker perched water tables, as indicated by monitoring wells.

The $\delta^{18}\text{O}$ signature of snowpacks varied most from that of PWTs in January and February (Table 4.1). In January, the $\delta^{18}\text{O}$ signatures of PWTs were approximately 1‰ greater than the respective snowpacks as a result of mixing of soil water with infiltrating snowmelt (Table 4.1). In February, the snowpack in the intact forest displayed a 1‰ positive shift in $\delta^{18}\text{O}$ in response to a warm storm event. This shift was not present in the snowpack of cleared forests, which may indicate the presence of a canopy effect. The snowpack was 0.5 m thicker in the cleared forest, and therefore the volume of water in the rain event may not have been large enough to change the signature of the snowpack. As a result, the $\delta^{18}\text{O}$ signature of PWTs in the forest display a 0.6‰ increase compared to PWTs in cleared forest (Table 4.1). In March and April, snowmelt was rapid, and no measurable differences were detected between the $\delta^{18}\text{O}$ signatures of snowpack, perched water, and streams.

Table 4.1. The $\delta^{18}\text{O}$ signature of perched water tables, snowpack, and streams in 2000.

Month 2000	PWT Cleared	PWT Forest	Snowpack Cleared	Snowpack Forest	1 st Order Stream	2 nd Order Stream
$\delta^{18}\text{O}\text{‰}$						
January	-14.6	-14.9	-15.8 [†]	-16.2 [†]	--	--
February	-14.9	-14.3	-16.5 [†]	-14.2	-15.1	-14.9
March	-16.0	-15.2	-15.7	-15.6	-15.9	-15.5
April	-15.5	-15.2	--	--	-15.2	-15.2

[†] indicates a measurable difference from that of the respective PWT that are greater than the standard deviation 0.5‰ and analytical precision of 0.3‰.

[‡] indicates detectable differences from that of streams that are greater than the standard deviation 0.5‰ and analytical precision of 0.3‰.

-- indicates that no sample was collected

Subtle differences in isotopic composition were observed between snowpack and other compartments of water, but they do not differ to the extent that hydrograph separations can be performed. The $\delta^{18}\text{O}$ signature of 1st and 2nd order stream samples were identical and displayed no detectable difference from that of PWTs (Table 4.1). The stream signatures were ~1.5‰ greater than the snowpack in the cleared forest in February. Moreover, the $\delta^{18}\text{O}$ signatures of streams and PWTs did not change significantly in response to the snowmelt in February (Table 4.1). This is indirect evidence suggesting that a majority of stream flow is influenced by lateral throughflow of PWTs rather than surface runoff of snowmelt.

One shortcoming of this experiment was that no direct measurements of snowmelt or rainfall were made. We assumed that the $\delta^{18}\text{O}$ signature of the entire snowpack, which was a mixture of rain and snow events, was identical to the signature of meltwater. In addition, preferential flow of infiltrating precipitation

through snowpacks has been observed to occur, and may be significant in the thin snow of the intact forest (Unnikrishna et al., 2002).

Regional trends of Cl^- depth profiles

To illustrate regional differences in ground-water recharge we measured Cl^- distributions for three major valley soils that are representative of the eastern Palouse. The various types of soils sampled include: 1) Fragiaqualfs at the Troy study site that occupy narrow valleys in the eastern margin of the Palouse; 2) Argixerolls that occupy large expansive lowlands throughout the eastern Palouse; and 3) Haploxerolls that represent drainage systems of the east-central portion of the Palouse.

The Cl^- depth profiles illustrate that pore-water residence times in valley soils is controlled by the degree of soil development. The Fragiaqualf and the Argixeroll soils both have hydraulically restrictive horizons, and as a result, Cl^- depth profiles display similar attributes. Both soils have high $[\text{Cl}^-]$ ranging from 25 to 100 mg L^{-1} , which is indicative of long pore-water residence times (Fig. 4.6). Peaks in $[\text{Cl}^-]$ are associated with water-restrictive B horizons. In addition, zones of low $[\text{Cl}^-]$ are associated with seasonally saturated E and BE horizons with reduced matrix.

Hydraulically restrictive horizons are not present in the Haploxeroll soils, and therefore, $[\text{Cl}^-]$ is low indicating short pore-water residence times. The $[\text{Cl}^-]$ decreases rapidly from 80 mg L^{-1} within the top 10 cm of the root zone to less than 15 mg L^{-1} throughout most of the profile (Fig. 4.6).

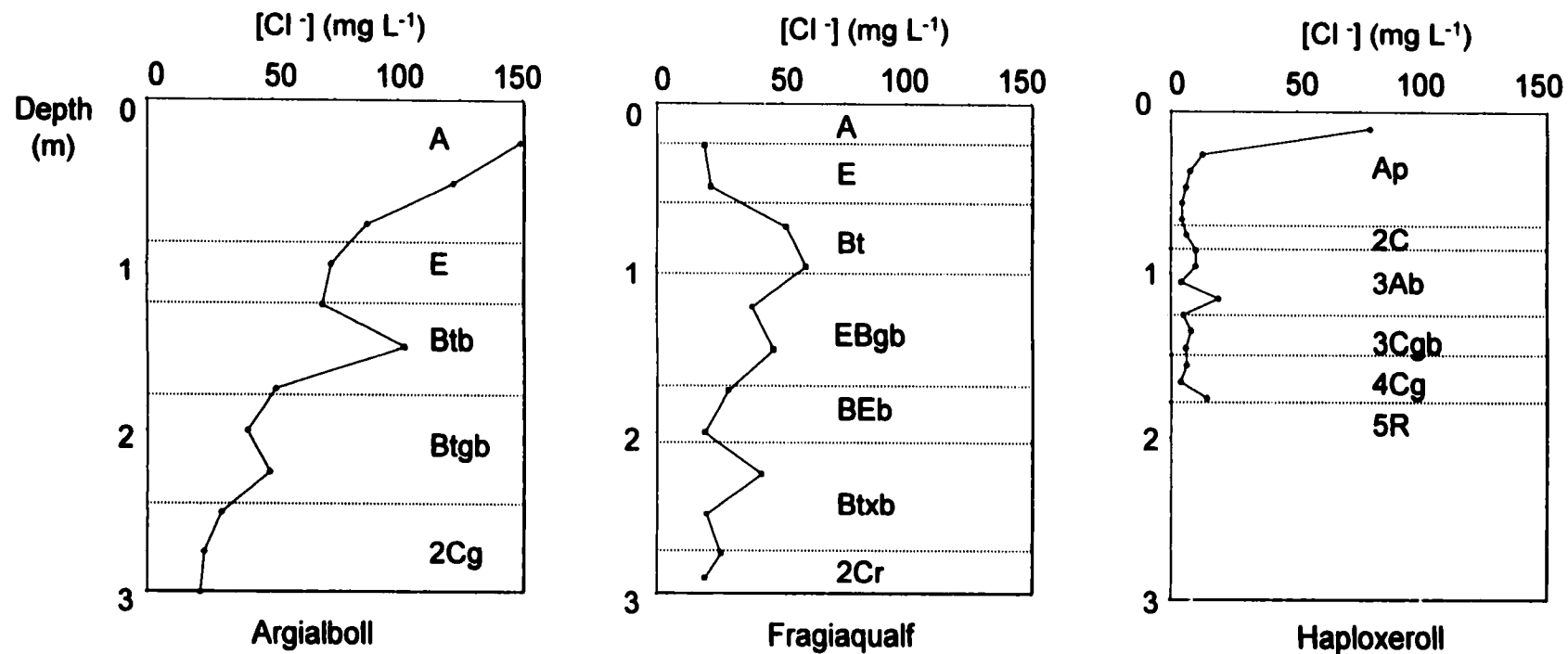


Figure 4.6. Chloride depth profiles at representative valley soils in the eastern Palouse Basin.

Conclusions

Valley soils occupy approximately 17,000 ha in the Palouse Basin. Although these landscape positions constitute only 16% of the Basin, they play an important role in the regional hydrologic processes. Results of hydrometric monitoring and natural tracer data indicate that PWTs of valley soils contribute to ground-water recharge and stream flow. Deep percolation is inhibited by hydraulically restrictive paleosols interstratified within the vadose zone. A combination of hydrometric and natural tracer measurements indicate that ground-water recharge occurs as bypass flow through vertical conduits of strata more permeable to water. Results from stable isotope analysis provide indirect evidence that stream flow is largely a result of lateral throughflow of perched water tables.

Representative Cl⁻ distributions of valley soils illustrate that regional trends in the degree of soil development influence ground water recharge rates. Further study of these dynamic hydrologic units is needed. Moreover, much could be learned from anthropogenic tracers such as tritium to more accurately identify the complex transport processes associated with bypass flow through heterogeneous strata.

References

Allison, G.B. and M.W. Hughes, 1983. The use of natural tracers as indicators of soil-water movement in a temperate semiarid region. *J. Hydrol.* 60:157-173.

- Allison, G.B., G.W. Gee and S.W. Tyler, 1994. Vadose-zone techniques for estimating ground-water recharge in arid and semiarid regions. *Soil Sci. Soc. Am. J.* 58:6-14.
- Bathke, G.R. and D.K. Cassel, 1991. Anisotropic variation of profile characteristics and saturated hydraulic conductivity in an Ultisol landscape. *Soil Sci. Soc. Am. J.* 55:333-339.
- Barker, R.J., 1981. Soil Survey of Latah County area, Idaho. USDA-SCS. U.S. Gov. Print. Office, Washington, D.C.
- Bazemore, D.E., K.N. Eshleman and K.J. Hollenbeck, 1994. The role of soil water in stormflow generation in a forested headwater catchment: Synthesis of natural tracer and hydrometric evidence. *J. Hydrol.* 162:47-75.
- Brooks, E.S., P.A. McDaniel and J. Boll, 2000. Hydrologic modeling in watersheds of the eastern Palouse: Estimation of subsurface flow conditions. Presented at the 2000 Pacific Northwest Region Meeting, Paper no. PNW2000-10. ASAE, St. Joseph, MI.
- Cooper, L.W., 1998. Isotopic fractionation in snow cover. In: Kendall, C., McDonnell, J.J. (Eds). *Isotope Tracers in Catchment Hydrology*. Elsevier, Amsterdam, pp.119-136.
- Dawson, T.E. and J.R. Ehleringer, 1998. Plants, isotopes and water use: A catchment-scale perspective. In Kendall, C. and McDonnell J.J. (Eds.). *Isotope Tracers in Catchment Hydrology*. Elsevier: Amsterdam, pp. 203-238.
- Eptstein, S. and T.K. Mayeda, 1953. Variation of ^{18}O content of waters from natural sources. *Geochim. Cosmochim. Acta* 5:213-224.

Gonfiantini, R., K. Frohlich, L. Araguas-Araguas and K. Rozanski, 1998.

Isotopes in groundwater hydrology. In Kendall, C. and McDonnell J.J. (Eds.).

Isotope Tracers in Catchment Hydrology Elsevier: Amsterdam, pp. 203-238.

Harris, D.M., J.J. McDonnell and A. Rodhe, 1995. Hydrograph separation using continuous open system isotope mixing. *Water Resour. Res.* 31:157-171.

Kelliher, F.M., R. Leuning and E.D. Schulze, 1993. Evaporation and canopy characteristics of coniferous forests and grasslands. *Oecologia* 95:153-163.

Kemp, R.A., P.A. McDaniel and A.J. Busacca, 1998. Genesis and relationship of macromorphology and micromorphology to contemporary hydrological conditions of a welded Argixeroll from the Palouse in NW, USA. *Geoderma* 83:309-329.

McDaniel, P.A., G.R. Bathke, S.W. Buol, D.K. Cassel and A.L. Falen, 1992.

Secondary manganese/iron ratios as pedochemical indicators of field-scale throughflow water movement. *Soil Sci. Soc. Am. J.* 56:1211-1217.

McDaniel, P.A. and A.L. Falen, 1994. Temporal and spatial patterns of episaturation in a Fragixeralf landscape. *Soil Sci. Soc. Am. J.* 58:1451-1457.

McDaniel, P.A., R.W. Gabehart, A.L. Falen, J.E. Hammel and R.J. Reuter, 2001. Perched water tables on Argixeroll and Fragixeralf hillslopes. *Soil Sci. Soc. Am. J.* 65:805-810.

McDonnell, J.J., 1990. A rationale for old water discharge through macropores in a steep, humid catchment. *Water Resour. Res.* 26:2821-2832.

- Marc, V., J. Didon-Lescot and C. Michael, 2001. Investigation of the hydrological processes using chemical and isotopic tracers in a small Mediterranean forested catchment during autumn recharge. J. Hydrol. 247:215-229.**
- Murray, J., 2002. Development of a GIS database for recharge assessment of the Palouse Basin. MS thesis. Univ. of Idaho, Moscow, ID.**
- Neal, M., C. Neal and G. Brahmmer, 1997. Stable isotope variations in rain, snow, and streamwaters at the Schluchsee and Villingen sites in the Black Forest, SW Germany. J. Hydrol. 190:102-110.**
- O'Brien, R., C.K. Keller and J.L. Smith, 1996. Multiple tracers of shallow groundwater flow and recharge in hilly loess. Ground Water 34:675-682.**
- O'Geen, T., J. Boll, E.S. Brooks, J.I. Linard, P.A. McDaniel, J.B. Sisson and A. Wylie, 2001. Detection of multiple perched water tables using natural tracers and multilevel tensiometers in deep loess. EOS Trans. AGU 82 p.47 Fall Meet. Suppl. Abstract H52A-0383.**
- O'Geen, A.T., P.A. McDaniel and J. Boll, in press. Chloride distributions as indicators of vadose zone stratigraphy in Palouse loess deposits. Vadose Zone Journal.**
- Park, S.J. and T.P. Burt, 1999. Identification of throughflow using the distribution of secondary iron oxides in soils. Geoderma 93:61-84.**
- Regan, M. P., 2000. Perched water table dynamics and hydrologic processes in an eastern Palouse catchment. MS thesis. Univ. of Idaho, Moscow, ID.**

- Reuter, R.J., P.A. McDaniel, J.E. Hammel and A.L. Falen, 1998. Solute transport in seasonal perched water tables in loess-derived soils. *Soil Sci. Soc. Am. J.* 62:977-983.
- Rodhe, A. and L. Nyberg, 1996. Transit times for water in a small till catchment from a step shift in the oxygen 18 content of the water input. *Water Resour. Res.* 32:3497-3511.
- Tang, F. and X. Feng, 2001. The effect of soil hydrology on the oxygen and hydrogen isotopic compositions of plants' source water. *Earth and Planet. Sci. Letters* 185:355-367.
- Unnikrishna, P.V., J.J. McDonnell and C. Kendall, 2002. Isotope variations in a Sierra Nevada snowpack and their relation to meltwater. *J. Hydrol.* 260:38-57.

APPENDIX 1

Chloride distributions

Eastern Basin Summit (Santa)

Depth (cm)	[Cl] _{IC}	[Cl] _{IC} mg L ⁻¹	mean [Cl]	water %	[Cl] pore H ₂ O mg L ⁻¹
40	6.6	6.8	6.7	22.3	30.6
60	4.1	4.1	4.1	21.0	19.8
80	3.5	3.5	3.5	17.9	19.3
94	5.0	4.9	5.0	12.1	40.7
114	5.6	5.6	5.6	12.5	45.0
134	4.9	4.9	4.9	12.0	41.2
154	5.3	5.3	5.3	12.7	42.0
174	4.2	4.2	4.2	14.0	30.1
184	4.5	4.6	4.6	13.9	33.5
224	1.2	1.1	1.1	16.0	7.1
238	4.5	4.5	4.5	16.4	27.4
244	3.3	3.2	3.2	13.0	24.4
257	4.5	4.4	4.4	16.7	26.5
274	3.7	3.7	3.7	13.2	28.0
286	4.8	4.9	4.9	15.8	31.1
303	4.7	4.7	4.7	14.2	33.0
318	5.1	5.2	5.2	15.7	33.0
334	8.4	8.2	8.3	13.6	60.6
352	6.1	6.1	6.1	15.6	38.9
371	6.5	6.7	6.6	15.3	43.7
395	7.2	7.3	7.3	14.4	50.7
404	8.9	8.8	8.9	16.3	54.1
428	11.1	11.1	11.1	17.2	64.4
448	13.2	13.1	13.1	17.3	75.8
474	10.4	10.5	10.4	12.9	81.0
500	8.1	8.2	8.1	16.0	50.9
522	7.9	7.8	7.9	15.4	50.9
548	11.1	11.3	11.2	17.6	63.8
572	11.7	11.6	11.7	16.9	68.7
595	10.7	10.7	10.7	16.3	65.7
606	11.3	11.2	11.3	16.5	68.0

Eastern Basin side slope 1(Santa)

Depth (cm)	[Cl] _{IC}	[Cl] _{IC} mg L ⁻¹	mean [Cl]	water %	[Cl] pore H ₂ O mg L ⁻¹
25	2.0		2.0	29.0	6.8
50	1.7	1.7	1.7	23.1	7.3
75	1.0	2.1	1.6	18.9	8.2
100	1.0	1.0	1.0	16.9	6.1
125	1.6	1.6	1.6	17.6	8.9
145	1.6	1.6	1.6	16.3	9.8
170	2.8	2.9	2.8	15.4	18.3
200	3.3	3.1	3.2	17.5	9.5
240	3.1	3.0	3.0	17.7	18.0
270	3.8	3.7	3.8	20.3	15.1
295	4.8	4.8	4.8	16.5	22.6
320	5.8	5.6	5.7	17.5	27.4
340	7.9	7.7	7.8	17.3	32.7
360	8.1	8.1	8.1	20.8	37.5
400	5.1	4.9	5.0	22.1	36.4
428	4.2	4.2	4.2	17.6	28.3
460	2.8	2.8	2.8	16.6	25.3
480	2.6	2.6	2.6	18.9	14.6
500	2.7	2.6	2.6	19.9	13.0
520	1.6	1.6	1.6	21.5	12.2
548	1.8	1.6	1.7	19.7	8.5
560	1.6	1.6	1.6	20.8	8.1
580	1.5	1.5	1.5	19.5	8.0
600	1.5	1.4	1.5	20.4	19.8
670	2.4	2.3	2.4	19.8	51.0
700	3.2	3.1	3.1	20.1	44.9
730	1.5	1.5	1.5	19.0	45.2
762	1.8	2.1	1.9	22.4	57.9
800	1.1	1.0	1.1	19.8	7.6
822	6.1	6.1	6.1	19.3	40.4
853	2.9	2.9	2.9	20.6	14.3
880	1.9	1.9	1.9	22.4	10.3
914	1.6	1.6	1.6	23.2	34.5
924	2.4	2.3	2.4	23.0	21.8
945	3.2	3.1	3.1	22.6	13.7
975	1.5	1.5	1.5	24.4	6.2
1005	1.8	2.1	1.9	22.7	8.2
1036	1.1	1.0	1.1	22.4	4.7
1067	6.1	6.1	6.1	25.0	24.2
1155	2.9	2.9	2.9	34.1	7.7

1186	1.9	1.9	1.9	15.8	12.0
1216	1.6	1.6	1.6	13.8	11.7

Eastern Basin side slope 2 (Santa)

Depth (cm)	[Cl] _{IC}	[Cl] _{IC} mg L ⁻¹	[Cl] _{IC}	mean [Cl]	water %	[Cl] pore H ₂ O mg L ⁻¹
113	1.5	1.1	1.1	18.9	1.2	6.5
135	1.3	1.3	1.3	19.0	1.3	6.9
157	2.6	2.7	2.7	18.4	2.7	14.5
179	4.0	4.0	4.0	18.2	4.0	21.9
211	4.0	4.0	4.1	19.2	4.0	20.9
259	6.4	6.3	6.3	18.7	6.3	33.9
281	6.6	6.6	6.6	20.3	6.6	32.5
303	7.7	7.6	7.6	20.2	7.6	37.6
325	7.2	7.4	7.2	18.0	7.3	40.4
347	7.4		7.4	18.8	7.4	39.2
369	7.3	7.4	7.3	17.9	7.3	40.9
391	6.9	6.9	6.9	18.6	6.9	37.1
416	6.4	6.3	6.4	17.8	6.4	35.7
441	7.9	7.8	8.1	22.7	8.0	35.0
466	6.2	6.2	6.2	22.1	6.2	27.9
491	4.9	5.0	4.9	25.1	5.0	19.7
516	4.4	4.4	4.3	22.1	4.3	19.7
541	4.8	4.8	4.8	24.7	4.8	19.4
575	3.9	4.0	4.0	26.9	4.0	14.8
606	4.1	4.0	4.0	28.8	4.0	14.0
631	3.4	3.4	3.4	26.3	3.4	13.0
656	3.8	3.7	3.6	22.8	3.7	16.3
691	2.6	2.5	2.5	21.7	2.6	11.8
725	2.2	2.2	2.2	21.6	2.2	10.1
784	5.3	5.2	5.3	15.5	5.3	34.1

Eastern Basin side slope 3 (Santa)

Depth (cm)	[Cl] _{IC}	[Cl] _{IC} mg L ⁻¹	mean [Cl]	water %	[Cl] pore H ₂ O mg L ⁻¹
20	10.3	10.3	10.1	27.9	36.1
40	4.6	4.9	4.5	24.4	18.4
60	4.4	4.5	4.2	21.0	20.0
80	5.3	5.5	5.1	21.9	23.3
114	4.0	4.2	3.8	16.8	22.7
134	6.2	6.1	5.9	15.8	37.2
160	2.1	2.0	1.8	16.1	11.1
180	4.6	4.6	4.4	17.7	24.6

200	9.6	9.7	9.4	17.5	53.5
220	6.6	6.7	6.4	18.1	35.2
250	7.8	8.3	7.8	15.2	51.2
270	9.4	9.5	9.2	18.8	48.8
295	15.3	14.1	14.4	18.4	78.2
320	15.3	15.8	15.3	18.9	81.0
346	19.1	18.5	18.6	17.8	104.5
370	18.1	18.8	18.1	17.6	103.0
390	25.3	25.1	24.9	18.8	132.9
412	29.0	28.5	28.5	19.2	148.7
423	21.7	21.6	21.4	17.1	124.8
441	19.1	19.1	18.8	15.9	118.1
462	23.7	24.2	23.7	15.7	151.3
486	22.2	22.2	21.9	18.4	119.4
500	10.9	10.8	10.6	14.9	70.7
527	10.4	10.5	10.2	17.0	59.9
545	11.1	11.0	10.8	16.2	66.6
565	9.3	9.2	9.0	15.6	57.5
587	10.1	10.1	9.8	17.3	56.8
606	10.3	11.0	10.3	16.7	61.9

Eastern Basin side slope 4 (Santa)

Depth (cm)	[Cl] _{IC}	[Cl] _{IC} mg L ⁻¹	mean [Cl]	water %	[Cl] pore H ₂ O mg L ⁻¹
20	10.3	10.3	10.1	27.9	36.1
40	4.6	4.9	4.5	24.4	18.4
60	4.5	4.4	4.2	21.0	20.0
80	5.5	5.3	5.1	21.9	23.3
114	4.2	4.0	3.8	16.8	22.7
134	6.1	6.2	5.9	15.8	37.2
160	2.0	2.1	1.8	16.1	11.1
180	4.6	4.6	4.4	17.7	24.6
200	9.6	9.7	9.4	17.5	53.5
220	6.7	6.6	6.4	18.1	35.2
250	8.3	7.8	7.8	15.2	51.2
270	9.5	9.4	9.2	18.8	48.8
295	14.1	15.3	14.4	18.4	78.2
320	15.3	15.8	15.3	18.9	81.0
346	18.5	19.1	18.6	17.8	104.5
374	18.8	18.1	18.1	17.6	103.0
390	25.1	25.3	24.9	18.8	132.9
412	28.5	29.0	28.5	19.2	148.7
423	21.6	21.7	21.4	17.1	124.8

441	19.1	19.1	18.8	15.9	118.1
462	24.2	23.7	23.7	15.7	151.3
486	22.2	22.2	21.9	18.4	119.4
500	10.8	10.9	10.6	14.9	70.7
527	10.5	10.4	10.2	17.0	59.9
545	11.1	11.0	10.8	16.2	66.6
565	9.2	9.3	9.0	15.6	57.5
587	10.1	10.1	9.8	17.3	56.8
606	10.3	11.0	10.3	16.7	61.9
618	34.7				

Eastern Basin valley 1(Taney)

Depth (cm)	[Cl] _{IC}	[Cl] _{IC} mg L ⁻¹	mean [Cl]	water %	[Cl] pore H ₂ O mg L ⁻¹
20	1.8	1.8	1.8	32.6	5.6
40	1.7	1.8	1.7	28.5	6.1
60	2.0	2.0	2.0	24.6	8.3
80	24.9	24.8	24.8	28.9	86.2
100	11.7	11.5	11.6	22.3	52.4
120	2.2	2.2	2.2	22.1	9.8
140	2.4	2.4	2.4	19.3	12.4
160	2.2	2.2	2.2	21.9	10.0
180	2.3	2.3	2.3	22.6	10.2
200	2.8	2.9	2.9	21.1	13.5
220	2.7	2.7	2.7	20.2	13.2
240	3.2	3.3	3.2	21.7	14.9
260	3.6	3.6	3.6	20.2	17.8
280	16.3	16.3	16.3	22.4	72.8
300	4.3	4.3	4.3	21.3	20.4
320	8.3	8.1	8.2	20.8	39.7
340	4.4	4.3	4.3	18.1	24.2
360	6.3	6.2	6.2	21.9	28.5
380	5.9	5.8	5.8	21.8	27.0
400	5.4	5.4	5.4	25.0	21.7
433	5.5	5.6	5.5	26.5	20.8
458	3.3	3.2	3.2	12.6	25.9
483	3.7	3.6	3.6	17.1	21.4
508	2.3	2.3	2.3	10.0	23.1
533	3.0	2.9	2.9	11.1	26.6
558	2.5	2.4	2.5	12.4	20.2
579	2.6	2.6	2.6	9.4	27.4

Eastern Basin valley 2 (Santa)

Depth (cm)	[Cl] _{IC}	[Cl] _{IC} mg L ⁻¹	mean [Cl]	water %	[Cl] pore H ₂ O mg L ⁻¹
25	7.2		7.2	36.9	19.5
50	5.1	5.4	5.2	23.1	21.9
75	13.0	13.0	13.0	24.8	52.7
100	13.7	14.4	14.0	23.0	59.4
125	7.3	10.3	8.8	18.5	39.8
150	10.3	5.5	7.9	21.5	48.1
175	5.3	4.4	4.9	18.1	29.5
200	4.3	10.0	7.1	21.5	20.0
225	9.9	4.7	7.3	23.0	43.0
250	4.7	6.8	5.8	22.5	20.9
275	6.7	3.9	5.3	25.3	26.6
290	4.0	7.7	5.8	19.5	20.4
330	7.6		7.6	10.7	71.1

Central Basin summit (Garfield)

Depth (cm)	[Cl] _{IC}	[Cl] _{IC} mg L ⁻¹	mean [Cl]	water %	[Cl] pore H ₂ O mg L ⁻¹
20	1.00	0.97	0.98	19	5.16
40	0.98	0.99	0.99	19	5.19
60	0.94	0.91	0.93	19	4.89
80	1.21	1.23	1.22	18	6.77
100	1.31	1.27	1.29	19	6.78
120	0.74	0.75	0.75	19	3.93
140	0.96	0.99	0.98	21	4.65
160	0.93	0.89	0.91	22	4.14
180	1.12	1.15	1.13	23	4.93
200	1.00	1.00	1.00	22	4.56
220	0.35	0.83	0.59	25	2.36
240	1.41	1.45	1.43	23	6.21
260	2.18	1.99	2.08	23	9.06
280	0.94	0.87	0.91	23	3.95
300	1.29	1.32	1.31	24	5.44
320	1.73	1.78	1.76	23	7.64
340	1.55	1.55	1.55	22	7.05
360	1.66	1.65	1.66	18	9.21
380	1.65	1.70	1.68	25	6.70
400	1.26	1.29	1.28	21	6.07
420	1.74	1.73	1.74	22	7.89
440	2.11	2.17	2.14	22	9.73
460	1.45	1.46	1.45	22	6.59

480	1.34	1.35	1.34	23	5.83
500	1.16	1.20	1.18	23	5.14
520	1.45	1.49	1.47	23	6.37

Central Basin concave side slope (Palouse/Thatuna)

Depth (cm)	[Cl] _{IC}	[Cl] _{IC} mg L ⁻¹	mean [Cl]	water %	[Cl] pore H ₂ O mg L ⁻¹
20	0.0	0.8	0.4	10	4.2
40	1.1	1.1	1.1	16	6.8
60	1.2	1.4	1.3	21	6.1
80	1.7	1.4	1.6	30	5.3
100	1.3	1.2	1.3	34	3.7
120	1.4	1.4	1.4	33	4.2
140	1.1	1.1	1.1	18	6.0
160	0.8	0.8	0.8	23	3.5
180	2.4	2.5	2.4	25	9.9
200	1.1	1.2	1.1	21	5.4
220	1.3	1.4	1.4	21	6.7
240	1.0	1.0	1.0	21	4.8
260	1.7	1.6	1.7	23	7.3
280	0.9	0.9	0.9	23	4.0
300	1.0	1.0	1.0	23	4.4
320	0.9	1.0	0.9	23	4.0
340	1.6	1.7	1.6	23	7.0
360	1.5	1.6	1.5	39	3.9
380	1.3	1.2	1.2	23	5.4
400	1.4	1.5	1.5	23	6.4
420	1.6	1.7	1.7	23	7.3
440	0.8	0.9	0.8	24	3.6
460	0.6	0.6	0.6	24	2.5
480	0.9	0.7	0.8	23	3.3
500	0.8	0.8	0.8	25	3.3
520	1.1	1.1	1.1	26	4.3
540	1.1	1.0	1.0	27	3.7
560	0.5	0.5	0.5	30	1.8
580	0.9	1.0	0.9	30	3.1
600	0.8	0.8	0.8	30	2.7

Central Basin convex side slope (Naff)

Depth (cm)	[Cl] _{IC}	[Cl] _{IC} mg L ⁻¹	mean [Cl]	water %	[Cl] pore H ₂ O mg L ⁻¹
20	2.3	2.3	2.3	17	13.2
40	0.7	0.8	0.8	19	4.0
60	1.7	1.8	1.7	22	8.0
80	1.4	1.5	1.4	20	7.0
100	1.1	1.0	1.0	22	4.7
120	4.3	4.3	4.3	23	18.6
140	1.9	1.9	1.9	24	7.8
160	0.7	0.8	0.8	25	3.0
180	1.0	1.0	1.0	22	4.6
200	4.1	4.0	4.0	24	16.6
220	1.6	1.6	1.6	26	6.3
240	3.5	3.6	3.5	23	15.0
260	2.3	2.3	2.3	25	9.3
280	2.1	1.9	2.0	25	8.1
300	3.2	2.9	3.1	28	10.8
320	2.4	2.4	2.4	26	9.3
340	2.7	2.6	2.7	28	9.5
360	2.6	2.7	2.6	28	9.4
380	3.1	3.1	3.1	26	12.0
400	1.4	1.4	1.4	26	5.3
420	5.2	5.2	5.2	27	19.6
440	3.9	3.9	3.9	29	13.7
460	5.5	5.5	5.5	31	17.8

Central Basin valley (Latahco)

Depth (cm)	[Cl] _{IC}	[Cl] _{IC} mg L ⁻¹	[Cl] _{IC}	mean [Cl]	water %	[Cl] pore H ₂ O mg L ⁻¹
20	2.0	2.3	2.3	2.2	13	16.7
40	2.6	2.6	2.3	2.5	16	15.3
60	3.7	3.7	3.9	3.8	23	16.4
80	1.7	2.0		1.9	29	6.5
100	1.6	1.8	1.7	1.7	30	5.6
120	0.0	1.5	1.4	1.5	26	5.6
140	1.6	2.0	1.8	1.8	22	8.2
160	1.7			1.7	24	7.1
180	2.0	2.4		2.2	28	8.1
200	1.2	7.0	7.3	5.2	25	20.4
220	0.0	6.4	5.4	5.9	29	20.5
240	1.9		7.1	4.5	26	17.1
260	3.6	3.9	3.6	3.7	26	13.9

280	4.6	5.2	5.2	5.0	28	18.0
300	5.9	5.8	5.9	5.9	30	19.8
320	1.3	3.5	3.4	2.7	29	9.4
340	2.2			2.2	27	8.5
360	0.0	3.5	3.3	3.4	22	15.5
380	1.5	3.5	3.3	2.8	29	9.7
400	4.0	4.1	4.5	4.2	34	12.4
420	3.3	3.7	3.6	3.5	31	11.5
440	5.9	6.1	6.1	6.1	33	18.6
460	4.6			4.6	42	11.2
480	1.7	4.3	3.9	3.3	32	10.4
500	2.3	2.5	2.5	2.4	33	7.3
520	3.8	4.0	4.0	3.9	36	10.9

Central Basin hanging valley (Cumulic Palouse)

Depth (cm)	[Cl] _{IC}	[Cl] _{IC} mg L ⁻¹	mean [Cl]	water %	[Cl] pore H ₂ O mg L ⁻¹
20	1.30	1.23	1.27	21	6.13
40	1.33	1.30	1.31	23	5.60
60	1.65	1.55	1.60	26	6.22
80	0.67	0.69	0.68	26	2.67
100	0.78	0.81	0.80	19	4.09
120	1.77	1.74	1.75	23	7.68
140	1.63	1.63	1.63	28	5.92
160	1.13	1.06	1.10	22	5.09
180	0.93	1.04	0.98	19	5.06
200	0.60	0.60	0.60	23	2.58
220	4.67	4.52	4.60	23	20.01
240	0.85	0.86	0.85	25	3.45
260	1.59	1.59	1.59	27	5.95
280	1.39	1.34	1.37	27	4.99
300	1.25	1.27	1.26	26	4.87
320	6.33	5.94	6.14	26	23.87
340	1.80	1.77	1.79	27	6.65
360	2.34	2.23	2.29	28	8.03
380	1.35	1.23	1.29	27	4.86
400	2.43	2.34	2.39	26	9.29
420	2.08	2.11	2.09	29	7.32
440	1.37	1.32	1.34	27	5.06
460	1.19	1.16	1.18	29	4.04
480	4.72	4.50	4.61	26	17.62
500	1.19	1.16	1.18	26	4.50
520	2.06	2.00	2.03	24	8.43

Western Basin summit (Naff)

Depth (cm)	[Cl] _{IC}	[Cl] _{IC} mg L ⁻¹	mean [Cl]	water %	[Cl] pore H ₂ O mg L ⁻¹
20	2.68	2.68	2.68	19	14.13
40	2.38	2.00	2.19	27	8.15
60	2.59	2.23	2.41	30	7.99
80	1.67	1.54	1.60	22	7.14
100	1.15	0.10	0.62	20	3.05
120	2.07	1.72	1.89	22	8.70
140	1.24	1.18	1.21	22	5.59
160	0.00	0.00	0.00	23	0.00
180	0.00	0.00	0.00	24	0.00
200	1.37	1.39	1.38	24	5.70
220	1.20	1.20	1.20	25	4.90
240	1.04	0.10	0.57	24	2.35
260	1.25	1.23	1.24	24	5.08
280	1.69	1.61	1.65	25	6.51
300	1.22	1.27	1.24	25	4.88
320	1.31	1.35	1.33	25	5.38
340	1.27	1.23	1.25	23	5.49
360	1.30	1.26	1.28	22	5.80
380	1.26	1.21	1.23	23	5.28
400	4.41	1.34	2.88	24	12.05
420	2.00	2.17	2.09	25	8.51
440	1.06	1.07	1.06	25	4.19
460	1.24	1.46	1.35	27	4.99
480	1.50	1.52	1.51	28	5.31
500	1.69	1.66	1.68	24	7.06
520	1.10	0.10	0.60	24	2.47

Western Basin side slope (Palouse)

Depth (cm)	[Cl] _{IC}	[Cl] _{IC} mg L ⁻¹	mean [Cl]	water %	[Cl] pore H ₂ O mg L ⁻¹
20	0.8	0.0	0.4	10	4.3
40	1.1	1.1	1.1	16	7.0
60	1.4	1.2	1.3	21	6.3
80	1.4	1.7	1.6	30	5.2
100	1.2	1.3	1.3	34	3.7
120	1.4	1.4	1.4	33	4.2
140	1.1	1.1	1.1	18	6.0
160	0.8	0.8	0.8	23	3.5
180	2.5	2.4	2.4	25	9.7
200	1.2	1.1	1.1	21	5.3

220	1.4	1.3	1.4	21	6.5
240	1.0	1.0	1.0	21	4.8
260	1.6	1.7	1.7	23	7.2
280	0.9	0.9	0.9	23	4.0
300	1.0	1.0	1.0	23	4.4
320	1.0	0.9	0.9	23	4.1
340	1.7	1.6	1.6	23	7.2
360	1.6	1.5	1.5	39	3.9
380	1.2	1.3	1.2	23	5.4
400	1.5	1.4	1.5	23	6.4
420	1.7	1.6	1.7	23	7.2
440	0.9	0.8	0.8	24	3.5
460	0.6	0.6	0.6	24	2.5
480	0.7	0.9	0.8	23	3.3
500	0.8	0.8	0.8	25	3.2
520	1.1	1.1	1.1	26	4.3
540	1.0	1.1	1.0	27	3.8
560	0.5	0.5	0.5	30	1.8
580	1.0	0.9	0.9	30	3.0
600	0.8	0.8	0.8	30	2.7

Western Basin valley (Thatuna)

Depth (cm)	[Cl] _{IC}	[Cl] _{IC} mg L ⁻¹	mean [Cl]	water %	[Cl] pore H ₂ O mg L ⁻¹
20	1.82	1.83	1.82	10	18.76
40	6.28	6.28	6.28	11	57.49
60	9.53	9.51	9.52	19	51.23
80	1.98	1.93	1.95	33	6.00
100	3.46	3.40	3.43	29	12.11
120	1.77	1.76	1.77	25	6.95
140	2.81	2.79	2.80	29	9.57
160	2.61	2.64	2.63	25	10.55
180	13.59	13.56	13.58	29	46.64
200	2.32	2.39	2.35	36	6.52
220	1.11	1.11	1.11	35	3.18
240	1.06	1.05	1.05	34	3.14
260	1.84	1.88	1.86	37	4.90
280	12.69	12.65	12.67	35	36.62
320	2.14	2.18	2.16	46	4.65
340	2.80	2.81	2.81	38	7.35
360	1.79	1.76	1.78	30	6.05
380	1.24	1.24	1.24	32	3.84
400	1.54	1.61	1.58	30	5.20
420	2.05	2.09	2.07	30	6.74

APPENDIX 2
Stable isotope data

Eastern Basin

Summit		Side Slope		Valley	
Depth (cm)	O-18 _{VSMOW}	Depth (cm)	O-18 _{VSMOW}	Depth (cm)	O-18 _{VSMOW}
50	-13.03	50	-13.30	50	-12.55
50	-12.80	50	leak	50	-12.89
100	-10.98	75	-13.49	100	-12.07
100	-10.79	75	leak	100	-12.00
125	-12.70	100	-10.12	125	-11.81
125	-12.53	100	-10.50	125	-11.67
150	-13.16	150	-11.70	150	-11.78
175	-13.11	150	-12.49	150	-12.38
200	-13.45	200	leak	175	-12.58
200	-12.94	200	-13.31	175	-12.22
225	-13.15	225	-13.39	200	-11.97
250	-13.11	225	-13.68	200	-12.64
275	-13.24	250	-14.12	250	-13.03
300	-13.32	250	-13.77	250	-12.93
350	-13.12	275	-14.31	300	-13.20
350	leak	300	-13.81	300	-13.06
375	-13.56	325	-14.33	350	-12.81
400	-13.63	350	-9.41	350	-13.04
400	-14.14	350	-13.90	400	-13.02
425	-14.68	375	-13.71	400	-12.74
		375	-13.81	425	-13.29
		400	-7.53	425	-13.03
		400	-14.33		
		425	-13.63		
		425	-13.80		
		450	-14.70		
		450	-14.77		
		475	-14.25		
		475	-13.62		
		500	-14.75		
		500	-14.09		
		525	-13.06		
		550	-14.46		
		550	-14.01		
		575	-14.82		
		600	-14.39		

Central Basin

Summit		Side slope		Valley	
Depth (cm)	O-18 _{VSMOW}	Depth (cm)	O-18 _{VSMOW}	Depth (cm)	O-18 _{VSMOW}
100	-12.83	100	-13.20	100	-13.04
100	-12.62	100	-13.02	100	leak
150	-13.12	150	-13.41	150	-12.68
150	-13.44	200	leak	150	leak
200	-12.66	200	-12.41	200	-13.14
200	-12.30	250	-12.88	200	-13.41
250	-11.48	250	-12.91	250	-13.58
250	-11.84	300	-13.00	250	-13.45
300	-11.67	350	-13.17	300	leak
300	-11.96	400	-13.39	300	-13.79
350	-11.96	400	-13.02	350	-13.81
350	-12.37	450	-13.13	350	-13.73
400	-11.90	450	-12.97	400	-13.66
400	leak	500	-12.81	400	-14.36
450	-12.60	500	-13.37	450	-13.80
450	-12.54	550	-13.16	450	-14.50
500	leak	550	-13.71	500	-14.35
500	-12.45	600	-13.52	500	-8.80
550	-12.97	600	-13.51	550	-14.75
550	-13.54			550	-14.25
600	-2.02				
600	-12.97				

Western Basin

Summit		Side slope		Valley	
Depth (cm)	O-18 _{VSMOW}	Depth (cm)	O-18 _{VSMOW}	Depth (cm)	O-18 _{VSMOW}
40	-14.73	75	-13.30	75	-13.30
80	-13.60	125	-13.49	100	-13.49
120	-13.09	150	-13.09	150	-13.09
160	-13.29	175	-11.83	200	-13.15
200	-14.03	225	-13.70	225	-13.79
220	-13.08	250	-13.22	250	-13.64
240	-13.39	275	-13.31	275	-13.27
260	-13.52	300	-13.02	325	-13.48
280	-13.18	325	-13.48	375	-14.18
300	-14.71	375	-13.72	400	-14.02
320	-12.07	400	-13.32	425	-14.05
340	-13.65	425	-13.05		
360	-13.27	450	-13.72		
400	-12.61	475	-13.24		
420	-12.59	500	-13.32		
440	-13.55	525	-13.02		
460	-13.28	550	-13.70		
480	-13.24				
500	-13.87				
520	-13.13				
540	-13.76				
560	-14.00				

APPENDIX 3

Stratigraphic measurements

Secondary Mn and Fe measured from cores of the eastern catchement

Valley						
Depth (cm)	%Mn a	% Mn b	ave MN%	% Fe a	% Fe b	Ave % Fe
20	0.111	0.116	0.114	1.069	0.861	0.965
40	0.090	0.081	0.086	0.822	0.793	0.807
50	0.018	0.017	0.017	0.716	0.689	0.703
60	0.040	0.049	0.044	0.686	0.663	0.674
80	0.008	0.010	0.009	0.789	0.814	0.802
100	0.067	0.062	0.064	1.483	1.439	1.461
120	0.061	0.050	0.055	1.125	1.106	1.116
140	0.032	0.036	0.034	1.006	1.055	1.030
160	0.025	0.024	0.025	0.693	0.672	0.682
180	0.035	0.037	0.036	0.969	1.050	1.009
200	0.010	0.009	0.009	1.235	1.138	1.186
220	0.006	0.007	0.006	0.768	0.804	0.786
240	0.014	0.011	0.013	1.101	0.959	1.030
260	0.010	0.009	0.009	0.793	0.684	0.739
280	0.012	0.015	0.014	0.859	0.887	0.873
300	0.014	0.013	0.014	0.903	0.949	0.926
320	0.036	0.038	0.037	0.801	0.783	0.792
340	0.033	0.034	0.033	0.821	0.860	0.840
360	0.010	0.011	0.011	0.630	0.670	0.650
380	0.046	0.038	0.042	0.670	0.672	0.671
400	0.010	0.010	0.010	0.588	0.576	0.582
420	0.008	0.007	0.008	0.580	0.532	0.556
433	0.006	0.007	0.007	0.965	1.033	0.999
458	-	0.004	0.004	-	0.195	0.195
483	-	0.001	0.001	-	0.237	0.237
508	-	0.002	0.002	-	0.130	0.130
533	-	0.004	0.004	-	0.155	0.155
558	-	0.005	0.005	-	0.400	0.400

Secondary Mn and Fe measured from cores of the eastern catchment

Side slope

Depth (cm)	Mn a	Mnb	Ave Mn	Fe a	Feb	Ave Fe
20	0.08	-	0.08	-	1.21	1.21
50	0.05	0.03	0.04	1.55	1.38	1.46
75	0.07	0.05	0.06	1.42	1.58	1.50
100	0.05	0.06	0.05	1.78	1.73	1.76
125	0.05	0.05	0.05	1.89	1.46	1.67
145	0.14	0.14	0.14	1.57	1.47	1.52
170	0.04	0.04	0.04	1.71	1.20	1.46
195	0.04	0.04	0.04	1.23	1.56	1.39
220	0.05	0.05	0.05	1.42	1.75	1.59
245	0.05	0.05	0.05	1.81	1.69	1.75
270	0.03	0.04	0.04	1.63	1.59	1.61
295	0.03	-	0.03	1.83	1.56	1.69
315	0.06	0.06	0.06	1.61	1.70	1.66
340	0.06	0.05	0.06	1.33	1.35	1.34
356	0.07	0.07	0.07	1.69	1.62	1.66
381	0.04	0.04	0.04	1.39	1.46	1.42
408	0.07	0.06	0.06	1.74	1.71	1.72
428	0.05	0.05	0.05	1.33	1.44	1.39
448	0.07	0.07	0.07	1.71	1.80	1.75
468	0.06	0.06	0.06	1.56	1.69	1.63
488	0.05	0.05	0.05	1.60	1.58	1.59
508	0.07	0.07	0.07	1.88	1.73	1.81
528	0.05	0.04	0.04	1.56	1.54	1.55
558	0.04	0.05	0.04	1.38	-	1.38
670	0.05	0.05	0.05	1.69	1.64	1.66
762	0.09	0.10	0.09	2.23	2.10	2.16
822	0.06	0.06	0.06	1.78	1.84	1.81
914	0.05	0.04	0.05	1.52	1.67	1.60
944	0.10	0.11	0.10	2.04	2.02	2.03
975	0.03	-	0.03	1.80	1.71	1.76
1005	0.02	0.02	0.02	1.80	1.89	1.84
1036	0.03	0.03	0.03	2.68	2.70	2.69
1066	0.14	0.09	0.11	4.43	4.50	4.47
1150	0.03	0.03	0.03	4.45	4.40	4.43
1188	0.04	0.03	0.03	0.70	0.77	0.74
1219	0.01	-	0.01	0.10	-	0.10

Secondary Mn and Fe measured from cores of the eastern catchment

Summit						
Depth (cm)	Mn a	Mn b	Ave % Mn	% Fe a	%Fe b	Ave % Fe
20	0.09	0.09	0.09	1.22	1.22	1.22
40	0.06	0.06	0.06	1.26	1.28	1.27
60	0.01	0.02	0.02	1.24	1.14	1.19
94	0.03	0.03	0.03	1.14	1.12	1.13
114	0.04	0.04	0.04	1.17	1.07	1.12
134	0.07	0.04	0.06	1.16	1.12	1.14
154	0.06	0.05	0.06	1.21	1.12	1.16
174	0.04	-	0.04	1.20	-	1.20
204	0.03	0.03	0.03	1.10	1.09	1.09
224	0.04	-	0.04	1.20	-	1.20
238	0.08	0.07	0.08	1.45	1.62	1.54
244	0.07	0.08	0.07	1.74	1.88	1.81
257	0.04	0.04	0.04	1.73	1.64	1.68
274	0.04	0.04	0.04	1.66	1.73	1.69
286	0.04	-	0.04	1.56	-	1.56
303	0.05	0.03	0.04	1.55	1.42	1.49
318	-	0.12	0.12	-	1.62	1.62
334	0.04	0.04	0.04	1.58	1.60	1.59
352	0.04	0.05	0.05	1.69	1.70	1.70
371	0.04	0.06	0.05	1.78	1.97	1.88
395	0.04	0.04	0.04	1.70	1.71	1.70
404	0.03	0.03	0.03	1.85	1.73	1.79
428	0.03	0.03	0.03	1.71	1.75	1.73
448	0.03	0.03	0.03	1.59	1.45	1.52
474	0.05	0.04	0.05	1.48	1.41	1.45
500	0.04	0.04	0.04	1.44	1.54	1.49
522	0.04	0.05	0.04	1.45	1.33	1.39
548	0.06	0.06	0.06	1.59	1.50	1.54
572	0.05	0.05	0.05	1.48	1.49	1.48
580	0.03	0.03	0.03	1.25	1.31	1.28
595	0.04	0.03	0.04	1.31	1.40	1.35
618	0.07	0.08	0.07	1.59	1.59	1.59

Soil Strength of core samples from the eastern catchment.

Valley	A	B	C	Ave
Depth (cm)	kg cm ⁻²			
20	0.25	0.2	0.15	0.2
40	0.2	0.25	0.2	0.2
50	0.75	0.7		0.7
60	1	1.25	1.2	1.2
80	1.9	1.75	1.75	1.8
100	2.25	2	2.5	2.3
120	4.5	4.25	4.3	4.4
140	1.25	1.3	1.5	1.4
160	1.3	1.1	2	1.5
180	0.9	0.9	1.1	1.0
200	1.25	1.2	1.2	1.2
220	1.25	0.75	0.75	0.9
240	1.25	1.25	1	1.2
260	1.25	1.45	1.15	1.3
280	1.1	1.25	1.6	1.3
300	0.65	0.4	0.85	0.6
320	0.65	0.75	0.75	0.7
340	1.5	0.9	1	1.2
360	1.1	1.6	1	1.2
380	1.7	1.6	1.79	1.7
400	0.8	0.8	0.9	0.8
420	0.8	1.2	0.8	0.9
433	1.5	1.35	1.25	1.4

Soil Strength of core samples from the eastern catchment.

Side slope	A	B	C	Ave
Depth	kg cm ⁻²			
20	1.1	1.1	0.65	1.0
50	1.1	1.1	1.25	1.2
75	1.8	1.8	1.45	1.7
100	2.25	3.25	3.9	3.1
125	4.5	4.5	4.5	4.5
145	4.5	3.5	4.5	4.2
175	3.25	3.65	3.8	3.6
195	1.8	1.8	1.7	1.8
220	1.5	1.1	1.2	1.3
245	2.45	2.45	2.75	2.6
270	1.45	1.1	1.2	1.3
295	1.5	1.25	1.6	1.5
315	4.5	4.5	4.5	4.5

340	1	1.2	1.1	2.0
356	1.25	1.7	2	2.0
381	3.4	3.5	3.25	3.4
408	4.5	4.5	4.5	4.5
428	2.8	2.45	2.5	2.6
448	3.15	3.5	2.65	3.1
468	2	2.5	1	1.8
488	1.5	1.1	1	1.2
508	1.25	0.5	1	0.9
528	1.25	1.25	1.5	1.3
558	2.25	2.26	2.2	2.2
670	1.85	2.25	1.5	1.9
762	4.5	4.5	4.5	4.5
820	3.25	4.5	4.5	4.1
914	4.5	4.5	4.5	4.5
945	4.5	4	4.5	4.3
975	3.5	4.5	4.5	4.2
1005	4.5	4.5	4.5	4.5
1036	4.5	4.5	4.5	4.5
1067	4.5	3.8	4	4.1
1155	2.5	2.1	2.9	2.5
1186	1.9	1.1	2	1.7
1216	2.25	2	1.6	2.0

Soil Strength of core samples from the eastern catchment.

Summit	A	B	C	Ave
Depth	kg cm ⁻²			
20	0.9	0.5	0.6	0.7
40	1.15	0.8	1.1	1.0
60	1.75	1.5	1.65	1.6
80	2.5	2.7	2.2	2.5
94	2.45	2.5	3.25	2.7
114	1.6	2	1.5	1.7
134	2.5	2.5	1.75	2.3
154	1	1	0.9	1.9
174	1.5	2	1.2	4.0
184	1.5	1.5	1.5	4.5
204	1.5	2	1.75	4.2
224	1.5	1	1.6	3.5
238	1	0.7	0.5	0.7
244	0.6	0.5	0.5	0.5
257	1	1.5	0.7	1.1
274	1.7	1.5	1	1.4
286	1	1.5	1.5	1.3

303	1.1	1	0.8	1.0
318	0.75	1	1.2	1.0
334	3.2	3.25	2.4	3.0
352	2.5	4	3.6	3.4
371	3.5	3	3.25	3.3
395	2.2	2.5	1.75	2.2
404	0.75	2	1.5	1.4
428	1.25	1.1	1	1.1
448	1.25	1.75	1.5	2.5
474	2	2.2	1.9	2.0
500	1.5	0.9	0.75	1.1
522	1.65	1.2	0.9	1.3
548	1.4	1.45	1.3	1.4
572	1.25	0.9	0.9	1.0
595	1.9	2.5	2.75	2.4
618	1.5	1.5	1.75	2.5

Clay content of core samples from the eastern catchment.

Summit

Depth (cm) Clay (%)

20	22.0
40	19.0
60	26.0
80	34.5
114	30.1
134	29.1
154	34.8
174	33.9
184	22.8
204	35.0
224	28.3
238	22.2
244	25.3
274	26.3
286	23.3
303	23.3
318	18.5
334	19.2
352	30.6
371	26.3
395	26.5
404	29.1
428	34.1
448	29.9

474	20.4
500	22.9
522	25.6
548	28.8
572	26.9
595	27.3
618	27.5

Clay content of core samples from the eastern catchment.

Side slope

Depth (cm)	Clay (%)
25	18.5
50	15.7
75	21.9
100	26.4
125	38.1
145	32.7
170	31.8
200	26.7
240	29.4
270	23.5
295	34.2
320	32.5
340	23.2
360	24.6
400	36.3
428	26.0
460	23.8
480	23.3
500	25.6
520	26.3
548	20.2
560	17.8
580	17.4
600	20.9
670	24.9
700	26.8
730	33.3
762	37.7
800	27.0
822	27.9
853	29.2
880	31.0
914	35.1

924	30.7
945	25.6
975	42.4
1005	35.8
1036	31.3
1067	36.4
1155	43.2
1186	20.8
1216	21.4

Clay content of core samples from the eastern catchment.

Valley

Depth (cm)	Clay (%)
20	18.7
40	19.5
60	39.0
80	46.7
100	37.0
120	46.1
140	27.7
160	28.4
180	28.1
200	28.4
220	28.8
240	29.5
260	35.0
280	32.7
300	26.7
320	20.2
340	24.9
360	29.7
380	30.9
400	31.8
420	29.6
433	33.7
458	9.2
483	10.1
508	9.8
533	8.4
558	8.7
579	9.9

APPENDIX 4

Diffusion calculations

	Diffusion coefficient (cm ² day ⁻¹)	Diffusion coefficient (m ² s ⁻¹)	Time @ 0.25 m s	Time @ 0.25 m yr	Time @ 0.5 m s	Time @ 0.5 m yr
Litoral sediment	1.66	1.9213E-09	32530120.5	1	130120481.9	4
Clay-sand mix	0.54	6.25E-10	100000000	3	400000000	13
Clay	0.08	9.25926E-11	675000000	21	2700000000	86